2011

Effects of Age and Early Life Ozone Exposure on the Developmental Dynamics of Afferent Airway Neurons in Postnatal Rats

Leor C. Zellner
West Virginia University

Effects of Age and Early Life Ozone Exposure on the Developmental Dynamics of Afferent Airway Neurons in Postnatal Rats

Leor C. Zellner

Dissertation submitted to the
School of Medicine
at West Virginia University
in partial fulfillment of the requirements
for the degree of

Doctor of Philosophy
in
Cellular and Integrative Physiology

Richard D. Dey, Ph.D., Advisor and Chair
Kathleen M. Brundage, Ph.D.
Jeffrey S. Fedan, Ph.D.
S. Jamal Mustafa, Ph.D.
Adrienne Salm, Ph.D.

Department of Neurobiology and Anatomy

Morgantown, West Virginia
2011

Keywords: Substance P, sensory neurons, Nerve Growth Factor, airway innervation

ABSTRACT

Effects of Age and Early Life Ozone Exposure on the Developmental Dynamics of Afferent Airway Neurons in Postnatal Rats

Leor C. Zellner

The environmental irritant ozone (O_3) plays a role in airway inflammation and is known to cause airway hyperresponisiveness especially in susceptible populations such as asthmatics and young children. O_3 exposure increases nerve growth fact (NGF) mRNA and protein levels in the airways, and alters the expression of substance P (SP) in nodose and jugular afferent airway neurons and in sensory nerve fibers in the airways. The growth and development of vagal afferent neurons is in part regulated by NGF, and because these sensory neurons continue to develop throughout postnatal life O_3 exposures during this period may adversely affect their development. The objectives of these studies were to 1) characterize the normal postnatal development of vagal ganglia sensory neurons, tracheal epithelial innervation, and NGF levels in lung lavage and 2) investigate changes in nodose and jugular ganglia neuron number and SP content following acute O_3 exposure in early postnatal life.

Initial studies determined that NGF levels in bronchoalveolar lavage fluid (BALF) and tracheal epithelial nerve fiber density (NFD) changed in an age-related manner, and both were maximally increased on postnatal day (PD) 10. Preliminary studies conducted to determine an efficient and accurate method for quantifying vagal sensory neurons used retrograde tracing techniques to identify afferent airway neurons located in the nodose and jugular ganglia. A novel quantification technique combining neuronal isolation, immunocytochemistry and flow cytometry was developed. Age-related changes were also noted in afferent airway neurons, which corresponded to the changes measured in NFD and NGF levels. These findings indicated that the early postnatal development of airway sensory neurons and innervation occurs in a rapid manner and may be influenced by NGF.

In the next set of studies, rats were exposed to O_3 (2ppm for 3 hrs) on PD5 to evaluate possible changes in neuronal development and SP content. A significant decrease in the total number of nodose and jugular ganglia neurons was noted 16 days after the O_3 exposure (PD21), and the number of SP-containing airway neurons was markedly increased on PD28 (23 days after O_3) compared with filtered air (FA) controls. No differences in the total number of airway neurons between O_3 and FA exposed groups were noted. These findings reveal that early life O_3 exposure can significantly alter vagal sensory neuron development.

In conclusion, sensory neuron development is significantly altered by exposure to O_3 in early postnatal life, and increases in the number of SP containing airway neurons so far removed from the exposure, may provide insight into why early life O_3 exposure enhances airway responses to subsequent irritant exposures later in life.

Acknowledgements

I would first like to express my heartfelt appreciation to my adviser, Dr. Richard Dey, for all of the support and encouragement he has given me throughout my graduate education. Through his mentoring I have grown as a researcher and developed skills that will serve me throughout my career. I would also like to thank the members of my committee, Dr. Jeffrey Fedan, Dr. Adrienne Salm, Dr. Jamal Mustafa, and Dr. Kathy Brundage, for their guidance and assistance in troubleshooting my research project. I am especially grateful to Dr. Kathy Brundage for all of her advice and for sharing her extensive knowledge of flow cytometry, which were essential for developing my neuron quantification experiments.

There are no words that can fully convey how truly grateful I am for the endless love and support of my parents Margaret and Alan. They have always been my greatest teachers, best role models and biggest fans. They helped to fuel my sense of adventure and are my daily reminder that age is a state of mind, rather than an issue of time. I could not have wished for more perfect parents!

Beth Lyons and her family adopted me as one of their own, provided me with a home away from home and a introduced me to the joys of Progressive Rummy, Five Crowns and Scrabble. I can never thank them enough! My sister Kerry has always challenged me to do better, and has been there to help me through some very rough patches, which I appreciated more than words can express. My brother Jeff and sister-in-law Holly, have been ready to lend a helping hand or kind word when I needed it most, I am thankful that they are in my life. My nieces Amie and Kennedy and my nephew Everett can always be counted on for hours of fun and laughter and I look forward to watching them grow-up.

I would also like to acknowledge Jill Hardee, Erica Freeman, Paul Cunningham, Casey Nestor, Dr. Tandy McClung, the wonderful people at BlissBlissBliss, Jeff Altemus, Dr. Dawn Hunter, Tom Batchelor, past members of the Dey Lab and the staff of both the Neurobiology and Anatomy and Physiology Departments.

Lastly, I need to thank my friends here at WVU for all of the support they provided through the years! My soccer family and the “foreigners” helped me to remember that there was life outside of graduate school and have given me memories that will last a lifetime. I would never have made it through without them!

I would be remiss if I did not thank Keith Fulk. Through his efforts I was able to come to Morgantown and meet all of my wonder friends, and for that I will always be grateful!

Table of Contents

List of Figures

Chapter 1

Chapter 3

Chapter 4

Chapter 5

Chapter 6

Abbreviations

ANOVA	analysis of variance
BALF	bronchoalveolar lavage fluid
Beads	Fluorescent RetroBeads™
BDNF	brain derived neurotrophic factor
BrdU	bromo-deoxyuridine
BSA	bovine serum albumin
DAPI	4’6-diamindio-2-phenylindole
DMEM/F12	Dulbecco’s Modified Eagle Medium: Nutrient Mixture F12
EdU	5-ethynyl-2'-deoxyuridine
FA	filtered air
FACS	Fluorescence-activated cell sorting
FITC	fluorescein isothiocyanate
HBSS	Hank’s Balanced Salt Solution
NFD	nerve fiber density
NGF	nerve growth factor
NTs	neurotrophins
O_3	ozone
PBS	phosphate buffered saline
PD	postnatal day
PGP-9.5	protein gene product 9.5
ppm	parts per million
RPE	R-Phycoerythrin
SP	substance P

CHAPTER 1:

Introduction and Literature Survey

Childhood asthma is a growing concern in major cities around the world. Understanding how the airways change during development and how they are affected by exposures to environmental air pollutants, such as ozone, is becoming of greater concern. This chapter discusses afferent sensory innervation of the airways, the postnatal development of afferent airway sensory neurons in the nodose and jugular ganglia, as well as how irritant exposures in early life can alter airway growth and maturation. The information presented here will provide a basis for comprehending the experiments discussed later on.

1.1 Structure of Lower Airway

1.1.1 General Structure and Function

The lower airway is comprised of two functional regions: the conducting region and the respiratory region. The conduction region is made up of the trachea, main stem bronchi, lobar bronchi, segmental bronchi, bronchioles, and terminal bronchioles. This region functions to transport air to and from the respiratory region, as well as playing a role in the humidification and temperature regulation of the inspired air (131). The conducting airways also filter and remove particles from the air, and have antibacterial functions to aide in immunologic defense of the body. The respiratory region contains respiratory bronchioles, alveolar ducts, alveolar sacs and alveoli. This is the area of the airway where gas exchange occurs (131).

The conducting region can further be divided into extrapulmonary airway, outside of the lung parenchyma, and intrapulmonary airway, within the lungs. The trachea and main bronchi comprise the extrapulmonary airway, while the remaining bronchi and bronchioles, comprise the intrapulmonary airway (131).

1.1.2 Airway wall structure

Below the basement membrane of the respiratory epithelium is the lamina propria, which consists of connective tissues, blood and lymph vessels, resident immune cells including, macrophages and mast cells, and autonomic and sensory nerve fibers, some of which may be the intraepithelial fibers that have been detected in rats (3, 8). The trachea and main-stem bronchi contain rings of C-shaped cartilage that act to prevent the airway from collapsing. The cartilage is located on the anterior and lateral walls, and bands of smooth muscle run along the posterior wall connecting the two ends of cartilage. Below the lamina propria is the submucosal layer containing serous and mucous glands, additional sensory and autonomic nerve fibers, and

blood vessels. Surrounding the extrapulmonary airway is the adventia, which acts as support for the external wall of the airways, and contains blood vessels, nerves and lymphatic vessels.

As the airways transition from conducting to respiratory, the number of ciliated cells in the respiratory epithelium gradually decreases as do the number of mucous glands and goblet cells. Cartilage rings become plates and progressively decline, while smooth muscle becomes helical shaped and gradually increases until the level of the respiratory bronchioles. At the level of the terminal bronchioles, the epithelium is mostly comprised of cuboidal cells. In the respiratory region, the epithelium is simple squamous epithelium, which helps to facilitate gas exchange by decreasing the distance oxygen must diffuse to enter the pulmonary capillaries (~0.5μm). The dense network of pulmonary capillaries encircling each of the ~300 million alveoli creates a blood-air interface with a surface area of ~75m^2, further facilitating gas exchange by increasing the diffusion rate for oxygen (131).

1.1.3 Cellular Components

Lining the airway is respiratory epithelium, which is characterized by a pseudostratified columnar, ciliated epithelium with mucus-secreting goblet cells. The function of the respiratory epithelium is to expel particulate matter that becomes trapped in mucus coating the epithelium, which is moved upward by the beating of the cilia. The epithelial cells of the respiratory epithelium fall into two classifications: ciliated and non-ciliated cells (135). Brush cells, serous cells, mucous goblet cells, neuroendocrine cells (113), basal cells and Clara cells (found primarily in the smaller bronchioles) fall into the latter class. The distribution of these cells is not uniform through out the lower airways, and differs depending on the species (121).

Sensory innervation in the airways is a very important component in the maintenance of pulmonary homeostasis. Under normal physiological conditions, sensory afferent activation following noxious stimuli results in protective mechanisms designed to limit irritant infiltration in the airways. Understanding afferent sensory innervation in the airways is important because during chronic inflammatory and pathological states hypersensitivity of sensory afferents result in exaggerated and injurious reflexes.

1.2 Development of Fetal Lung and Airway Innervation

Mammalian fetal lung maturation begins during embryogensis, which in humans starts near the end of the 4th week of gestation. Lung growth then progress through three distinct phases the pseudoglandular, canalicular and saccular stages with continued development

extending well into postnatal life (reviewed in 119). These stages of lung development have been described in several different species including rats, primates, sheep and mice, though timing of the phases will differ depending on species specific gestational periods (reviewed in 119). Figure 1-1 shows a comparison of human and rat fetal lung development. In both rats and humans, postnatal life is a period of rapid and ongoing alveolarization, as the lung grows to meet increasing metabolic demands. The accelerated rate of rat postnatal development makes comparison with human postnatal development more challenging, however in general postnatal day (PD) 2-6 are roughly equivalent to the period from infancy through preschool age in humans. PD10-PD21 most closely correspond with school aged children through prepubescent teenagers, with early adolescences and the onset of puberty in humans equating to PD28-42 in rats (reviewed in 119).

Figure 1-1 (1)

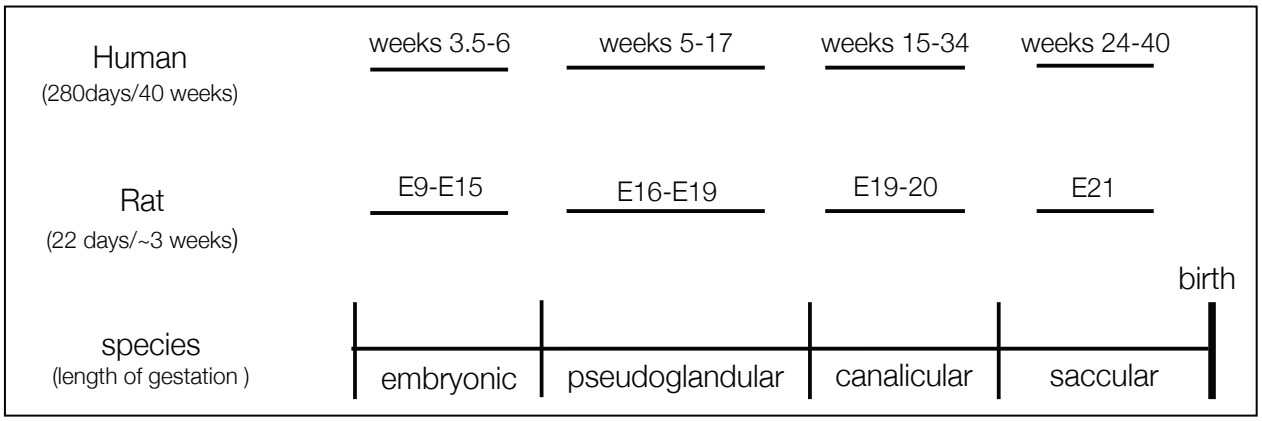

Figure 1-1. Comparison of human and rat fetal lung development. Timeline of prenatal lung development in humans and rats.

The following table (Table 1-1) highlights important developmental milestones in lung development including the formation of airway innervation (summarized from 136).

Table 1-1

Developmental Phase	Fetal Lung Development	Development of Airway innervation
Embryonic	* Formation of lung bud - Rapid division as series of tubules branching in dichotomous pattern - Branching morphogenesis of epithelial tubules (ET) forms proximal tracheobronchial tree	* Neural crest cells (NCC) migrate from foregut to lungs; differentiate - Will become intrinsic pulmonary neurons
Pseudoglandular	* Branching morphogenesis at peak levels - Segmental bronchi present - Critical developmental stage for formation of conducting airways * Lung lobular organization completed * Airway smooth muscle (ASM) laid down at sites of new growth of ET - ET elongation = formation of continuous ASM layer from trachea to growing tips *BY END OF PHASE*: * Branching virtually complete	* ET surrounded by interconnect precursor ganglia and loose nerve bundles * Vagus nerve trunks visible * Neural process connecting vagi to trachea and 1° bronchi likely contain afferent sensory fibers from vagal sensory ganglia * Functional innervation of ASM * Prolific amounts of vesicle traffic observed *BY END OF PHASE*: * Precursor neural tissues done proliferating * Differentiating into mature neurons
Canalicular	* Dramatic changes in lung morphology * Differentiation of pulmonary epithelium - Formation of future air/blood barrier * Surfactant synthesis * Arterioles of bronchial circulation appear adjacent to nerve trunks and bundles * Capillary canalization of lungs begins * Conducting and gas exchange regions are easily distinguished	* Spatial separation between ganglia due to increased lung growth * Ganglia become compact and spherical; migrate away from nerve bundles * Decrease in nerve bundle diameter * Mucosal innervation is established followed by mucosal vasculature * Appearance of neurotransmitters - SP^+ fibers in ASM (humans) - $CGRP^+$ fibers in epithelium (rat & humans), trachea, bronchial SM, and around blood vessels (rat)

Developmental Phase	Fetal Lung Development	Development of Airway innervation
Saccular	* Rapid lung growth - Peripheral airways form widened airspaces (saccules) * Significant expansion of gas exchange region * Bronchial mucosal circulation complexity increases - Developing into microvessel network * Arterioles follow nerve bundles	* Increased spatial separation between ganglia * Maturation of ganglia and nerves * Ganglia neurons and axons in nerve bundles are ensheathed by glial cell processes * Full expression of neurotransmitters * SP^+ C-fibers in epithelium (humans), lamina propria (rats)
Postnatal	* Branching morphogenesis * Enlargement of airways and gas exchange region * Alveolarization * Cellular differentiation - Continues throughout lifespan of all species - Tracheal epithelial differentiation is the most extensively characterized	*IN HUMANS* * Formation of basal nerve plexus - Composed of sensory and motor neurons - Lays just above basement membrane in epithelium * Nerves from plexus ascend between epithelial cells; arborize; spread varicose fibers over apical surface of epithelium - Varicose fibers terminate in one or more swollen varicosities containing SP & CRGP - These varicose fibers are C-fibers

1.3 Sensory Innervation of the Airway

1.3.1 Afferent Fiber Type

Numerous retrograde and anterograde tracing studies established that nearly the entirety of sensory innervation in the lower airway originates in the nodose and jugular ganglia located on the vagus nerves, with a smaller contribution coming from sensory fibers originating in the dorsal root ganglia(7, 14, 38, 66, 80, 127, 137). The trachea and main bronchi are innervated by fibers carried in the vagal branches of the superior laryngeal and recurrent laryngeal nerves. Smaller branches of the vagus nerve innervate the remaining portions of the airway (7, 14, 38, 66, 80, 127, 137). There are three types of afferent sensory nerve fibers typically identified in the airway below the larynx: slowly adapting stretch receptors (SAR), rapidly adapting stretch receptors (RAR) and bronchopulmonary C-fibers (31, 60).

1.3.2 Slowly Adapting Stretch Receptors

SARs are an example of afferent nerves that respond to non-harmful distention of the lung. This type of stretch-sensitive mechanosensor exhibits slow adaptation responses to sustained lung distention. While highly sensitive to mechanical stimulation SARs are relatively insensitive to chemical stimulation (60). Signal transduction in these nerve fibers is conducted via myelinated A-δ fibers that are between 1-5 μm in diameter and have conduction velocities between 5-30 m/s (90, 101).

1.3.3 Rapidly Adapting Stretch Receptors

RARs are stretch-sensitive mechanosensors that rapidly adapt during maintained inflation. They have the ability to readily respond to changes in the mechanical properties of the airways and are functionally important in airway defensive mechanisms, including initiation of the cough reflex (14). The greatest concentration of RARs in the airways, established through electrophysiological studies, is around the carina, hilum, and main bronchi, though they are found throughout the airways (60, 109). Upon activation, signals from RARs are also conducted via A-δ fibers, though generally they have slower conduction rates than SARs (17, 31). The most striking difference between RARs and SARs is that RARs are able to respond to a variety of stimuli including inhaled irritants and endogenous mediators of inflammation (14, 60).

1.3.4 Bronchopulmonary C-fibers

C-fibers are classified as such due to their slow conduction velocities (0.6-2 m/s; 45). The slow propagation of action potentials can be attributed to the fact that they are thin (0.1-1 um), unmyelinated nerve fibers. C-fibers are highly chemosensitive, and in nearly every mammalian respiratory system. They are vigorously activated by capsaicin, the active ingredient in peppers of the Capsicum family (14, 84).

Histological and functional studies carried out in cats found that thin, unmyelinated fibers account for the majority of afferent nerve fibers in the airways (4). Bronchopulmonary C-fiber is the collective terminology for two classifications of C-fiber afferents in the airways: bronchial C-fibers and pulmonary C-fibers. A distinction was made between the two, based on their anatomic location within the airway; bronchial C-fibers are found within the airway mucosa, pulmonary C-fiber afferents innervate intrapulmonary lung tissue. Bronchial C-fibers are most accessible to chemicals injected into the bronchial circulation, while chemicals injected into the pulmonary circulation were more readily accessed by pulmonary C-fibers (32, 83). This distinction however, is not generally made in rats, since the circulatory accessibility is not as clear in smaller animals (17, 61).

Though bronchial and pulmonary C-fibers have differing sensitivities and responses to lung inflation, activation of bronchopulmonary C-fibers evokes a multitude of defensive reflexes including rapid shallow breathing, apnea, bronchoconstriction, mucus secretion and extravasation of plasma and cough (31, 32, 35, 148).

1.3.5 Connection to Central Nervous System

These three types of afferent nerve fibers travel within the vagus nerves and synapse with second order neurons in the nucleus of the solitary tract (NTS). Though the three fiber types generally terminate in the middle and caudal portions of the NTS (73, 74), each fiber terminates in specific non-overlapping regions (34, 42, 79).

Appreciating the classifications of afferent sensory terminals in the airways and the different fiber types involved in signal transduction is an important first step toward understanding the consequences of hypersensitivity in these nerve terminals during chronic inflammatory states. It is also pertinent to elucidate what is happening in the soma of these afferents, upon activation.

1.4 Nodose & Jugular Ganglia Neurons

1.4.1 Anatomical Organization and Embryonic Origin

As previously mentioned, retrograde and anterograde tracing studies demonstrated that the majority of airway afferent sensory innervation is from C-fibers originating in the nodose and jugular ganglia (4, 7, 38, 66, 80, 127, 137). The nodose (inferior) and jugular (superior) ganglia, located on the left and right vagus nerves at the level of the jugular foramen (Figure 1-2), bilaterally innervate the lower airways, and also provide sensory afferent innervation for other viscera including the heart and GI tract. In rats and adult mice, the nodose and jugular ganglia are present as a single fused ganglion containing the jugular ganglion in the rostral portion, and the nodose ganglion in the caudal region (112).

Despite being in a single fused ganglion, nodose and jugular neurons exhibit differences in afferent fiber type, sensitivity to pharmacological stimuli and airway irritants, as well as variations in neuropeptide expression and reliance on differing growth factors during development. These differences might be attributed to the differing embryonic origin of the two ganglia. D'Amico-Martel and Noden (33) using the technique of embryonic tissue transplantation, illustrated that jugular ganglion neurons originate from the neural crest, while neurons in the nodose ganglion are derived from the third and fourth epibranchial placodes.

Figure 1-2 (2)

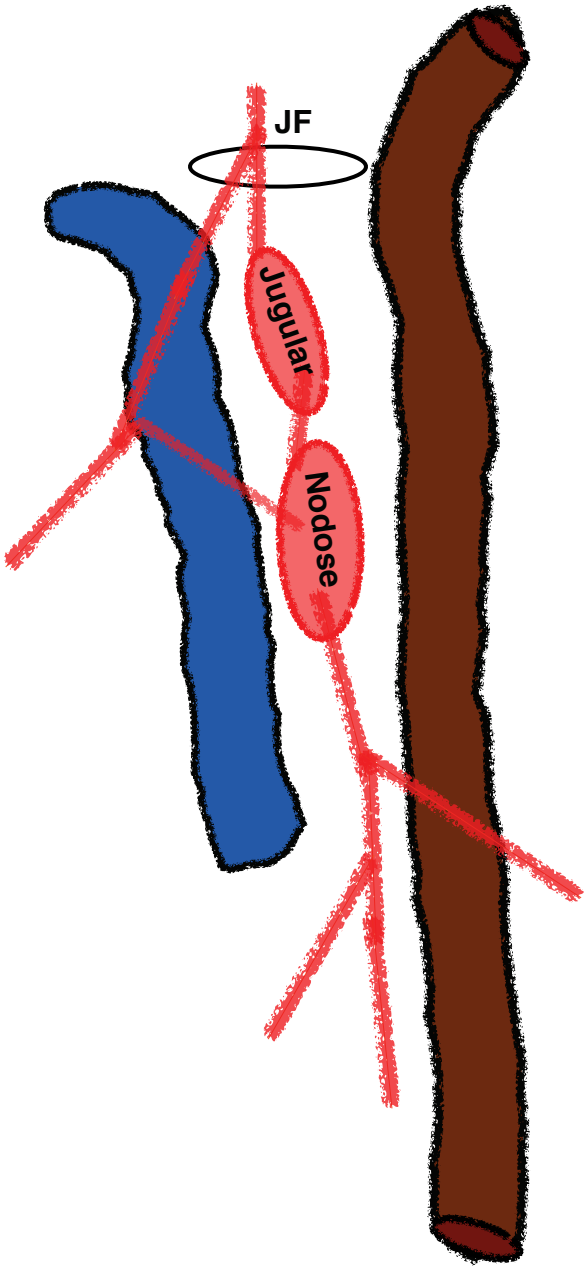

Figure 1-2. Anatomical orientation of the nodose and jugular ganglia.
The nodose (inferior) and jugular (superior) ganglia are on the vagus nerve (CNX) and are located just distal of the jugular foramen (JF) where the vagus nerve exits the brainstem.

1.4.2 Fiber Type and Sensitivity to Pharmacological Agents and Airway Irritants

Electrophysiological studies conducted in rats demonstrate that a large percentage (75%) of afferent fibers originating in the nodose ganglion are C-fibers (90). This work also determined that nodose ganglion neuron afferents have two additional classifications of fiber type. Both are myelinated, fast conducting A-type fibers (>10m/s conduction velocity); however, the fibers termed “Ah-type” had conduction velocities as low as 4m/s and had broad action potentials (>2ms) that closely resemble those of unmyelinated C-fibers. This study did not determine which tissue(s) these afferent fibers were innervating; however, this does not rule out the possibility of airway innervation via nodose C-fibers.

Another study using rats, attempting to discern if afferent fiber type of nodose and jugular neurons could be determined on the basis of morphological markers as well as response to pharmacological stimuli, utilized differences in the calcium transients of cultured nodose and jugular neurons following capsaicin treatment as a way to determine the associated fiber type (30). Capsaicin sensitivity, which was first characterized in dorsal root ganglion, is considered the standard identifying trait of nociceptive, C-fibers (150).

It was established that 58% of the viable neurons examined were capsaicin-sensitive. Of neurons exhibiting increased calcium transients in response to a low dose of capsaicin, 60% were nodose neurons, and 56% were jugular neurons (30). When a maximal dose of capsaicin was administered, jugular ganglion neurons were significantly more responsive than nodose ganglion neurons. From these results it was concluded that jugular ganglion neurons have a significantly higher sensitivity to capsaicin (30), which might indicate a higher concentration of C-fibers in jugular neurons. However, as in the Li and Schild (90) study, the site of innervation was not established, in this instance due to the use of cultured neurons.

As far as identifying afferent fiber type on the basis of morphology (soma size, surface texture, color, or shape), no morphological differences were noted between nodose and jugular neurons that responded to capsaicin treatment. However, it was documented that capsaicin-sensitive neurons in both ganglia were predominantly less than 35 μm in diameter, and that as soma size increased, the percentage of neurons responsive to capsaicin decreased (30).

A much clearer picture of the origin of sensory afferent nerve fibers in the airways exists in the guinea pig. Studies have ascertained that the afferent fibers of nodose ganglion neurons are myelinated, fast conducting A-δ fibers, whereas the afferent fibers of jugular ganglion neurons are an equal mixture of myelinated A-δ fibers and unmyelinated C-fibers (127). Though some differences have been noted, these findings have, for the most part, been generally accepted as the organization of vagal sensory afferents in other mammalian species.

An additional study employing electrophysiology examined the sensitivity of rat airway vagal afferents to pharmacological (capsaicin), irritant (cigarette smoke), and lung inflation stimuli in relation to conduction velocities (60). This investigation concluded that in rat airways, a small percentage of A-δ fibers are mildly stimulated by chemical irritants, but C-fibers are the primary chemosensitive afferents; however, location of the soma associated with the nerve fibers was not determined (60). Studies in guinea pigs have determined that nodose ganglion A-δ afferents are stimulated during allergic airway inflammatory events, resulting in increased tachykinin gene expression (49). Taken together with the findings of the Ricco et al. (127) study, the conclusions of the Ho et al. (60) study indicate that the A-δ fibers stimulated following irritant exposure could be afferents originating in nodose neurons.

1.4.3 Neuropeptide Expression

Neuropeptides constitute one of the largest families of extracellular messengers, and can act as neurotransmitters, hormones, and paracrine factors. In the airways the release of neuropeptides such as the tachykinin, substance P (SP), results in vasodilation, increased vascular permeability, and edema.

In primary cultures of rat postnatal nodose and jugular ganglia neurons, SP immunoreactive cell bodies were detected in soma from both ganglia (99). However, in cultures containing both nodose and jugular neurons the levels of SP produced and the numbers of immunoreactive cell bodies were 2-3 times higher when compared with primary cultures containing exclusively nodose ganglion neurons. Interestingly, the amount of SP measured in nodose only primary cultures increased the longer the neurons remained in culture (97).

SP immunoreactivity in nodose and jugular ganglia neurons of rats, mice and guinea pigs colocalizes with the neuropeptides neurokinin A (NKA) and calcitonin-gene related peptide (CGRP; 39, 58, 104). NKA is a potent bronchoconstrictor, while CGRP acts as a vasodilator. Though neurons in both ganglia express the same neuropeptides, the amounts of each varied between nodose and jugular neurons, which might account for the differing responses of nodose and jugular neurons following afferent nerve activation.

1.4.4 Growth Factor Reliance

Numerous studies in several different species have established that neurons in the nodose and jugular ganglion require different growth factors for their survival. MacLean et al. (98) found that adding the neurotrophin, nerve growth factor (NGF) to primary cultures of early postnatal nodose neurons had no effect on neuronal survival.

Work employing the use of transgenic mice has helped to elucidate trophic needs of vagal sensory neurons. Experiments using NGF -/- mice determined that there was no change in neuron number in nodose ganglia; however, there was a significant depletion in the number of jugular neurons, when compared to wild type controls (reviewed in 134). However, Forgie et al. (50), using a different NGF -/- transgenic model, found that there were a small population of nodose neurons that were supported by NGF.

When brain derived neurotrophic factor (BDNF) knock out mice were examined, significant losses in nodose neurons were detected, while the number of jugular ganglia neurons remained unchanged (reviewed in 134). A group using transgenic mice that over-express BDNF found that the number of neurons in the nodose ganglion was selectively increased, while the number of neurons in other ganglia did not change in number (86).

Nodose and jugular ganglia neurons have differing trophic support requirements, as well as differences in embryonic origin, neuropeptide expression and sensitivity to inhaled irritants. These dissimilarities may all be important factors in determining the severity of the response that is generated upon activation of airway afferent nerves.

1.5 Afferent Nerve Action

The afferent sensory nerve fibers in the airways, can be activated by a multitude of noxious stimuli including: capsaicin, cigarette smoke, ozone, allergens, bradykinin, low pH, ether, formalin, SO_2, (TDI), histamine, methylcholine, prostaglandins, leukotrienes, cold air, and hypertonic saline (reviewed in 94, 100). The action potentials generated as a result of depolarizing events at sensory nerve endings are propagated toward the central nervous system, as well as through the antidromic conduction of impulses through terminal arborizations of sensory afferent nerve fibers. The peripheral signals being conducted at the collateral branches to unstimulated nerve endings have been termed an axon reflex (10).

Information arriving at the NTS in the brainstem, from nodose and jugular afferents in the airways, elicits differing responses depending on which receptor type (SAR, RAR, C-fiber) was activated in the airways(78). Signals conducted via SARs affect the Breuer-Hering reflex. RAR stimulation initiates gasping and cough reflexes. C-fiber afferent transmission results in rapid, shallow breathing and apnea (78).

Within the airways, antidromic stimulation of nociceptive afferent fibers initiates neuropeptide release from sensory nerve endings, leading to neurogenic inflammation in the airways (10). A number of physiological and pathological functions in the airways are mediated by nodose and jugular sensory afferents and the neuropeptides released from these nerve fibers.

1.6 Neuropeptides in the Airway

SP was first described in 1931 by von Euler & Gaddum in the brain and intestine as a smooth muscle-contracting substance, and a vasodepressor (147). SP is an 11-amino acid peptide (29) localized in nodose and jugular neurons as well as in peripheral nerve fibers within and beneath the respiratory epithelium, amongst bundles of smooth muscle, encircling blood vessels and submucosal glands, and in close relationship to resident immune cells (72). The synthesis of SP in nodose and jugular ganglia neurons is the result of preprotachykinin-1 gene expression. This gene contains four different transcripts capable of producing SP, thereby increasing the probability that SP will be generated upon gene expression (124). Helke et al. (58) found that post-translation

modifications of SP occur during peptide storage in vesicles and axonal transport to nerve terminals.

SP exerts its effects in the airway through preferentially binding with neurokinin 1 (NK-1) receptors, though it may also act through the NK-2 and NK-3 receptors (116). In the lower airways receptors have been localized on the epithelium, small blood vessels and glands in the lamina propria (19, 111, 118, 129). Binding of SP with NK-1 initiates receptor-mediated inflammatory responses characterized by plasma extravasation, vasodilation and mucus secretion (8, 68, 96). The actions of SP in the airways are terminated through rapid degradation by the tissue peptidase neutral endopeptidase and angiotensin-converting enzymes, which have been localized to tissues that also have NK-1 receptors (19, 75, 111, 118, 129). Cigarette smoke-induced neurogenic inflammation in rat has been show to be partially mediated by SP NK-1 interaction, characterized by plasma extravasation and goblet cell exocytosis (108). NK-1 receptors are localized to endothelial cells in postcapillary venules and SP binding with NK-1 results in endocytosis of the ligand receptor complex. Vagal stimulation increased the number of NK-1 immunoreactive endothelial cell endosomes, indicating that SP may have a direct effect on endothelial cells (20). This direct effect of SP on plasma extravasation in endothelial cells of the postcapillary venules in rat trachea was later demonstrated through i.v. injections of SP. Within 20 sec of injection intracellular gaps appeared between endothelial cells, peaking in numbers after 1 min, and then decreasing with a half life of 3.2 min (106). The gaps between endothelial cells accounted for ~ 3% of the surface area of postcapillary venules.

SP release from sensory afferents in the airways has also been shown to modulate immune cell functions, including T-lymphocytes proliferation, macrophage activation, enhanced macrophage and neutrophil phagocytosis, lymphocyte, neutrophil, eosinophil, and monocyte chemotaxis, enhanced cytokine release from activated monocytes and endothelial cell proliferation (9, 28, 55, 72, 81, 102, 115, 139).

Under normal physiological conditions the actions of SP described here are important in protecting the airways when noxious stimuli are encountered. It is when pathological states induced by chronic inflammatory events, that the effects of SP have detrimental consequences.

1.7 Neurotrophins

The neurotrophins (NTs) are a group of structurally related proteins whose primary function is regulating the survival and differentiation of neurons in both the peripheral and central nervous system (24). The group includes NGF, BDNF, neurotrophin-3 (NT-3), and neurotrophin 4/5 (NT-4/5). NTs act primarily as target-derived paracrine and autocrine trophic factors (125), and are released from nerve-associated cells such as glial cells, Schwann cells and fibroblasts (88, 89).

As previously discussed, the NTs, NGF and BDNF, are responsible for the survival of nodose and jugular ganglia neurons, and have been shown to differentially affect the capsaicin-sensitivity of airway C-fibers in vitro (151). To exert their effects on particular neuronal subsets, NGF and BDNF act through specific high affinity (KD10-11) tropomyosin-related kinase (Trk) receptor tyrosine kinases. NGF preferentially binds to TrkA, BDNF and NT-4/5 to TrkB, and NT-3 to TrkC (114). NTs can also bind the low affinity (KD10-9) pan-neurotrophin receptor p75NT(82).

Studies have determined that NTs also act as mediators of inflammation, by altering the expression of neuropeptides that are released from sensory nerve terminals and through direct interactions with immune cells in both human and animal models (18, 21). Tachykinin production in nodose and jugular ganglia neurons is increased when levels of NGF and BDNF are increased (65, 91, 97, 138). The respiratory epithelium and immune cells, including mast cells, T and B-lymphocytes, and activated macrophages that are present in or recruited to the airways during inflammatory events, produce and release NTs (21, 22, 43, 76, 87, 141, 144). The interaction of NTs, neuropeptides, and immune cells in the airways leads to inflammation that is characteristically seen in asthma.

1.8 Neurogenic Inflammation

Neurogenic inflammation is the term coined by Jancso et al (69), to describe the increase in vascular permeability, plasma extravasation, and tissue swelling occurring in the skin and eyes when sensory nerves were stimulated by topical administration of irritants or by antidromic electrical stimulation (68, 69). Lundberg et al (95) were the first group to describe neurogenic inflammation in the airway. They found that inhalation of cigarette smoke, administration of capsaicin or electrical stimulation of the vagus nerve,

induced an increase in plasma protein extravasation in the airways. The effects were abolished following pretreatment with capsaicin or a SP antagonist, and it was noted that exogenous SP given following depletion of SP from sensory nerve fibers elicited the same effects as the noxious stimuli. These results led them to hypothesize that SP released from capsaicin-sensitive nerve fibers mediates neurogenic inflammation in the airways (93, 96).

When a noxious stimulus such as ozone, cigarette smoke, or house dust mite allergen is introduced into the airways of a sensitized subject many processes are initiated. Cells in the respiratory epithelium increase mucus secretion and in some cases epithelial cell sloughing is noted. The epithelium releases BDNF, NGF, other growth factors, and inflammatory cytokines, which activate and recruit immune cells to the airway. As well, airway wall thickness increases through smooth muscle hyperplasia and a thickening of the lamina reticularis. Activated T-cells release mediators (cytokines, NTs) that cause goblet cell metaplasia, along with activating B-cells and mast cells. Mast cell degranulation results in the release of histamine, which acts on the epithelial cells and goblet cells, as well as activating sensory nerve terminals initiating an axon reflex. The antidromic and central signaling in nodose and jugular sensory afferents leads to bronchoconstriction, vasodilation and increased vascular permeability through the actions of neuropeptides released at terminal arborizations (Figure 1-3). The increase in SP levels in the airways also stimulates mast cell activation. The release of NTs from immune cells and the epithelium causes an increase in nodose and jugular neuron SP production and release (51).

Several different studies have shown that neurotrophins can mediate neuronal plasticity in inflammatory conditions, such as asthma (40, 41, 91), which has only fueled the search for ways to translate these basic science discoveries into clinically relevant treatments.

Figure 1-3 (3)

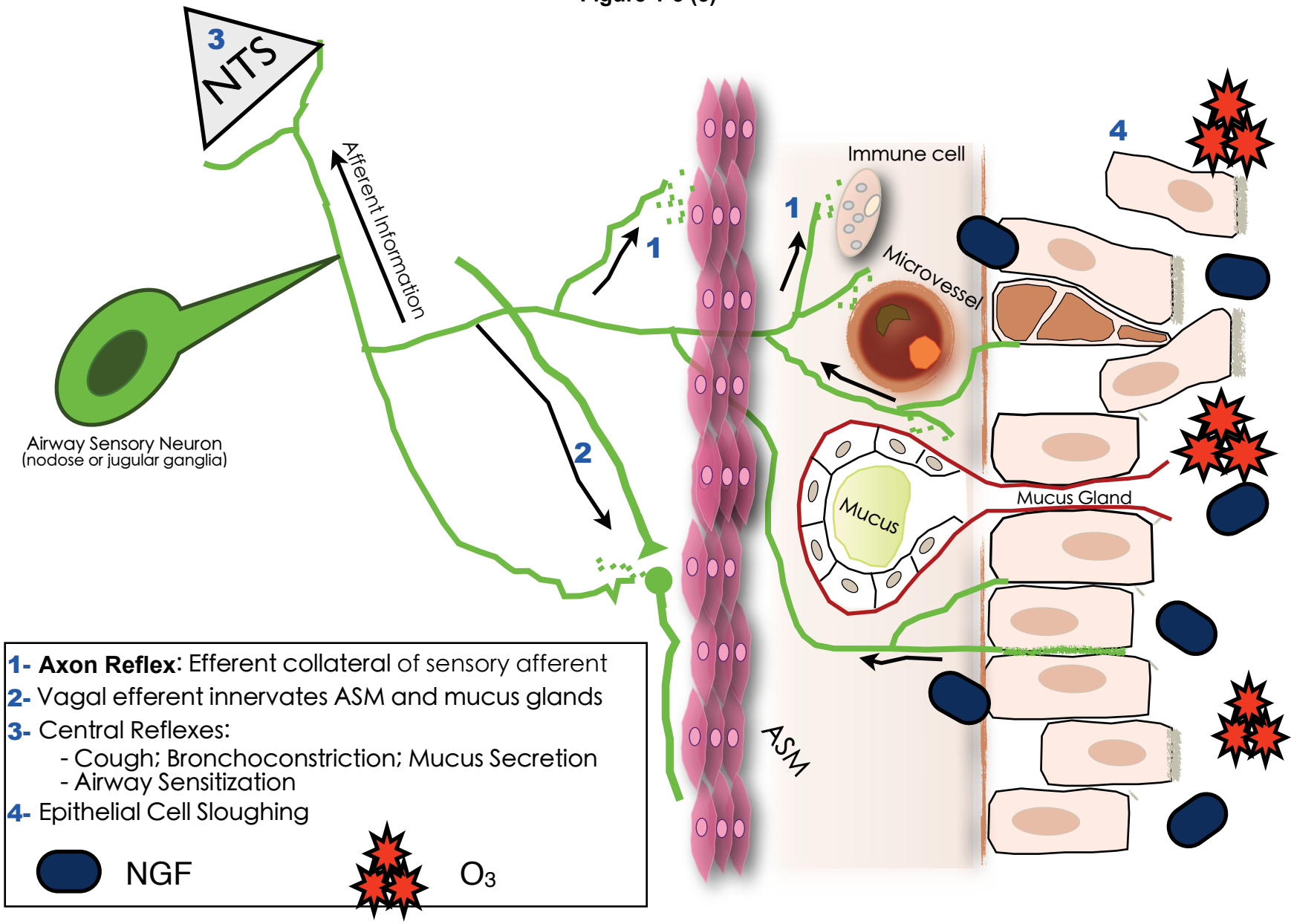
3
NTS
Afferent Information
Airway Sensory Neuron
(nodose or jugular ganglia)
1
2
Immune cell
1
Microvessel
4
Mucus
Mucus Gland
ASM
1- Axon Reflex: Efferent collateral of sensory afferent
2- Vagal efferent innervates ASM and mucus glands
3- Central Reflexes:
- Cough; Bronchoconstriction; Mucus Secretion
- Airway Sensitization
4- Epithelial Cell Sloughing
NGF
O3

1.9 Neurotrophins and Respiratory Disorders

Although neurotrophins were initially thought to be involved exclusively in the survival and maintenance of neuronal populations, as is evident from the explanation of neurogenic inflammation above, neurotrophins have a more diverse role, particularly in pathological conditions such as asthma. Asthma is characterized by airway inflammation, bronchoconstriction, and airway obstruction and is associated with altered neuronal control of the airways (24, 44, 48).

In searching for the role that neurotrophins have in asthma pathogenesis, several interesting discoveries have been made by examining human asthmatics. Increased levels of neurotrophins were noted in the bronchoalveolar lavage fluid (BALF) of allergic asthma patients following allergen challenge (146). Another study found that NGF is increased in the serum of asthma patients (18); this increase was continuous and independent of a recent asthma attack.

The role of neurotrophins in other airway inflammatory disorders has been examined using animal models. Respiratory syncytial virus (RSV) infects nearly all children before they are two years old (54), and it is thought to be a risk factor for developing asthma later in life (117). It has been demonstrated that NGF is increased in the lungs following RSV infection (63). This same group showed that after pretreatment with anti-NGF antibodies, the neurogenic inflammation seen following RSV infection was abolished. In addition, NGF is released in the airways following irritant exposures (27, 64, 130, 145, 149, 152), and neurotrophins can enhance airway responses to inflammatory stimuli (15, 16, 122, 123). In an allergic airway inflammation model it was shown that treatment with BDNF or anti-BDNF antibodies did not affect inflammation (23). However, it was demonstrated that treatment with exogenous BDNF increased airway responsiveness, and that treatment with anti-BNDF antibodies attenuated the hyperresponsiveness seen in ovalbumin-sensitized mice (23). This indicates that NGF and BDNF may be working in concert to produce the symptoms seen in asthma patients. As neurotrophins have a role in inducing tachykinin gene expression (91), and act as mediators of inflammation, attempting to elucidate the exact role that NGF has in asthma and other inflammatory respiratory disorders is of great importance.

1.10 Ozone and Early Life Exposures

1.10.1 Ozone (O_3)

Ground level O_3 is a pollutant and a main component in urban photochemical smog. It poses a “significant health risk” to susceptible populations, particularly asthmatic children(1). Ground level O_3 is the product of a sunlight-catalyzed chemical reaction between volatile organic compounds (VOC) and nitrogen oxides (NOx) present in the air (25). Sources of VOC and NOx include gasoline vapors, and automobile exhaust as well as industrial manufacturing and electric utilities emissions (25). O_3 can act to remove hydrocarbons like those found in gasoline vapors, from the atmosphere; however, the products of that reaction are also key components of photochemical smog (25). This type of air pollution is present in nearly every city, though it more prevalent urban areas located in warm, sunny, dry climates where warm upper air can prevent vertical circulation (6). Metropolitan areas such as Houston and Los Angeles with a substantial number of vehicles on the road each day are examples of O_3-prone areas in the United States (1, 2).

O_3 acts as an oxidizing agent and inhalation of O_3 can cause clinical symptoms ranging from mild headaches and burning eyes, to shortness of breath, chest pain, wheezing, and coughing (107). O_3 exposure can also exacerbate emphysema and asthma symptoms, augment lung inflammation and cause attenuated lung function (13, 57). These effects can be both transient and prolonged. Increased numbers of emergency room admissions for respiratory illnesses, like asthma, have been correlated with high concentration of ground level O_3 (26, 128, 142, 154). A recent article by Jerret et al., described a significant increase in the rates of respiratory related deaths following long-term exposure to increasing concentration of O_3 (70). This study also revealed that the risk of death from a respiratory related illness or disease is 30% more likely for people living in metropolitan areas prone to the highest levels of O_3 when compared to areas with the lowest measured O_3 concentrations (70).

To demonstrate the physiological effects of O_3 exposure studies in human subjects (62) and numerous animals models including rats (46), mice (110), dogs (105), and guinea pigs (53) and have been conducted. O_3 exposure causes pathological changes including damage to airway epithelium, airway hyperresponsiveness (AHR) and pulmonary inflammation (12, 56, 85, 140, 153). Neutrophil influx in the trachea and

bronchoalveolar space and increased serum protein levels in lavage fluid are characteristic inflammatory responses observed following exposure to O_3 (5, 11, 36, 37, 77, 120). A characteristic feature of AHR, increased airway smooth muscle (ASM) response to broncho-constricting agonists, is also noted (59). Though the downstream effects of O_3 exposure such as the induction and release of neurotrophins and tachykinins are well documented, the exact mechanisms responsible remain unclear.

1.10.2 Early Life Exposures

Emerging evidence in both human and animals models of asthma and other respiratory disorders shows that early life exposures can alter airway responses to noxious-stimuli later in life. Early life ozone exposures in mice have been shown to have detrimental effects on airway functions and are known to cause AHR (46, 132, 155), a defining feature of asthma. Studies examining the effects of early life ozone exposure on postnatal rats have revealed that multi-day O_3 exposures between PD1 and PD15 result in an increased percentage of SP immunoreactive nerve fibers in ASM 24 hrs after O_3 when compared with controls (67). No differences were found in animals that were exposed to ozone later in postnatal life. As part of the same investigation Hunter et al., demonstrated that combining early life (PD4) O_3 exposures with a subsequent exposure later in postnatal life (PD28) resulted in significant increases in SP innervation in ASM, as well as increased lung resistance and decreased dynamic compliance when compared to values measured from rat pups initially exposed to O_3 on PD21 (67). Rats exposed to ozone between postnatal days (PDs) 2 and 6 and then exposed to either filtered air or ozone on PD 28, had increased percentages of SP immunoreactive nerve fibers in airway smooth muscle when compared to unexposed animals or rat pups exposed later in life (67).

In studies examining the effects of early life exposure to sidestream cigarette smoke, mice were exposed to filtered air or cigarette smoke for 10 consecutive days, beginning at three different time points, i.e., gestational day (GD) 7, PD2 or PD21, and then exposed to cigarette smoke on PD59 (152). Groups initially exposed to cigarette smoke on either GD7 or PD2 had significantly altered lung function, increased percentage of SP immunoreactive nerve fibers in the airways, and increased levels of NGF in lavage fluid measured 24 hrs after reexposure to sidestream smoke on PD 59, when compared to mice initially given cigarette smoke on PD21 or those exposed to only FA at GD7 or PD2 (152). Research done in neonatal rats has found that side-stream

tobacco smoke exposure during the gestational and postnatal periods produced reductions in lung functions at eight weeks of age even when smoke exposure was terminated at PD 21 (71).

These studies point towards the possibility of the existence of a critical period during the postnatal development of the airways, when noxious stimuli can more significantly affect normal defensive airway functions regulated by sensory nerve afferents, causing them to become increasingly sensitive to later insults. To examine the possible role of NGF in this proposed critical period, Hunter et al. (64) first measured the concentration of NGF in the bronchoalveolar lavage fluid, and relative levels of NGF mRNA in tracheal epithelial cells, from animals exposed to ozone at PD 6 and then reexposed on PD 28. On PD 29, both NGF protein in lavage fluid and relative NGF mRNA levels were significantly increased over all other groups, including animals that were initially exposed to ozone on PD 21. In a second set of experiments, animals were administered NGF intratracheally at PD 6 and then exposed to ozone on PD 28. Increases in SP immunoreactivity in both the nerve fibers innervating the extrapulmonary smooth muscle, and cell bodies of airway specific neurons in vagal ganglia were noted (64). This study demonstrates that NGF released in the airways during early life may play a key role in the development of the afferent nerve hypersensitivity that is seen following ozone exposure later in life.

Studies examining the effects of early life exposures in humans have found that early respiratory infections correlate with persistent wheezing and asthma in children (103) and severe viral infections in infancy are associated with asthma in teens (133). It has also been shown that in children, ozone can cause increases in asthmatic symptoms even at concentrations below the U.S. Environmental Protection Agency standard (52), and hospital admissions for asthma increase on days of high ambient ozone concentrations (47, 143). Studies have found that high ozone levels in Mexico City have been positively correlated with infant mortality (92). Inhalation of environmentally relevant levels of ozone causes increased specific airway resistance and breathing frequency and a decrease in tidal volume, forced vital capacity and total lung capacity (13, 57). One study was conducted to examine if air pollution can influence the airway inflammation and decreased lung function seen in children with mild asthma, who live in urban centers (126). The children were moved from the urban area to a rural area in an attempt to discern if decreased air pollution would result in an attenuation of

their asthma symptoms. Lung function, along with inflammatory biomarkers, such as numbers of nasal eosinophils were measured before and seven days after the move to the rural area. Rapid decreases in airway inflammation and marked improvement in lung function were noted within the seven-day period of being in an area of better air quality (126).

1.11 Conclusions

Taken together, these studies demonstrate not only the immense influence that early life exposures have on developing airways, but the need for a clearer understanding of the underlying mechanisms at work in the process of airway neural remodeling.

References

1. United States Environmental Protection Agency. Ozone. [Webpage]. August, 19, 2010 [cited 2011 July 26]. Available from: http://www.epa.gov/ozone.

2. United States Environmental Protection Agency. Air quality criteria for ozone and related photochemical oxidants. Research Triangle Park, NC: National Center for Environmental Assesment-RTP Office; 2006.

3. Adriaensen D, Timmermans JP, Brouns I, Berthoud HR, Neuhuber WL, Scheuermann DW. Pulmonary intraepithelial vagal nodose afferent nerve terminals are confined to neuroepithelial bodies: An anterograde tracing and confocal microscopy study in adult rats. *Cell Tissue Res* 1998;293:395-405.

4. Agostoni E, Chinnock JE, De Daly MB, Murray JG. Functional and histological studies of the vagus nerve and its branches to the heart, lungs and abdominal viscera in the cat. *J Physiol* 1957;135:182-205.

5. Aris RM, Christian D, Hearne PQ, Kerr K, Finkbeiner WE, Balmes JR. Ozone-induced airway inflammation in human subjects as determined by airway lavage and biopsy. *Am Rev Respir Dis* 1993;148:1363-1372.

6. Baird C, editor. Environmental Chemistry. 2nd edition, New York: W.H. Freeman and Co.; 1999.

7. Baluk P, Gabella G. Innervation of the guinea pig trachea: A quantitative morphological study of intrinsic neurons and extrinsic nerves. *J Comp Neurol* 1989;285:117-132.

8. Baluk P, Nadel JA, McDonald DM. Substance P-immunoreactive sensory axons in the rat respiratory tract: A quantitative study of their distribution and role in neurogenic inflammation. *J Comp Neurol* 1992;319:586-598.

9. Bar-Shavit Z, Goldman R, Stabinsky Y, Gottlieb P, Fridkin M, Teichberg VI, Blumberg S. Enhancement of phagocytosis - a newly found activity of substance P residing in its n-terminal tetrapeptide sequence. *Biochem Biophys Res Commun* 1980;94:1445-1451.

10. Barnes PJ. Neural control of human airways in health and disease. *Am Rev Respir Dis* 1986;134:1289-1314.

11. Basha MA, Gross KB, Gwizdala CJ, Haidar AH, Popovich J, Jr. Bronchoalveolar lavage neutrophilia in asthmatic and healthy volunteers after controlled exposure to ozone and filtered purified air. *Chest* 1994;106:1757-1765.

12. Beckett WS. Ozone, air pollution, and respiratory health. *Yale J Biol Med* 1991;64:167-175.

13. Beckett WS, McDonnell WF, Horstman DH, House DE. Role of the parasympathetic nervous system in acute lung response to ozone. *J Appl Physiol* 1985;59:1879-1885.

14. Belvisi MG. Sensory nerves and airway inflammation: Role of a delta and C-fibres. *Pulm Pharmacol Ther* 2003;16:1-7.

15. Bennedich Kahn L, Gustafsson LE, Olgart Hoglund C. Brain-derived neurotrophic factor enhances histamine-induced airway responses and changes levels of exhaled nitric oxide in guinea pigs in vivo. *Eur J Pharmacol* 2008;595:78-83.

16. Bennedich Kahn L, Gustafsson LE, Olgart Höglund C. Nerve growth factor enhances neurokinin A-induced airway responses and exhaled nitric oxide via a histamine-dependent mechanism. *Pulmonary Pharmacology & Therapeutics* 2008;21:522-532

17. Bergen DR, Peterson DF. Identification of vagal sensory receptors in the rat lung: Are there subtypes of slowly adapting receptors? *J Physiol* 1993;464:681-698.

18. Bonini S, Lambiase A, Angelucci F, Magrini L, Manni L, Aloe L. Circulating nerve growth factor levels are increased in humans with allergic diseases and asthma. *Proc Natl Acad Sci U S A* 1996;93:10955-10960.

19. Borson DB. Roles of neutral endopeptidase in airways. *Am J Physiol* 1991;260:L212-225.

20. Bowden JJ, Garland AM, Baluk P, Lefevre P, Grady EF, Vigna SR, Bunnett NW, McDonald DM. Direct observation of substance P-induced internalization of neurokinin 1 (NK1) receptors at sites of inflammation. *Proc Natl Acad Sci U S A* 1994;91:8964-8968.

21. Braun A, Appel E, Baruch R, Herz U, Botchkarev V, Paus R, Brodie C, Renz H. Role of nerve growth factor in a mouse model of allergic airway inflammation and asthma. *Eur J Immunol* 1998;28:3240-3251.

22. Braun A, Lommatzsch M, Mannsfeldt A, Neuhaus-Steinmetz U, Fischer A, Schnoy N, Lewin GR, Renz H. Cellular sources of enhanced brain-derived neurotrophic factor production in a mouse model of allergic inflammation. *Am J Respir Cell Mol Biol* 1999;21:537-546

23. Braun A, Lommatzsch M, Neuhaus-Steinmetz U, Quarcoo D, Glaab T, McGregor GP, Fischer A, Renz H. Brain-derived neurotrophic factor (BDNF) contributes to neuronal dysfunction in a model of allergic airway inflammation. *Br J Pharmacol* 2004;141:431-440.

24. Braun A, Lommatzsch M, Renz H. The role of neurotrophins in allergic bronchial asthma. *Clin Exp Allergy* 2000;30:178-186.

25. Brown TL, Lemay HE, Bursten BE, Murphy CJ, Woodward P, editors. Chemistry: Central science.11th edition: Prentice Hall; 2007.

26. Burnett RT, Dales RE, Raizenne ME, Krewski D, Summers PW, Roberts GR, Raad-Young M, Dann T, Brook J. Effects of low ambient levels of ozone and sulfates on the frequency of respiratory admissions to ontario hospitals. *Environ Res* 1994;65:172-194.

27. Cardenas S, Scuri M, Samsell L, Ducatman B, Bejarano P, Auais A, Doud M, Mathee K, Piedimonte G. Neurotrophic and neuroimmune responses to early-life pseudomonas aeruginosa infection in rat lungs. *Am J Physiol Lung Cell Mol Physiol* 2010;299:L334-344.

28. Carolan EJ, Casale TB. Effects of neuropeptides on neutrophil migration through noncellular and endothelial barriers. *J Allergy Clin Immunol* 1993;92:589-598.

29. Chang MM, Leeman SE, Niall HD. Amino-acid sequence of substance P. *Nat New Biol* 1971;232:86-87.

30. Chung E, Gu Q, Kwong K, Arden WA, Lee LY. Comparison of capsaicin-evoked calcium transients between rat nodose and jugular ganglion neurons. *Auton Neurosci* 2002;97:83-88.

31. Coleridge HM, Coleridge JC. Pulmonary reflexes: Neural mechanisms of pulmonary defense. *Annu Rev Physiol* 1994;56:69-91.

32. Coleridge JC, Coleridge HM. Afferent vagal C fibre innervation of the lungs and airways and its functional significance. *Rev Physiol Biochem Pharmacol* 1984;99:1-110.

33. D'Amico-Martel A, Noden DM. Contributions of placodal and neural crest cells to avian cranial peripheral ganglia. *Am J Anat* 1983;166:445-468.

34. Davies RO, Kubin L. Projection of pulmonary rapidly adapting receptors to the medulla of the cat: An antidromic mapping study. *J Physiol* 1986;373:63-86.

35. Davis B, Roberts AM, Coleridge HM, Coleridge JC. Reflex tracheal gland secretion evoked by stimulation of bronchial C-fibers in dogs. *J Appl Physiol* 1982;53:985-991.

36. DeLorme MP, Yang H, Elbon-Copp C, Gao X, Barraclough-Mitchell H, Bassett DJ. Hyperresponsive airways correlate with lung tissue inflammatory cell changes in ozone-exposed rats. *J Toxicol Environ Health A* 2002;65:1453-1470.

37. Devlin RB, McDonnell WF, Becker S, Madden MC, McGee MP, Perez R, Hatch G, House DE, Koren HS. Time-dependent changes of inflammatory mediators in the lungs of humans exposed to 0.4 ppm ozone for 2 hr: A comparison of mediators found in bronchoalveolar lavage fluid 1 and 18 hr after exposure. *Toxicol Appl Pharmacol* 1996;138:176-185.

38. Dey RD, Altemus JB, Zervos I, Hoffpauir J. Origin and colocalization of CGRP- and SP-reactive nerves in cat airway epithelium. *J Appl Physiol* 1990;68:770-778.

39. Dinh QT, Mingomataj E, Quarcoo D, Groneberg DA, Witt C, Klapp BF, Braun A, Fischer A. Allergic airway inflammation induces tachykinin peptides expression in vagal sensory neurons innervating mouse airways. *Clin Exp Allergy* 2005;35:820-825.

40. Dmitrieva N, Shelton D, Rice AS, McMahon SB. The role of nerve growth factor in a model of visceral inflammation. *Neuroscience* 1997;78:449-459.

41. Donnerer J, Schuligoi R, Stein C. Increased content and transport of substance P and calcitonin gene-related peptide in sensory nerves innervating inflamed tissue: Evidence for a regulatory function of nerve growth factor in vivo. *Neuroscience* 1992;49:693-698.

42. Donoghue S, Garcia M, Jordan D, Spyer KM. The brain-stem projections of pulmonary stretch afferent neurones in cats and rabbits. *J Physiol* 1982;322:353-363.

43. Ehrhard PB, Erb P, Graumann U, Otten U. Expression of nerve growth factor and nerve growth factor receptor tyrosine kinase Trk in activated CD4-positive T-cell clones. *Proc Natl Acad Sci U S A* 1993;90:10984-10988.

44. Ellis JL, Undem BJ. Antigen-induced enhancement of noncholinergic contractile responses to vagus nerve and electrical field stimulation in guinea pig isolated trachea. *J Pharmacol Exp Ther* 1992;262:646-653.

45. Erlanger J, Gasser HS, Bishop GH. The compound nature of the action current of nerve as disclosed by the cathode ray oscillograph. *Am J Physiol* 1924;70:624-666.

46. Evans TW, Brokaw JJ, Chung KF, Nadel JA, McDonald DM. Ozone-induced bronchial hyperresponsiveness in the rat is not accompanied by neutrophil influx or increased vascular permeability in the trachea. *Am Rev Respir Dis* 1988;138:140-144.

47. Fauroux B, Sampil M, Quenel P, Lemoullec Y. Ozone: A trigger for hospital pediatric asthma emergency room visits. *Pediatr Pulmonol* 2000;30:41-46.

48. Fischer A, Hoffmann B. Nitric oxide synthase in neurons and nerve fibers of lower airways and in vagal sensory ganglia of man. Correlation with neuropeptides. *American Journal of Respiratory and Critical Care Medicine* 1996;154:209-216

49. Fischer A, McGregor GP, Saria A, Philippin B, Kummer W. Induction of tachykinin gene and peptide expression in guinea pig nodose primary afferent neurons by allergic airway inflammation. *J Clin Invest* 1996;98:2284-2291.

50. Forgie A, Kuehnel F, Wyatt S, Davies AM. In vivo survival requirement of a subset of nodose ganglion neurons for nerve growth factor. *The European Journal of Neuroscience* 2000;12:670-676

51. Galli SJ, Tsai M, Piliponsky AM. The development of allergic inflammation. *Nature* 2008;454:445-454.

52. Gent JF, Triche EW, Holford TR, Belanger K, Bracken MB, Beckett WS, Leaderer BP. Association of low-level ozone and fine particles with respiratory symptoms in children with asthma. *JAMA* 2003;290:1859-1867.

53. Gordon T, Venugopalan CS, Amdur MO, Drazen JM. Ozone-induced airway hyperreactivity in the guinea pig. *J Appl Physiol* 1984;57:1034-1038.

54. Hall CB. Respiratory syncytial virus. In: Feigin RD, Cherry JD, editors. Textbook of pediatric infectious diseases, 4th ed. Philadelphia: WB Saunders Co; 1998. p. 2087.

55. Hartung HP, Wolters K, Toyka KV. Substance P: Binding properties and studies on cellular responses in guinea pig macrophages. *J Immunol* 1986;136:3856-3863.

56. Hazbun ME, Hamilton R, Holian A, Eschenbacher WL. Ozone-induced increases in substance P and 8-epi-prostaglandin F2 alpha in the airways of human subjects. *Am J Respir Cell Mol Biol* 1993;9:568-572.

57. Hazucha MJ. Relationship between ozone exposure and pulmonary function changes. *J Appl Physiol* 1987;62:1671-1680.

58. Helke CJ, Krause JE, Mantyh PW, Couture R, Bannon MJ. Diversity in mammalian tachykinin peptidergic neurons: Multiple peptides, receptors, and regulatory mechanisms. *FASEB J* 1990;4:1606-1615.

59. Hiltermann TJ, Stolk J, Hiemstra PS, Fokkens PH, Rombout PJ, Sont JK, Sterk PJ, Dijkman JH. Effect of ozone exposure on maximal airway narrowing in non-asthmatic and asthmatic subjects. *Clin Sci (Lond)* 1995;89:619-624.

60. Ho CY, Gu Q, Lin YS, Lee LY. Sensitivity of vagal afferent endings to chemical irritants in the rat lung. *Respir Physiol* 2001;127:113-124.

61. Hong JL, Kwong K, Lee LY. Stimulation of pulmonary C fibres by lactic acid in rats: Contributions of H+ and lactate ions. *J Physiol* 1997;500 (Pt 2):319-329.

62. Horstman DH, Folinsbee LJ, Ives PJ, Abdul-Salaam S, McDonnell WF. Ozone concentration and pulmonary response relationships for 6.6-hour exposures with five hours of moderate exercise to 0.08, 0.10, and 0.12 ppm. *Am Rev Respir Dis* 1990;142:1158-1163.

63. Hu C, Wedde-Beer K, Auais A, Rodriguez MM, Piedimonte G. Nerve growth factor and nerve growth factor receptors in respiratory syncytial virus-infected lungs. *Am J Physiol Lung Cell Mol Physiol* 2002;283:L494-502.

64. Hunter DD, Carrell-Jacks LA, Batchelor TP, Dey RD. Role of nerve growth factor in ozone-induced neural responses in early postnatal airway development. *Am J Respir Cell Mol Biol* 2010.

65. Hunter DD, Myers AC, Undem BJ. Nerve growth factor-induced phenotypic switch in guinea pig airway sensory neurons. *Am J Respir Crit Care Med* 2000;161:1985-1990.

66. Hunter DD, Undem BJ. Identification and substance P content of vagal afferent neurons innervating the epithelium of the guinea pig trachea. *Am J Respir Crit Care Med* 1999;159:1943-1948.

67. Hunter DD, Wu Z, Dey RD. Sensory neural responses to ozone exposure during early postnatal development in rat airways. *Am J Respir Cell Mol Biol* 2010;43:750-757.

68. Jancso N, Jancso-Gabor A, Szolcsanyi J. Direct evidence for neurogenic inflammation and its prevention by denervation and by pretreatment with capsaicin. *Br J Pharmacol Chemother* 1967;31:138-151.

69. Jancso N, Jancso-Gabor A, Szolcsanyi J. The role of sensory nerve endings in neurogenic inflammation induced in human skin and in the eye and paw of the rat. *Br J Pharmacol Chemother* 1968;33:32-41.

70. Jerrett M, Burnett RT, Pope CA, 3rd, Ito K, Thurston G, Krewski D, Shi Y, Calle E, Thun M. Long-term ozone exposure and mortality. *N Engl J Med* 2009;360:1085-1095.

71. Joad JP, Bric JM, Peake JL, Pinkerton KE. Perinatal exposure to aged and diluted sidestream cigarette smoke produces airway hyperresponsiveness in older rats. *Toxicol Appl Pharmacol* 1999;155:253-260.

72. Joos GF, Germonpre PR, Pauwels RA. Role of tachykinins in asthma. *Allergy* 2000;55:321-337.

73. Kalia M, Mesulam MM. Brain stem projections of sensory and motor components of the vagus complex in the cat: I. The cervical vagus and nodose ganglion. *J Comp Neurol* 1980;193:435-465.

74. Kalia M, Mesulam MM. Brain stem projections of sensory and motor components of the vagus complex in the cat: Ii. Laryngeal, tracheobronchial, pulmonary, cardiac, and gastrointestinal branches. *J Comp Neurol* 1980;193:467-508.

75. Katayama M, Nadel JA, Bunnett NW, Di Maria GU, Haxhiu M, Borson DB. Catabolism of calcitonin gene-related peptide and substance P by neutral endopeptidase. *Peptides* 1991;12:563-567.

76. Kerschensteiner M, Gallmeier E, Behrens L, Leal VV, Misgeld T, Klinkert WE, Kolbeck R, Hoppe E, Oropeza-Wekerle RL, Bartke I, Stadelmann C, Lassmann H, Wekerle H, Hohlfeld R. Activated human T cells, B cells, and monocytes produce brain-derived neurotrophic factor in vitro and in inflammatory brain lesions: A neuroprotective role of inflammation? *J Exp Med* 1999;189:865-870.

77. Krishna MT, Madden J, Teran LM, Biscione GL, Lau LC, Withers NJ, Sandstrom T, Mudway I, Kelly FJ, Walls A, Frew AJ, Holgate ST. Effects of 0.2 ppm ozone on biomarkers of inflammation in bronchoalveolar lavage fluid and bronchial mucosa of healthy subjects. *Eur Respir J* 1998;11:1294-1300.

78. Kubin L, Alheid GF, Zuperku EJ, McCrimmon DR. Central pathways of pulmonary and lower airway vagal afferents. *Journal of Applied Physiology (Bethesda, Md: 1985)* 2006;101:618-627

79. Kubin L, Kimura H, Davies RO. The medullary projections of afferent bronchopulmonary C fibres in the cat as shown by antidromic mapping. *J Physiol* 1991;435:207-228.

80. Kummer W, Fischer A, Kurkowski R, Heym C. The sensory and sympathetic innervation of guinea-pig lung and trachea as studied by retrograde neuronal tracing and double-labelling immunohistochemistry. *Neuroscience* 1992;49:715-737.

81. Laurenzi MA, Persson MA, Dalsgaard CJ, Ringden O. Stimulation of human B lymphocyte differentiation by the neuropeptides substance P and neurokinin A. *Scand J Immunol* 1989;30:695-701.

82. Lee FS, Kim AH, Khursigara G, Chao MV. The uniqueness of being a neurotrophin receptor. *Curr Opin Neurobiol* 2001;11:281-286.

83. Lee LY, Kou YR, Frazier DT, Beck ER, Pisarri TE, Coleridge HM, Coleridge JC. Stimulation of vagal pulmonary C-fibers by a single breath of cigarette smoke in dogs. *J Appl Physiol* 1989;66:2032-2038.

84. Lee LY, Pisarri TE. Afferent properties and reflex functions of bronchopulmonary C-fibers. *Respir Physiol* 2001;125:47-65.

85. Leikauf GD, Simpson LG, Santrock J, Zhao Q, Abbinante-Nissen J, Zhou S, Driscoll KE. Airway epithelial cell responses to ozone injury. *Environ Health Perspect* 1995;103 Suppl 2:91-95.

86. LeMaster AM, Krimm RF, Davis BM, Noel T, Forbes ME, Johnson JE, Albers KM. Overexpression of brain-derived neurotrophic factor enhances sensory innervation and selectively increases neuron number. *The Journal of Neuroscience: The Official Journal of the Society for Neuroscience* 1999;19:5919-5931

87. Leon A, Buriani A, Dal Toso R, Fabris M, Romanello S, Aloe L, Levi-Montalcini R. Mast cells synthesize, store, and release nerve growth factor. *Proceedings of the National Academy of Sciences of the United States of America* 1994;91:3739-3743.

88. Levi-Montalcini R. "Polypeptide growth factors" With special emphasis on wound healing. Introduction. *Cell Biology International* 1995;19:355

89. Lewin GR, Barde YA. Physiology of the neurotrophins. *Annu Rev Neurosci* 1996;19:289-317.

90. Li BY, Schild JH. Electrophysiological and pharmacological validation of vagal afferent fiber type of neurons enzymatically isolated from rat nodose ganglia. *J Neurosci Methods* 2007;164:75-85.

91. Lindsay RM, Harmar AJ. Nerve growth factor regulates expression of neuropeptide genes in adult sensory neurons. *Nature* 1989;337:362-364.

92. Loomis D, Castillejos M, Gold DR, McDonnell W, Borja-Aburto VH. Air pollution and infant mortality in mexico city. *Epidemiology* 1999;10:118-123.

93. Lundberg JM. Pharmacology of cotransmission in the autonomic nervous system: Integrative aspects on amines, neuropeptides, adenosine triphosphate, amino acids and nitric oxide. *Pharmacol Rev* 1996;48:113-178.

94. Lundberg JM, Hokfelt T, Martling CR, Saria A, Cuello C. Substance P-immunoreactive sensory nerves in the lower respiratory tract of various mammals including man. *Cell Tissue Res* 1984;235:251-261.

95. Lundberg JM, Saria A. Capsaicin-sensitive vagal neurons involved in control of vascular permeability in rat trachea. *Acta Physiol Scand* 1982;115:521-523.

96. Lundberg JM, Saria A. Capsaicin-induced desensitization of airway mucosa to cigarette smoke, mechanical and chemical irritants. *Nature* 1983;302:251-253.

97. MacLean DB, Lewis SF, Wheeler FB. Substance P content in cultured neonatal rat vagal sensory neurons: The effect of nerve growth factor. *Brain Res* 1988;457:53-62.

98. MacLean DB, Lewis SF, Wheeler FB. Substance P content in cultured neonatal rat vagal sensory neurons: The effect of nerve growth factor. *Brain Research* 1988;457:53-62

99. MacLean DB, Wheeler F, Hayes L. Basal and stimulated release of substance P from dissociated cultures of vagal sensory neurons. *Brain Res* 1990;519:308-314.

100. Maggi CA. Tachykinins and calcitonin gene-related peptide (CGRP) as co-transmitters released from peripheral endings of sensory nerves. *Prog Neurobiol* 1995;45:1-98.

101. Manzano GM, Giuliano LM, Nobrega JA. A brief historical note on the classification of nerve fibers. *Arq Neuropsiquiatr* 2008;66:117-119.

102. Marasco WA, Showell HJ, Becker EL. Substance P binds to the formylpeptide chemotaxis receptor on the rabbit neutrophil. *Biochem Biophys Res Commun* 1981;99:1065-1072.

103. Martinez FD, Stern DA, Wright AL, Taussig LM, Halonen M. Differential immune responses to acute lower respiratory illness in early life and subsequent development of persistent wheezing and asthma. *J Allergy Clin Immunol* 1998;102:915-920.

104. Martling CR. Sensory nerves containing tachykinins and CGRP in the lower airways. Functional implications for bronchoconstriction, vasodilatation and protein extravasation. *Acta Physiol Scand Suppl* 1987;563:1-57.

105. Matsui S, Jones GL, Woolley MJ, Lane CG, Gontovnick LS, O'Byrne PM. The effect of antioxidants on ozone-induced airway hyperresponsiveness in dogs. *Am Rev Respir Dis* 1991;144:1287-1290.

106. Matthiesen S, Bahulayan A, Kempkens S, Haag S, Fuhrmann M, Stichnote C, Juergens UR, Racke K. Muscarinic receptors mediate stimulation of human lung fibroblast proliferation. *Am J Respir Cell Mol Biol* 2006;35:621-627.

107. Menzel DB. Ozone: An overview of its toxicity in man and animals. *J Toxicol Environ Health* 1984;13:183-204.

108. Morimoto H, Yamashita M, Matsuda A, Miyake H, Fujii T. Effects of FR 113680 and FK 224, novel tachykinin receptor antagonists, on cigarette smoke-induced rat tracheal plasma extravasation. *Eur J Pharmacol* 1992;224:1-5.

109. Mortola J, Sant'Ambrogio G, Clement MG. Localization of irritant receptors in the airways of the dog. *Respir Physiol* 1975;24:107-114.

110. Mustafa MG, Elsayed NM, Quinn CL, Postlethwait EM, Gardner DE, Graham JA. Comparison of pulmonary biochemical effects of low-level ozone exposure on mice and rats. *J Toxicol Environ Health* 1982;9:857-865.

111. Nadel JA. Decreased neutral endopeptidases: Possible role in inflammatory diseases of airways. *Lung* 1990;168 Suppl:123-127.

112. Nassenstein C, Taylor-Clark TE, Myers A, Ru F, Nandigama R, Bettner W, Undem B. Phenotypic distinctions between neural crest and placodal derived vagal C-fibers in mouse lungs. *J Physiol* 2010.

113. Nettesheim P, Jetten AM, Inayama Y, Brody AR, George MA, Gilmore LB, Gray T, Hook GE. Pathways of differentiation of airway epithelial cells. *Environ Health Perspect* 1990;85:317-329.

114. Patapoutian A, Reichardt LF. Trk receptors: Mediators of neurotrophin action. *Curr Opin Neurobiol* 2001;11:272-280.

115. Payan DG, Brewster DR, Goetzl EJ. Specific stimulation of human T lymphocytes by substance P. *J Immunol* 1983;131:1613-1615.

116. Piedimonte G. Tachykinin peptides, receptors, and peptidases in airway disease. *Exp Lung Res* 1995;21:809-834.

117. Piedimonte G. Neural mechanisms of respiratory syncytial virus-induced inflammation and prevention of respiratory syncytial virus sequelae. *Am J Respir Crit Care Med* 2001;163:S18-21.

118. Piedimonte G, McDonald DM, Nadel JA. Glucocorticoids inhibit neurogenic plasma extravasation and prevent virus-potentiated extravasation in the rat trachea. *J Clin Invest* 1990;86:1409-1415.

119. Pinkerton KE, Joad JP. The mammalian respiratory system and critical windows of exposure for children's health. *Environ Health Perspect* 2000;108 Suppl 3:457-462.

120. Pino MV, Stovall MY, Levin JR, Devlin RB, Koren HS, Hyde DM. Acute ozone-induced lung injury in neutrophil-depleted rats. *Toxicol Appl Pharmacol* 1992;114:268-276.

121. Plopper CG, Mariassy AT, Wilson DW, Alley JL, Nishio SJ, Nettesheim P. Comparison of nonciliated tracheal epithelial cells in six mammalian species: Ultrastructure and population densities. *Exp Lung Res* 1983;5:281-294.

122. Prakash YS, Thompson MA, Pabelick CM. Brain-derived neurotrophic factor in TNF-alpha modulation of Ca2+ in human airway smooth muscle. *Am J Respir Cell Mol Biol* 2009;41:603-611.

123. Quarcoo D, Schulte-Herbruggen O, Lommatzsch M, Schierhorn K, Hoyle GW, Renz H, Braun A. Nerve growth factor induces increased airway inflammation via a neuropeptide-dependent mechanism in a transgenic animal model of allergic airway inflammation. *Clin Exp Allergy* 2004;34:1146-1151.

124. Rameshwar P. Substance p: A regulatory neuropeptide for hematopoiesis and immune functions. *Clin Immunol Immunopathol* 1997;85:129-133.

125. Renz H. Neurotrophins in bronchial asthma. *Respiratory Research* 2001;2:265-268

126. Renzetti G, Silvestre G, D'Amario C, Bottini E, Gloria-Bottini F, Bottini N, Auais A, Perez MK, Piedimonte G. Less air pollution leads to rapid reduction of airway inflammation and improved airway function in asthmatic children. *Pediatrics* 2009;123:1051-1058.

127. Ricco MM, Kummer W, Biglari B, Myers AC, Undem BJ. Interganglionic segregation of distinct vagal afferent fibre phenotypes in guinea-pig airways. *J Physiol* 1996;496 (Pt 2):521-530.

128. Romieu I, Meneses F, Sienra-Monge JJ, Huerta J, Ruiz Velasco S, White MC, Etzel RA, Hernandez-Avila M. Effects of urban air pollutants on emergency visits for childhood asthma in mexico city. *Am J Epidemiol* 1995;141:546-553.

129. Roques BP, Noble F, Dauge V, Fournie-Zaluski MC, Beaumont A. Neutral endopeptidase 24.11: Structure, inhibition, and experimental and clinical pharmacology. *Pharmacol Rev* 1993;45:87-146.

130. Scuri M, Chen BT, Castranova V, Reynolds JS, Johnson VJ, Samsell L, Walton C, Piedimonte G. Effects of titanium dioxide nanoparticle exposure on neuroimmune responses in rat airways. *J Toxicol Environ Health A* 2010;73:1353-1369.

131. Sherwood L. Fundamentals of physiology: A human perspective. Thomson Brooks/Cole; 2006.

132. Shore SA, Johnston RA, Schwartzman IN, Chism D, Krishna Murthy GG. Ozone-induced airway hyperresponsiveness is reduced in immature mice. *J Appl Physiol* 2002;92:1019-1028.

133. Sigurs N, Gustafsson PM, Bjarnason R, Lundberg F, Schmidt S, Sigurbergsson F, Kjellman B. Severe respiratory syncytial virus bronchiolitis in infancy and asthma and allergy at age 13. *Am J Respir Crit Care Med* 2005;171:137-141.

134. Snider WD. Functions of the neurotrophins during nervous system development: What the knockouts are teaching us. *Cell* 1994;77:627-638.

135. Souma T. The distribution and surface ultrastructure of airway epithelial cells in the rat lung: A scanning electron microscopic study. *Arch Histol Jpn* 1987;50:419-436.

136. Sparrow MP, Weichselbaum M. Development of the airway innervation. In: Harding R, Pinkerton KE, Plopper CG, editors. The lung: Devleopment, aging and the environment. London: Elsevier Academic Press; 2004. p. 33-53.

137. Springall DR, Cadieux A, Oliveira H, Su H, Royston D, Polak JM. Retrograde tracing shows that CGRP-immunoreactive nerves of rat trachea and lung originate from vagal and dorsal root ganglia. *J Auton Nerv Syst* 1987;20:155-166.

138. Springer J, Wagner S, Subramamiam A, McGregor GP, Groneberg DA, Fischer A. BDNF-overexpression regulates the reactivity of small pulmonary arteries to neurokinin A. *Regulatory Peptides* 2004;118:19-23

139. Stanisz AM, Befus D, Bienenstock J. Differential effects of vasoactive intestinal peptide, substance P, and somatostatin on immunoglobulin synthesis and proliferations by lymphocytes from peyer's patches, mesenteric lymph nodes, and spleen. *J Immunol* 1986;136:152-156.

140. Sterner-Kock A, Kock M, Braun R, Hyde DM. Ozone-induced epithelial injury in the ferret is similar to nonhuman primates. *Am J Respir Crit Care Med* 2000;162:1152-1156.

141. Tam SY, Tsai M, Yamaguchi M, Yano K, Butterfield JH, Galli SJ. Expression of functional Trk A receptor tyrosine kinase in the HMC-1 human mast cell line and in human mast cells. *Blood* 1997;90:1807-1820.

142. Thurston GD, Ito K, Kinney PL, Lippmann M. A multi-year study of air pollution and respiratory hospital admissions in three new york state metropolitan areas: Results for 1988 and 1989 summers. *J Expo Anal Environ Epidemiol* 1992;2:429-450.

143. Tolbert PE, Mulholland JA, MacIntosh DL, Xu F, Daniels D, Devine OJ, Carlin BP, Klein M, Dorley J, Butler AJ, Nordenberg DF, Frumkin H, Ryan PB, White MC. Air quality and pediatric emergency room visits for asthma in atlanta, georgia, USA. *Am J Epidemiol* 2000;151:798-810.

144. Torcia M, Bracci-Laudiero, L., Lucibello, M., Nencioni, L., Labardi, D., Rubartelli, A., Cozzonlino, F., Aloe, L., Garaci, E.,. Nerve growth factor is an autocrine survival factor for memory B lymphocytes. *Cell* 1996;85:345-356.

145. Urrego F, Scuri M, Auais A, Mohtasham L, Piedimonte G. Combined effects of chronic nicotine and acute virus exposure on neurotrophin expression in rat lung. *Pediatr Pulmonol* 2009;44:1075-1084.

146. Virchow JC, Julius P, Lommatzsch M, Luttmann W, Renz H, Braun A. Neurotrophins are increased in bronchoalveolar lavage fluid after segmental allergen provocation. *Am J Respir Crit Care Med* 1998;158:2002-2005.

147. von Euler US, Gaddum JH. An unidentified depressor substance in certain tissue extracts. *J Physiol Lond* 1931;72:74-87.

148. Widdicombe JG. Sensory innervation of the lungs and airways. *Prog Brain Res* 1986;67:49-64.

149. Wilfong ER, Dey RD. Nerve growth factor and substance P regulation in nasal sensory neurons after toluene diisocyanate exposure. *Am J Respir Cell Mol Biol* 2004;30:793-800.

150. Winter J. Characterization of capsaicin-sensitive neurones in adult rat dorsal root ganglion cultures. *Neurosci Lett* 1987;80:134-140.

151. Winter J. Brain derived neurotrophic factor, but not nerve growth factor, regulates capsaicin sensitivity of rat vagal ganglion neurones. *Neurosci Lett* 1998;241:21-24.

152. Wu ZX, Hunter DD, Kish VL, Benders KM, Batchelor TP, Dey RD. Prenatal and early, but not late, postnatal exposure of mice to sidestream tobacco smoke increases airway hyperresponsiveness later in life. *Environ Health Perspect* 2009;117:1434-1440.

153. Wu ZX, Lee LY. Airway hyperresponsiveness induced by chronic exposure to cigarette smoke in guinea pigs: Role of tachykinins. *J Appl Physiol* 1999;87:1621-1628.

154. Yang Q, Chen Y, Shi Y, Burnett RT, McGrail KM, Krewski D. Association between ozone and respiratory admissions among children and the elderly in vancouver, canada. *Inhal Toxicol* 2003;15:1297-1308.

155. Zhang LY, Levitt RC, Kleeberger SR. Differential susceptibility to ozone-induced airways hyperreactivity in inbred strains of mice. *Exp Lung Res* 1995;21:503-518.

CHAPTER 2:

Objectives and Rationale

2.1 Objective 1: Characterize the normal postnatal development of nodose and jugular ganglia sensory neurons, tracheal epithelial nerve fibers, and the concentration of NGF present in the airway lumen.

Previous studies examining the postnatal development of sensory neurons from rat nodose ganglia are contradictory in that one study indicated nodose neuron number decreased from birth until approximately PD15, while a separate group reported no change in nodose neuron number from birth through adulthood. However, neither of these studies evaluated specific subsets of neurons, such as those projecting to the airway, nor did they consider neurons in the jugular ganglia. Experiments examining changes in tracheal epithelial innervation have been conducted; however in many instances results are reported as changes in a specific peptide (e.g. SP). Studies utilizing protein gene product-9.5 (PGP-9.5) immunohistochemistry to identify all innervating nerve fibers have been completed but most determined changes in total nerve fiber density (NFD) following manipulation of normal development. Over-expression of NGF in the airways affects airway innervation and its actions as a trophic factor for sensory neurons innervating the airways has also been thoroughly documented. However, the levels of NGF present in the airways during normal postnatal development have not been extensively studied.

Chapter 3 presents studies that examined the normal postnatal development of tracheal epithelial innervation between PD6 and PD28, as well as quantifying the concentration of NGF measured in BALF during the same time period. Studies presented in Chapter 4 detail the preliminary experiments conducted to determine the optimal method for quantifying neurons. In Chapter 5, the quantification of both total nodose and jugular sensory neurons and neurons innervating the airway (airway neurons) during postnatal life is presented.

In Objective 1, I postulate that the sensory neural development of the airways (airway neuron number and tracheal epithelial NFD) will correlate with the levels of NGF present in early postnatal airways. I will test this hypothesis by taking measurements of all three parameters at specific postnatal ages (PD6, PD10, PD15, PD21, and PD28) and will then statistically analyze the results to determine if a correlation exists.

2.2 Objective 2: Determine the effect of an acute ozone exposure on the postnatal development and neuropeptide expression of nodose and jugular sensory neurons.

Mounting evidence indicates that fetal and early life exposures to inhaled environmental pollutants may play an important role in the pathogenesis of asthma seen initially in children and later in adults. NGF concentrations in the airways can be influenced by exposure to allergens, as well as environmental agents, such as ozone. Both NGF administration and ozone exposure can increase the percentage of SP-immunoreactive (SP-IR) neurons in nodose and jugular ganglia. However, it has not been determined what effects a single ozone exposure in early postnatal life may have on sensory neuron number and the number of SP airway neurons.

Chapter 5 presents the results of trials that quantified total neuron, airway neuron, SP neuron and SP- airway neuron number using a combination of primary neuron culture, immunocytochemistry and flow cytometry.

In Objective 2, I hypothesize that early life ozone exposure will have no effect on total nodose and jugular neuron number, and will increase both the number of airway neurons and the number of SP-IR airway neurons. To test this hypothesis I will expose PD5 aged rat pups to filtered air or 2 ppm O_3 and then quantify neuron numbers on PD10, PD15, PD21 or PD28.

CHAPTER 3:

Epithelium Nerve Fiber Density and NGF Levels in Early Postnatal Rat Airways

3.1 Introduction

Airway inflammation, a defining characteristic of asthma, is partially mediated by sensory afferent nerve fibers innervating the airways, which exert their influence through the release of neuropeptides from terminal arborizations (3). The majority of the sensory afferent innervation in the airways originates in cells bodies located within vagal sensory ganglia (1, 2, 7, 21). Early development of cell bodies in both ganglia is dependent on NGF for their growth and survival (10, 14). Although NGF is known to influence sensory neuronal development, the role of NGF in the development of airway innervation during early postnatal life has not been extensively studied. One study employing transgenic mice that over-express NGF specifically in the airways determined that, compared to wild type littermates, transgenic animals had hyperinnervated airways (12)

NGF is a protein in the neurotrophin family (15), which acts as a target–derived or paracrine trophic factor regulating the growth and survival of both peripheral and central neuronal populations. Initially neurotrophins were thought to be involved exclusively in the survival and maintenance of neuronal populations; however, it has been demonstrated that they have a more diverse role, particularly in inflammatory conditions of neural origin (8, 9, 16). As an inflammatory disease, the pathogenesis of asthma may involve the actions of neurotrophins including NGF (5, 6, 18-20). Increased levels of NGF have been seen in the BALF of allergic asthma patients following allergen challenge (23), and NGF is increased in the serum of asthma patients (4).

The rationale for conducting this study is that if over-expression of NGF in the airways results in hyperinnervated airways, the possibility exists that the levels of NGF present in the airways during normal postnatal development determine the level of innervation. Neuropeptides released from sensory afferents can mediate airway inflammation and hyperresponsiveness through interactions with immune cells and airway smooth muscle. An increased level of innervation heightens the possibility of increased amounts of neuropeptides present in sensory terminals. Upon noxious stimulation of the airways, more neuropeptides could be released into the airways, thereby exacerbating inflammation. For these reasons it is important to understand if changes in NGF concentrations in the airway during normal postnatal development can directly affect airway innervation levels. The objective of this study was to establish the normal patterns of sensory innervation in the airways, along with determining how levels of NGF change during postnatal development.

3.2 Materials and Methods

3.2.1 Experimental Design

In order to test the hypothesis, experiments were designed to determine the nerve fiber density in tracheal epithelium, and measure NGF protein levels in the airway from PD6 through PD28. To assess sensory innervation in the airways, tracheal epithelium was examined on PD6, 10, 15, 21, and 28, and the nerve fiber density calculated for each respective age group. On the same postnatal days BALF was collected to determine the NGF levels in the airway lumen.

3.2.2 Animals

Fischer 344 late gestation pregnant rats were purchased from Harlan Laboratories and shipped while pregnant. Upon arrival pregnant females were kept in filtered ventilated cages in a USDA-approved, specific pathogen-free and environmentally controlled animal facility. While in the facility, animals were provided with HEPA-filtered air, autoclaved diet and tap water ad libitum and housed under controlled light-cycle (12 hr light/ 12 hr dark) and temperature (22-24°C) conditions. After pups were born they were kept in the same cage as the mother. Rat pups were analyzed on PD6, 10, 15, 21, and 28. All procedures were done in accordance with IACUC regulations and approved IACUC protocols.

3.2.3 Immunohistochemistry

Animals were given an overdose of sodium pentobarbital (50 mg/ml). Tracheas of animals not receiving bronchoalveolar lavage were used for immunohistochemistry, as described in Hunter et al., (13). Tracheas were removed by cutting caudal to the larynx and cranial to the main bronchi. Tissues were immediately fixed in ice-cold picric-acid formaldehyde fixative containing 2% paraformaldehyde, 15% saturated picric acid and 0.15 M phosphate buffer (22). Three hrs later tracheas were washed twice in 0.1 M phosphate buffered saline containing 0.3% (v/v) Triton X-100 (PBS-TX, pH=7.8). Following the second rinse, the tissue remained in PBS-Tx overnight at 4°C. The following day, tracheas were oriented on corks so that the first sections would be taken from the dorsal aspect of the trachea closest to the smooth muscle side. The tissue was covered with Tissue Tek OCT (Sakura, Torrance, CA), frozen in isopentane cooled by liquid nitrogen, placed in air tight plastic bags and stored at -80°C.

Continuous serial sections (12 μm thickness) of the trachea were collected on gelatin-coated coverslips and briefly air-dried. In the smaller PD6 and 10 animals, the entire trachea was sectioned, whereas, in the larger PD15, 21 and 28 pups, only every 4^{th} section of trachea

was collected. Sections were incubated with an affinity purified rabbit monoclonal antibody against the pan neuronal marker, protein gene product 9.5 (PGP-9.5; Chemicon/Millipore, Temecula**,** CA; Thompson et al., 1983) diluted 1:50 in phosphate-buffered saline, 0.3% triton X 100 and 1% (w/v) bovine serum albumin (PBS-TX-BSA) in a humidified chamber overnight at 4°C. Sections were rinsed three times with PBS-TX-BSA, for 5 min each rinse then covered with a fluorescein isothiocyanate (FITC)-conjugated goat anti-rabbit immunoglobin IgG (Jackson ImmunoResearch, West Grove, PA**)**, diluted 1:100 in PBS-TX-BSA and incubated at 37°C for 30 minutes. Coverslips were again rinsed three times for 5-min intervals in PBS-TX-BSA. Fluoromount (Southern Biotechnology, Birmingham, AL) was used to mount the coverslips on glass slides. Controls for this experiment comprised a test of the specificity of the primary antibody in PGP-9.5-rich brain regions (positive control), or negative controls in which the primary monoclonal antibody was omitted.

3.2.4 Nerve Fiber Density (NFD) Measurement

To measure the total NFD of the tracheal epithelium, images of PGP-9.5-containing nerve fibers were collected in series using a Zeiss LSM 510 confocal microscope equipped with a fluorescein filter (excitation 495 nm and emission 520 nm) and an argon laser (Zeiss, Oberkochen, Germany). Ten sections per animal were selected randomly using standard light microscopy to avoid bias based on innervation density. A series of twenty images representing all of the tracheal epithelium in each section was collected, saved to a database, and exported as black and white digital TIF images. The TIF images were analyzed using Optimas software (Bioscan, Edmonds, WA) to determine the NFD. The perimeter of the epithelial region was outlined digitally and PGP-9.5- immunoreactive (IR) nerve fibers were identified by segmentation using user-defined threshold gray levels based on optimizing signal-to-noise appearance of the nerve fibers and background. The PGP-9.5 NFD was calculated by dividing the PGP-9.5-IR nerve fiber area by the total area of epithelium outlined.

3.2.5 Determination of Standard Lung Volume for Bronchoalveolar Lavage

Since the animals were used at different ages and the lungs were different sizes, special procedures were developed to facilitate comparisons of BALF protein between the age groups. A standard volume of PBS was instilled for each age group, which was determined by measuring the volume of PBS that could be instilled into lungs at a constant filling pressure (25 cm H_2O pressure). Briefly, a graduated syringe filled with a known volume PBS was attached to tubing that was inserted into the trachea of rat pups through a small incision. The water level

was maintained at 25 cm above the animal while the lungs were filling with the PBS. When all of the lobes of the lungs had visibly filled, the flow of PBS was stopped and the new volume in the syringe was recorded. The standard volume for each age group is the mean volume that was instilled in three animals in each age group. This method was modified from a protocol for fixing lungs for histological analysis (11). By maintaining a constant filling pressure, the conditions used for determining the volume of PBS used for BAL procedures in different ages are uniform.

3.2.6 Bronchoalveolar Lavage Fluid Collection

BALF was collected from rat pups on PD6, 10, 15, 21, and 28. Briefly, animals were overdosed with an i.p. injection of sodium pentobarbital (50 mg/ml), the thoracic cavity opened and the lungs exposed. A cannula was inserted into the trachea and phosphate buffered saline (PBS) was instilled into the lungs in situ. A standard volume of PBS was instilled for each age group. A single bolus of PBS at the standard volume was instilled and withdrawn through the lungs three times, collected in tubes after the 3rd withdrawl, and centrifuged at 10,000 rpm. The supernatant was removed, aliquoted into 1.5 ml microcentrifuge tubes and stored at -80°C until analysis was preformed.

3.2.7 NGF Enzyme-Linked Immunosorbent Assay (ELISA)

The concentration of NGF (7.8-250 pg/ml) in each lavage supernatant sample was assayed using the NGF Emax Immuno Assay System (Promega, Madison, WI) according to the manufacturer's instructions. The concentration of NGF in each lavage sample was determined using a standard curve, and then multiplied by the standard instilled volume for the respective age group to determine the amount of NGF in the entire lung. NGF concentrations were then normalized to the dry lung weight (g) for the respective postnatal ages (Table 3-1). All samples were run in duplicate or triplicate, and, as a negative control, triplicate PBS samples were run with each assay.

Table 3-1

Postnatal Age	Standard Volume Instilled (ml)	Standard Lung Dry Weight (g)
PD6	0.6 $\pm$ 0.05	0.049 $\pm$ 0.001
PD10	1.0 $\pm$ 0.06	0.063 $\pm$ 0.001
PD15	1.13 $\pm$ 0.08	0.077 $\pm$ 0.004
PD21	1.90 $\pm$ 0.10	0.082 $\pm$ 0.001
PD28	4.33 $\pm$ 0.28	0.091 $\pm$ 0.001

3.2.8 Statistical Analysis

Results of experiments are expressed as mean ± SE. Nerve fiber density results are expressed as a percentage of the area of PGP-9.5-IR nerve fibers in the total area of epithelium. An n of 6 animals were used for all groups except were noted. All data in these experiments were analyzed using a one-way ANOVA, followed by Tukey's post hoc examination when an effect was considered significant. Values were considered significant at $p < 0.05$.

3.3 Results

3.3.1 Epithelium Nerve Fiber Density

The amount of innervation in the epithelium was measured to determine if there were age related changes in innervation levels. Figure 3-1A shows a representative image of PGP-9.5^{+} nerve fibers in the tracheal epithelium. The level of innervation in the tracheal epithelium at both PD6 and PD10 was significantly increased over the NFD at PD28 (Figure 3-1B). The decrease in NFD observed at PD21 was determined to be significantly different from the NFD at PD10. Innervation levels did not significantly change between PD21 and PD28. Although, NFD at PD15 appeared to be increased above PD21 and PD28 innervation levels, no significant difference was found. Overall, the level of tracheal epithelium innervation attenuates significantly beginning around PD15 and then stablizes.

3.3.2 NGF concentration in BALF

Next we measured levels of NGF in the BALF. NGF concentrations in the BALF of PD10 animals were significantly higher than at any other age group examined (Figure 3-2). PD15 NGF levels were slightly higher than the levels seen at PD 6, 21, and 28; however, no significant differences were found.

Figure 3-1(4)

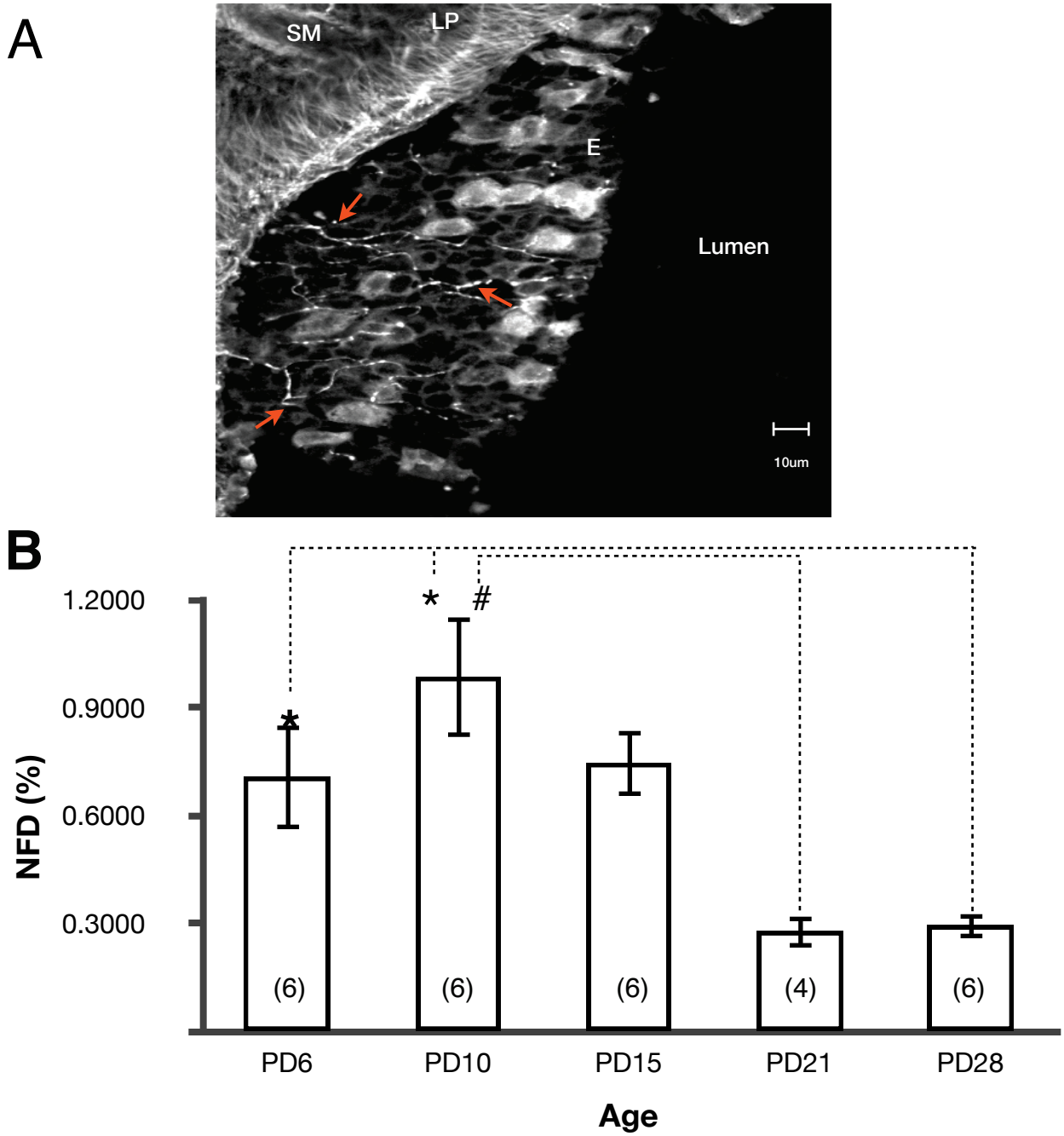

Figure 3-1. Total epithelium nerve fiber density (NFD) of postnatal day (PD) 6,10,15, 21 and 28 Rats. Nerve fibers in the epithelium were identified using PGP-9.5 immunohistochemistry and quantified. Quantifications were done using Optimas Imaging software. **(A)** Representative confocal image of airway from PD 10 rat pup. Arrows indicate PGP-9.5+ positive nerve fibers. E: epithelium; LP: lamina propria; SM: smooth muscle. **(B)** NFD is expressed as percent area and numbers represent the average of all animals sampled for a particular age group. The epithelium NFD in PD6 and PD10 animals were significantly higher than in PD28 rats (*p<0.05). PD10 NFD was also significantly increased above PD21 levels (#p<0.05). No difference was seen in PD15 rats. Numbers in parenthesis represent the n value for each age group.

Figure 3-2(5)

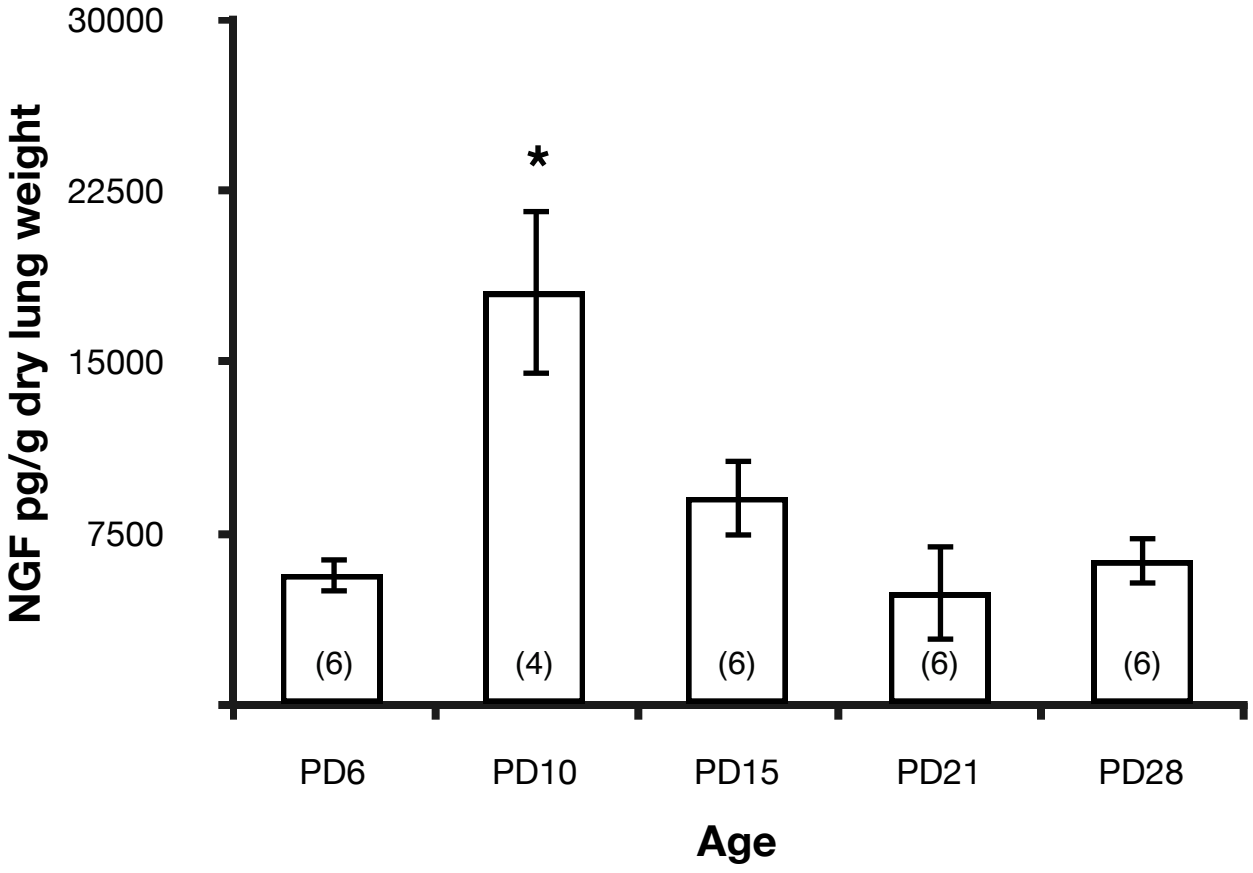

Figure 3-2. Nerve growth factor (NGF) protein concentration in bronchoalveolar lavage fluid (BALF) of postnatal day (PD) 6, 10, 15, 21 and 28 Rats. Lavage fluid was collected from animals and NGF protein levels were quantified according to manufacturer's specifications using the NGF Emax Immuno Assay System (Promega, Madison, WI). Protein levels are expressed in pg/g lung. PD10 animals had significantly increased NGF levels over all other age groups. .(*$p<0.05$). Numbers in parenthesis represent the n value for each age group.

Figure 3-3 (6)

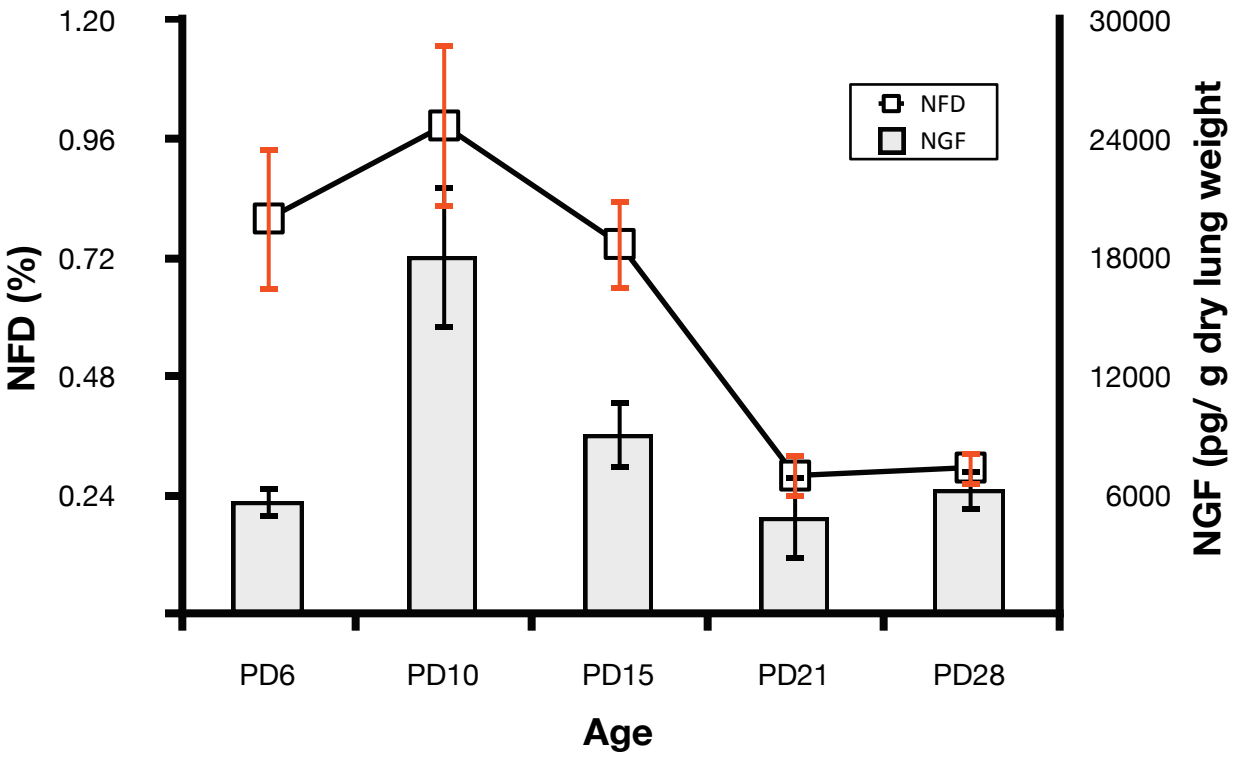

Figure 3-3. Nerve growth factor (NGF) protein concentration in bronchoalveolar lavage fluid (BALF) compared with epithelium nerve fiber density (NFD) of postnatal day (PD) 6, 10, 15, 21 and 28 rats. Both NGF levels in BALF (bars) and epithelium NFD (line) are maximally increased on PD10.

3.4 Discussion

The results of this study reveal that the levels of NGF in lavage fluid on PD10 were significantly greater than levels measured on any other day. Epithelium NFD was also greatest on PD10 and was significantly greater than the NFD measured in both PD21 and PD28 rat pups. PD6 rats had epithelium NFD levels that were significantly greater than NFD levels measured on PD28. Given the known effects of NGF on axonal growth, these findings suggest that a relationship exists between epithelium NFD and the levels of NGF measured in BALF during normal postnatal development.

In a study examining NGF levels in postnatal aged mice Lommatzsch et al., reported NGF concentrations measured in mouse whole lung homogenates during normal postnatal development decrease between PD1 and PD21 (17). We determined that the levels of NGF were significantly higher at PD10 than at any other day examined, and that NGF levels remained low after PD21 (Figure 3-2). Although our study looked at a more specific timeline, both studies describe decreased levels of NGF at PD21 that remained low at later time points.

A study conducted by Hoyle et al. (12) using transgenic mice that over-express NGF specifically in the lung found that the airways of the transgenic mice were hyperinnervated when compared to wild type. In our study, the changes occurring in both parameters followed a similar pattern, however, statistical analysis using a Pearson correlation revealed that epithelium NFD and NGF levels in lavage fluid did not correlate (r^2=0.5531). This discrepancy could be due to trophic support from within the epithelium itself that cannot be measured in the BALF, for instance, if it had not been released into the lumen. It is likely that the axons arborize upon reaching the epithelium and that this innervation might change as animals age or as target-derived trophic support is altered. Another possible variable is that the effect of elevated NGF may be delayed if it take a few days for axonal branching to reach their maximal level of growth.

3.4.1 Conclusions

While the correlation statistics do not indicate that the levels of NGF in the airways directly determine the extent of epithelium innervation, it is hard to ignore the similar pattern that epithelium NFD and NGF levels in BALF follow of both being maximally increased on PD10 and then decreasing from PD15 through PD28. When the two parameters are graphed together as shown in Figure 3-3, a potential relationship between the two emerges. If an increase in NGF levels measured at an earlier age were followed by an increase in NFD levels at a subsequent age, then a more direct relationship between the two might be elucidated. However, NGF levels

and airway innervation being significantly increased on the same day demonstrates that, while NGF may not be the only determining factor in airway innervation levels, NGF a likely modulator of airway epithelial nerve fiber development in early postnatal life.

References

1. Agostoni E, Chinnock JE, De Daly MB, Murray JG. Functional and histological studies of the vagus nerve and its branches to the heart, lungs and abdominal viscera in the cat. *J Physiol* 1957;135:182-205.

2. Baluk P, Gabella G. Innervation of the guinea pig trachea: A quantitative morphological study of intrinsic neurons and extrinsic nerves. *J Comp Neurol* 1989;285:117-132.

3. Baluk P, Nadel JA, McDonald DM. Substance p-immunoreactive sensory axons in the rat respiratory tract: A quantitative study of their distribution and role in neurogenic inflammation. *J Comp Neurol* 1992;319:586-598.

4. Bonini S, Lambiase A, Angelucci F, Magrini L, Manni L, Aloe L. Circulating nerve growth factor levels are increased in humans with allergic diseases and asthma. *Proc Natl Acad Sci U S A* 1996;93:10955-10960.

5. Braun A, Lommatzsch M, Renz H. The role of neurotrophins in allergic bronchial asthma. *Clin Exp Allergy* 2000;30:178-186.

6. Braun A, Quarcoo D, Schulte-Herbruggen O, Lommatzsch M, Hoyle G, Renz H. Nerve growth factor induces airway hyperresponsiveness in mice. *Int Arch Allergy Immunol* 2001;124:205-207.

7. Dey RD, Altemus JB, Zervos I, Hoffpauir J. Origin and colocalization of cgrp- and sp-reactive nerves in cat airway epithelium. *J Appl Physiol* 1990;68:770-778.

8. Dmitrieva N, Shelton D, Rice AS, McMahon SB. The role of nerve growth factor in a model of visceral inflammation. *Neuroscience* 1997;78:449-459.

9. Donnerer J, Schuligoi R, Stein C. Increased content and transport of substance p and calcitonin gene-related peptide in sensory nerves innervating inflamed tissue: Evidence for a regulatory function of nerve growth factor in vivo. *Neuroscience* 1992;49:693-698.

10. Forgie A, Kuehnel F, Wyatt S, Davies AM. In vivo survival requirement of a subset of nodose ganglion neurons for nerve growth factor. *The European Journal of Neuroscience* 2000;12:670-676

11. Gehr P, Weibel ER. Morphometric estimation of regional differences in the dog lung. *J Appl Physiol* 1974;37:648-653.

12. Hoyle GW, Graham RM, Finkelstein JB, Nguyen KP, Gozal D, Friedman M. Hyperinnervation of the airways in transgenic mice overexpressing nerve growth factor. *Am J Respir Cell Mol Biol* 1998;18:149-157.

13. Hunter DD, Wu Z, Dey RD. Sensory neural responses to ozone exposure during early postnatal development in rat airways. *Am J Respir Cell Mol Biol* 2010;43:750-757.

14. Katz DM, Erb M, Lillis R, Neet K. Trophic regulation of nodose ganglion cell development: Evidence for an expanded role of nerve growth factor during embryogenesis in the rat. *Experimental Neurology* 1990;110:1-10

15. Levi-Montalcini R. The nerve growth factor 35 years later. *Science (New York, NY)* 1987;237:1154-1162.

16. Lindsay RM, Harmar AJ. Nerve growth factor regulates expression of neuropeptide genes in adult sensory neurons. *Nature* 1989;337:362-364.

17. Lommatzsch M, Quarcoo D, Schulte-Herbruggen O, Weber H, Virchow JC, Renz H, Braun A. Neurotrophins in murine viscera: A dynamic pattern from birth to adulthood. *Int J Dev Neurosci* 2005;23:495-500.

18. Quarcoo D, Schulte-Herbruggen O, Lommatzsch M, Schierhorn K, Hoyle GW, Renz H, Braun A. Nerve growth factor induces increased airway inflammation via a neuropeptide-dependent mechanism in a transgenic animal model of allergic airway inflammation. *Clin Exp Allergy* 2004;34:1146-1151.

19. Renz H. Neurotrophins in bronchial asthma. *Respiratory Research* 2001;2:265-268

20. Renz H. The role of neurotrophins in bronchial asthma. *European Journal of Pharmacology* 2001;429:231-237.

21. Springall DR, Cadieux A, Oliveira H, Su H, Royston D, Polak JM. Retrograde tracing shows that cgrp-immunoreactive nerves of rat trachea and lung originate from vagal and dorsal root ganglia. *J Auton Nerv Syst* 1987;20:155-166.

22. Stefanini M, De Martino C, Zamboni L. Fixation of ejaculated spermatozoa for electron microscopy. *Nature* 1967;216:173-174.

23. Virchow JC, Julius P, Lommatzsch M, Luttmann W, Renz H, Braun A. Neurotrophins are increased in bronchoalveolar lavage fluid after segmental allergen provocation. *Am J Respir Crit Care Med* 1998;158:2002-2005.

CHAPTER 4:

Preliminary Neuron Studies

4.1 Introduction

Sensory innervation of the airways has been extensively investigated in many species. It is known that sensory afferent fibers in the respiratory tract have an important role in regulating inflammation and airway responsiveness in both physiologic and pathologic states. Although several studies have been conducted to examine changes in neuron numbers in the nodose and jugular ganglia, the soma responsible for the majority of sensory afferent innervation in the airways, those studies have been primarily conducted in adult animals and have focused more on changes in the neuropeptide content than on changes in neuron number.

Work conducted by Bakal and Wright (1) looking at postnatal development of nodose neurons has shown that the number of neurons in the nodose ganglia of rats decreases until approximately PD15. Studies done by Cooper (3) found that in rats, nodose ganglion neuron number did not change during postnatal development. The lack of consensus on neuron number combined with the fact that these studies did not evaluate specific subsets of neurons, such as those projecting to the airway, and they did not examine changes in neuron numbers in the jugular ganglia, indicated that further investigation is warranted.

A series of preliminary assessments were undertaken to ascertain the most effective way to quantify neurons in the nodose and jugular ganglia. Two different quantification methods were used, i.e., design-based stereology and flow cytometry. The first experiments used design-based stereology to count neurons by hand, in fixed sections of ganglia; however, findings from this initial work indicated possible methodological limitations in this approach. To address these possible issues, a second group of experiments was conducted to evaluate if flow cytometry would be a valid technique for counting dissociated nodose and jugular ganglia neurons. Results of these studies showed a very large, unexpected increase in total neuron number between PD15 and PD28. In order to elucidate the cause of this increase in neuronal number, a third set of experiments sought to determine if the large changes in neuron numbers analyzed using flow cytometry were due to nodose and jugular ganglia neuron proliferation. These studies used two different thymidine analogs, bromo-deoxyuridine (BrdU) and 5-Ethynyl-2'-deoxyuridine (EdU), which are incorporated into DNA during the active DNA synthesis occurring in proliferating cells. The first assessment of neuron proliferation using BrdU showed possible neuron proliferation; however, no definitive conclusions could be made due to the extensive tissue damage that occurred during the detection process. EdU was used in the second assessment of neuron proliferation, and EdU fluorescence was not detected in any neurons in

the nodose or jugular ganglia. It was, therefore, concluded that neuron proliferation did not explain the large increase in neuronal number. The final set of trials used flow cytometry as the quantification technique, however new staining protocols were employed to determine if the variability seen in the previous flow cytometry experiments could be minimized. The objectives of this study were to 1) determine the most effective method for quantification of nodose and jugular ganglia neurons, 2) determine if increases in neuron numbers observed in preliminary experiments are the result of neuron proliferation and to 3) optimize flow cytometry techniques used for the analysis of neuron numbers.

4.2 Materials and Methods

4.2.1 Experimental Design

4.2.1a Nodose and Jugular Airway Neuron Counts:

In order to establish a time course of airway sensory neuronal development, retrograde tracing was used to identify neurons in the nodose and jugular ganglia that specifically innervate the trachea epithelium. Fluorescent RetroBeads™ (beads, LumaFluor Inc., Durham, NC) are not cytotoxic, persist for long periods in retrogradely-labeled soma, do not transverse the basement membrane, and are compatible with immunocytochemical techniques (2, 6, 7). The beads were instilled into the tracheal lumen of all animals on PD2. All animals received bead instillations on the same day so that microspheres would be present in the airways throughout the time course of this study, and as a control for size variations between animals as they age.

For preliminary stereology studies pups were euthanized on PD6, PD10, PD15, PD28, and PD60. Ganglia were removed, fixed, frozen, sectioned, and counterstained with the nuclear stain 4'6-diamindio-2-phenylindole (DAPI). The number of airway neurons contained in the nodose and jugular ganglia was quantified through analysis using fluorescent microscopy in conjunction with *Stereo Investigator* software.

Preliminary studies performed using flow cytometry were conducted. Bead instillations were completed in the same manner as animals used for neuron quantification with stereology. Ganglia were excised, disassociated, and processed for flow cytometry. Animals were analyzed on PD6, PD10, PD15, and PD28. The total number of neurons in nodose and jugular ganglia and the number of airway neurons in both ganglia were quantified.

4.2.1b BrdU and EdU Experiments:

To determine if neuron proliferation is occurring in nodose and jugular ganglia, BrdU and EdU studies were undertaken. BrdU and EdU are nucleoside analogs of thymidine that when available in cells, are incorporated into the DNA of proliferating cells during S-phase. Any BrdU that is incorporated into DNA can then be detected using an anti-BrdU antibody. EdU DNA incorporation is detected via a copper-catalyzed covalent reaction between an azide and an alkyne. BrdU or EdU was administered via single intraperitoneal injection on PD22, PD24, and PD26. All animals were euthanized on PD28; nodose and jugular ganglia were removed, fixed, frozen, and prepared for BrdU / EdU detection. Immunohistochemistry for the pan neuronal marker, PGP-9.5, was performed in addition to BrdU / EdU detection. Sections of ganglia processed for PGP-9.5 and BrdU or EdU were visualized on a fluorescent microscope capable of detecting FITC, Rhodamine, and Alexa Fluor 647.

4.2.2 Animals

Late gestation pregnant female Fischer 344 rats were purchased from Harlan Laboratories and shipped while pregnant. Upon arrival pregnant females were kept in filtered ventilated cages in a USDA-approved, specific pathogen-free and environmentally controlled animal facility. While in the vivarium, animals were provided with HEPA-filtered air, autoclaved diet and tap water ad libitum and housed under controlled light-cycle (12 hr light/ 12 hr dark) and temperature (22-24°C) conditions. After pups were born they were kept in the same cage as the mother. Rat pups were analyzed on PD28. All procedures were done in accordance with IACUC regulations and approved IACUC protocols.

4.2.3 Fluorescent Microsphere Instillation

Retrograde tracers were instilled into the tracheal lumen in order to identify sensory neurons in the nodose and jugular ganglia that specifically innervate the airway epithelium. Briefly, on PD2, rat pups were anesthetized via ice immersion-induced hypothermia (3-5 min). The pups were placed inside a latex sleeve, to protect their skin. When sufficiently anesthetized, the trachea was exposed with a midline incision in the skin on the ventral surface of the neck. Next, for stereology studies, 2 µl of a mixture of Green and Red Fluorescent beads were instilled into the tracheal lumen using a 10 µl Hamilton syringe. For flow cytometry studies only green beads were used, as the flow cytometer was not equipped with the appropriate laser filter combination to detect the red beads. Incisions were closed using surgical glue. Rat pups were revived using gentle warming and artificially ventilated if needed. When animals regained

consciousness and were breathing normally, they were returned to their mother. As the beads need a minimum of four days to travel from the epithelium to the cell body and since the beads reach maximal uptake within seven days of instillation (6), animals were not examined prior to PD6.

4.2.4 Stereology

4.2.4a Sample Preparation

On PD6, 10, 15, 28 or 60, animals were euthanized with an i.p. injection of sodium pentobarbital (50 mg/ml), both vagus nerves were exposed and the left and right vagal ganglia were removed, as described in, Hunter et al. (5). Tissues were immediately fixed in ice-cold picric-acid formaldehyde fixative containing 2% paraformaldehyde, 15% saturated picric acid and 0.15 M phosphate buffer (9). Three hours later ganglia were washed twice in 0.1 M phosphate buffered saline containing 0.3% (v/v) Triton X-100 (PBS-TX, pH=7.8). Following the second rinse, the tissue remained in PBS-TX overnight at 4°C. The following day, ganglia were oriented on corks in parallel alternated positions, with one ganglia rotated 180°. The tissue was covered with Tissue Tek OCT (Sakura, Torrance, CA), frozen in isopentane cooled by liquid nitrogen, placed in airtight plastic bags and stored at -80°C.

Continuous serial sections (2 5µm thickness) of the ganglia were collected on gelatin-coated cover slips and briefly air-dried; every section of ganglia was collected. Following section collection slips were then mounted onto slides using ProLong® Gold antifade with DAPI (Invitrogen, Carlsbad, CA). Slides were allowed to cure overnight and were then sealed with clear nail polish before being analyzed.

4.2.4b Analysis: Airway Neuron Counts

Using *Stereo Investigator* software (MBF Bioscience, Williston, VT), sensory neurons in the nodose and jugular whose axons specifically innervate the tracheal epithelium can be identified. Briefly, at low magnification sections are defined as regions of interest, then at higher magnification airway neurons are distinguished from other neurons if they contain red or green beads. A feature of the software called Meander Scanning is used to ensure that neurons are only counted once. The meander scan moves the motorized microscope stage to a new area of the region of interest. Airway neurons are then identified and labeled using a marker (Figure 4-1).

4.2.5 BrdU or EdU Injections

BrdU or EdU injections were used to determine if cell proliferation was occurring in the nodose and jugular ganglia between PDs 21 and 28. Briefly, on PDs 22, 24 and 26 animals were placed in a restraint of known mass and then weighed to determine animal weight. BrdU (Zymed Laboratories, San Francisco, CA), EdU (Molecular Probes / Invitrogen, Carlsbad, CA) or PBS was administered intraperitoneally (i.p), at a concentration of 1 ml/100 g body weight, with the appropriate dose being determined from body weight measurement on each day. Weight measurements and injections occurred at the same time each day.

4.2.6 Immunohistochemistry

Ganglia were excised and prepared for immunohistochemical studies as described in the "Stereology Sample Preparation" section. Continuous serial sections (12 µm thickness) of the ganglia were collected on gelatin-coated cover slips and briefly air-dried, and every 4^{th} section of ganglia was collected. In an attempt to increase section adherence to cover slips, sections fixed to slides using an acetone / methanol mixture (1:1), for 10 min at 4°C and then allowed to air-dry at 37°C for 30 min. After drying, sections were incubated with an affinity purified rabbit monoclonal antibody against diluted 1:50 in PBS-TX + 1% (w/v) bovine serum albumin (PBS-TX-BSA) in a humidified chamber overnight at 4°C. Sections were rinsed three times with PBS-TX-BSA, for 5 min each rinse then covered with a rhodamine-conjugated goat anti-rabbit immunoglobin IgG (Jackson ImmunoResearch, West Grove, PA**)**, diluted 1:100 in PBS-TX-BSA and incubated at 37°C for 30 min. Cover slips were again rinsed three times for 5-min intervals in PBS-TX-BSA. Cover slips were then processed for BrdU detection.

In EdU assays, EdU detection was performed prior to immunohistochemistry for PGP-9.5. To allow for visualization of EdU conjugated to Alexa Fluor® 647, a FITC-conjugated goat anti-rabbit secondary antibody (Jackson ImmunoResearch, West Grove, PA**)** was used to detect PGP-9.5, rather than a rhodamine conjugated secondary antibody. Controls for this experiment comprised a test of the specificity of the primary antibody in PGP-9.5 rich brain regions (positive control), or negative controls in which the primary monoclonal antibody was omitted.

4.2.7 Flow Cytometry

4.2.7a Nodose and Jugular Ganglia Neuron Isolation

At PD 10, 15, 21, or 28 pups were euthanized with an i.p. injection of sodium pentobarbital (50 mg/ml), both vagus nerves were exposed and the left and right nodose and jugular ganglia were removed. Neurons were isolated using a method previously described by Kwong and Lee (8). Briefly, following removal, ganglia were desheathed, cut into smaller pieces and placed in a 0.125% collagenase type IV in Dulbecco's Modified Eagle Medium: Nutrient Mixture F12 (DMEM/F12) media solution overnight at 37°C. To terminate collagenase activity, the suspension was pelleted (150g, 5 min) and resuspended in a solution of 0.15% trypsin EDTA in Hank's Balanced Salt Solution (HBSS) (<1 min) repelleted (150g, 5 min) and resuspended in modified DMEM/F12 solution. This final suspension, containing a mixture of cells and cellular connective tissue fragments was layered on top of a solution of 15% bovine serum albumin (BSA) in DMEM/F12. Subsequent centrifugation (500g, 8 min) through the BSA solution resulted in the trapping of myelinated debris such that the remaining pellet contained mostly neurons free of cellular and connective tissue fragments. The pelleted neurons were collected and then prepared for flow cytometry.

4.2.7b Staining and Analysis

Cell pellets containing isolated neurons were resuspended in 500 µl of DMEM/F12 media with 250 µl of BD Cytofix/Cytoperm Kit (BD Biosciences, San Jose, CA) for 20 minutes to fix and permeabilize them. Cells were incubated with a guinea pig primary antibody (Chemicon/Millipore, Temecula**,** CA) against PGP-9.5 for 30 min at 4°C. After incubation, cells were washed twice to remove any unbound primary antibody, followed by the addition of a R-Phycoerythrin (RPE) conjugated donkey anti-guinea pig antibody (Jackson ImmunoResearch, West Grove, PA). Cells were incubated with the secondary antibody for 30 min at 4°C, then washed twice to remove any unbound antibody, and resuspended in a final volume of 300 µl. Prior to analysis, samples were passed through a 70µm cell strainer to remove cellular debris. Cells were analyzed on a BD FACSAria (BD Biosciences, San Jose, CA) located in the WVU Flow Cytometry Core Facility using DIVA 6.1 software. For each sample, data was collected using a constant flow rate for 60 seconds. Events were deemed neurons if they were PGP-9.5 positive and their size and amount of cellular granulation were consistent with the characteristics of neurons. Neurons that innervate the airways were identified as being FITC positive as an indicator of the retrograde transport of green beads.

To calculate the number of neurons in each sample the following equation was used:

$$\frac{\text{Number of Events}}{\text{Volume Sampled}} = \frac{\text{Neuron Number}}{\text{Total Sample Volume}}$$

For each sample set analyzed, a tube containing a known volume of buffer was run through the FACSAria for the same time and at the same flow rate used for sample analysis. The volume sampled was determined by measuring the amount remaining in the tube.

4.2.7c DAPI Counterstaining

In experiments that utilized the new staining protocol neuronal isolates were incubated with DAPI (1:5000) for ten minutes at 4°C following immunohcytochemical staining for PGP-9.5. Cells were then washed, filtered through a 70 µm cell strainer, and resuspended in a final volume of 300 µl. An event was considered an intact cell if it was DAPI positive.

4.2.8 Cell Proliferation Detection

4.2.8a BrdU Detection

In order to detect BrdU incorporation in nodose and jugular neurons, the Zymed BrdU Staining Kit (Zymed Laboratories, San Francisco, CA) was used. This kit employs a biotinylated monoclonal anti-BrdU for detection and the presence of BrdU is revealed using a highly sensitive streptavidin-biotin staining system. BrdU was detected in accordance with manufacturer instructions. Briefly, following immunohistochemical detection of PGP-9.5, sections were treated with 0.3% hydrogen peroxide to quench endogenous peroxidase activity. Sections were then treated with trypsin and a denaturing solution in order to increase the permeability of sections, thereby enhancing antibody penetration. After rinses with PBS, sections were blocked with a blocking solution to minimize non-specific binding. After rinsing, sections were then incubated with a biotinylated mouse-anti-BrdU antibody at room temperature for 60 min. Slides were rinsed in PBS, and then incubated with a streptavidin-FITC conjugated secondary antibody for 60 min at room temperature. Sections were rinsed again in PBS to remove any unbound antibody, and then Fluoromount (Southern Biotechnology, Birmingham, AL) was used to adhere cover slips to the slides, in order to preserve the fluorescence. Both positive and negative control sections were included in the study. Sections of gut from animals receiving BrdU injections, and those receiving PBS injections, were processed simultaneously

with ganglia sections. Gut was used because of the high proliferation rates of intestinal epithelial cells. Slides were protected from light and stored at 4°C until visualized on the microscope. Images were taken using a LSM510 confocal microscope equipped with the appropriate laser / filter combinations to allow for visualization of both FITC and rhodamine.

4.2.8b EdU Detection

EdU incorporation was detected using the Click-iT® EdU Imaging Kit (Molecular Probes / Invitrogen, Carlsbad, CA). This kit uses a copper-catalyzed covalent reaction between an azide and an alkyne for EdU detection. In this application, the EdU contains the alkyne and the Alexa Fluor® 647 dye contains the azide. EdU detection was performed in accordance with manufacturer instructions. Briefly, following sectioning and collection of samples on gelatin-coated cover slips, sections were incubated with the Click-iT® reaction cocktail (containing copper sulfate and Alexa Fluor® azide component) for 30 min at room temperature in an opaque humidified chamber to protect sections from the light. Cover slips were washed with PBS containing 3% BSA. Cover slips were then processed for immunohistochemical detection of PGP-9.5 and mounted onto slides using Fluoromount (Southern Biotechnology, Birmingham, AL). Both positive and negative control sections were included in the study. Sections of gut from animals receiving EdU injections, and those receiving PBS injections were processed simultaneously with ganglia sections. Sections of ganglia that were processed without adding the Alexa Flour 647 azide, and ganglia sections from animals receiving PBS in *vivo* were also done. Slides were protected from light and stored at 4°C until visualized on the microscope. Images were taken using a LSM510 Confocal microscope equipped with the appropriate laser / filter combinations to allow for visualization of both FITC and Alexa Flour 647.

4.2.9 Statistical Analysis

Results of stereology experiments are expressed as means. Results of flow cytometry experiments are expressed as means $\pm$ SEM. An n of 6 animals was used for all groups except where noted. All data in these experiments were analyzed using a one-way ANOVA, followed by Tukey's post hoc examination when an effect was considered significant. Values were considered significant at a p-value < 0.05.

4.3 Results

4.3.1 Neuron Counts

4.3.1a Airway Neuron Counts: Stereology

Airway neurons were counted to determine if age-related changes in neuron number exist in this subpopulation of nodose and jugular ganglia neurons. Figure 4-2A shows a representative image of nodose and jugular ganglia section that is positively stained for DAPI, while 4-2B is a representative image of cell bodies in the nodose and jugular ganglia containing retrogradely transported beads from the airways. The number of airway neurons in PD6 animals 262 $\pm$ 13 (n=3) was significantly different from all other age groups (Figure 4-2C). PD10 rat pups had 153 $\pm$12 (n=5) labeled airway neurons, where as the numbers of airway neurons in PD15, 28 and 60 were 130 $\pm$ 10.6, 104 $\pm$ 8 (n=2), and 107 $\pm$ 8 (n=2), respectively. No other statistical differences were noted. These studies indicate that as animals age the number of neurons specifically innervating the airway decreases.

4.3.1b Neuron Counts: Flow Cytometry without DAPI counter-staining

Using flow cytometry without DAPI counter-staining it was determined that airway neuron numbers in PD28 2,334 $\pm$ 468 (n=13) animals were significantly different from neuron numbers in PD10 722 $\pm$ 197 (n=10) and PD15 913 $\pm$ 177 (n=7) rats (Figure 4-3A). Airway neuron numbers in PD6 rats 1,050 $\pm$ 208 (n=8) were not significantly different from neuron numbers in any other age groups. The number of total neurons in PD28 rat pups 165,678 $\pm$ 53,570 (n=13) was significantly different from neuron numbers in PD6 12,485 $\pm$ 2,194 (n=8) animals (Figure 4-3B). PD10 rats had 42,979 $\pm$ 5,636 (n=7) total neurons, whereas PD15 animals had 69,829 $\pm$ 16,858 (n=10) total nodose and jugular ganglia neurons. No other significant differences were found. While neuron numbers in PD15 and PD28 rats were not significantly different, the large increase in neuron numbers between the two age groups was unexpected and so studies to determine why such an increase was seen were conducted.

4.3.2 Cell Proliferation Studies

4.3.2a BrdU Detection

In order to establish if increases in total nodose and jugular neuron numbers between PD12 and PD28 were due to neuron proliferation, BrdU studies were performed. Figure 4-4 (A and B) shows representative images of sections of gut from animals administered BrdU in vivo (A) and those receiving PBS in vivo (B). Images of PGP-9.5 and BrdU staining in nodose and jugular ganglia are shown in Figure 4-4C and D. Extensive tissue degradation made

confirmation of BrdU staining in neurons impossible, so a second study to look for proliferation in the nodose and jugular ganglia was undertaken.

4.3.2b EdU Detection

In an attempt to determine if nodose and jugular ganglia neurons are proliferating between PD15 and PD28, EdU studies were conducted. Representative images from EdU experiments are shown in Figure 4-5. Figure 4-5A shows gut from an animal that was administered PBS in vivo and 4-5B is gut from an animal receiving EdU in vivo. Images of ganglia from a rat administered EdU in vivo (Alexa Flour 647 not included in Click-iT® reaction cocktail) and a rat receiving PBS in vivo are shown in Figure 4-5 C and D, respectively. A ganglia section from a rat administered EdU in vivo and stained for PGP-9.5 is shown in Figure 4-5E. Observations of images collected from animals administered EdU in vivo revealed no EdU staining in nodose or jugular ganglia neurons and it was, therefore, concluded that neuronal proliferation was not the cause for the large increase in neuron number between PD15 and PD28.

4.3.3 Neuron Counts: Flow Cytometry (new staining protocol)

As no EdU staining was visualized in nodose and jugular ganglia neurons, amended staining protocols for the flow cytometer assay were attempted. It was decided to counterstain all neuronal isolates with DAPI to identify nuclei in cells. Whole cells were deemed neurons if they were both DAPI positive PGP-9.5 positive. Neurons that innervate the airways were identified as being FITC positive as an indicator of the retrograde transport of green beads.

Statistical analysis to determine if differences existed between the two staining protocols was not performed, however, total nodose and jugular ganglia neuron numbers measured in DAPI stained samples were substantially lower than neuron numbers measured in samples not stained with DAPI (Table 4-1). Based on these results, it was determined that neuron counts would be conducted employing flow cytometry for determination of nodose and jugular neuron number, and all future studies would use DAPI counterstaining.

Table 4-1

Table 4-1. Comparison of Staining Protocols: with DAPI vs. without DAPI				
	PD6	**PD10**	**PD15**	**PD28**
Airway Neuron Number				
PGP-9.5^{+}/DAPI^{+}	83	429	344	453
PGP-9.5^{+}/DAPI^{-}	1051	914	723	2334
Total Neuron Number				
PGP-9.5^{+}/DAPI^{+}	924	8197	12435	6765
PGP-9.5^{+}/DAPI^{-}	12496	42979	69830	165679

Figure 4-1 (7)

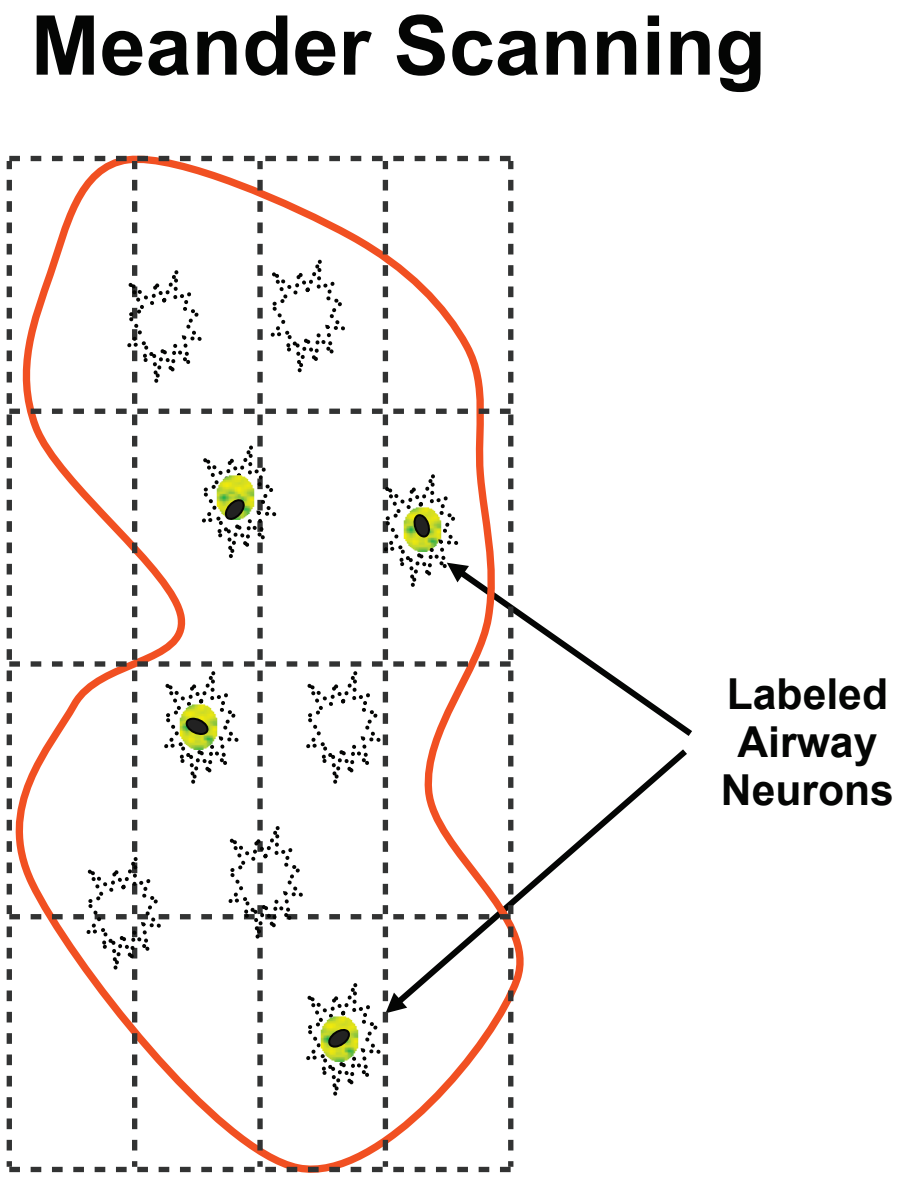

Figure 4-1. Visual representation of meander scanning technique for airway neuron counts. A section of nodose and jugular ganglia is visualized on the microscope at 10x magnification. A tracing of the entire section is drawn, identifying the ganglia as the region of interest (ROI). At 40x airway neurons were identified as containing red or green beads. The meander scan feature of the software overlays a grid on the ROI, and then the motorized stage of the microscope moves within the grid to a new area on the ROI, until all areas of the grid have been counted.

Figure 4-2 (8)

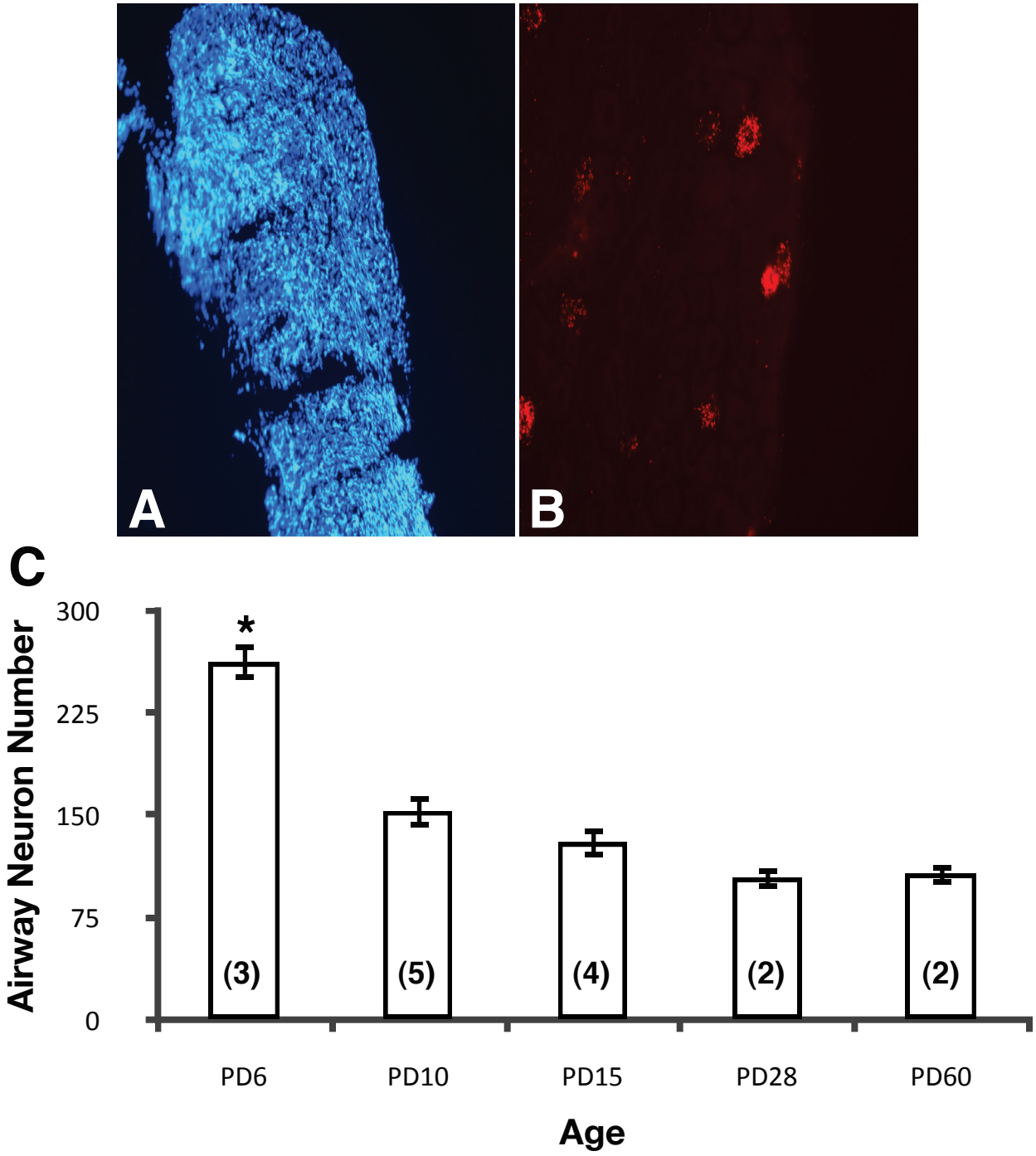

Figure 4-2. Number of airway neurons contained in nodose and jugular ganglia of postnatal day (PD) 6,10,15, 28 and 60 rats as determined by stereology. **(A)** Representative image of nodose and jugular ganglia nuclei stained with DAPI. **(B)** Representative image of neurons labeled with fluorescent microspheres retrogradely transported from the airway. **(C)** A one-way ANOVA followed by Tukey's post-hoc examination found that airway neuron numbers in PD6 animals were significantly higher than in PD10, PD15, PD28 and PD60 animals (* $p<0.05$). Neuron numbers represent the average of all animals sampled for a particular age group. Numbers in parenthesis represent the n value for each age group.

Figure 4-3 (9)

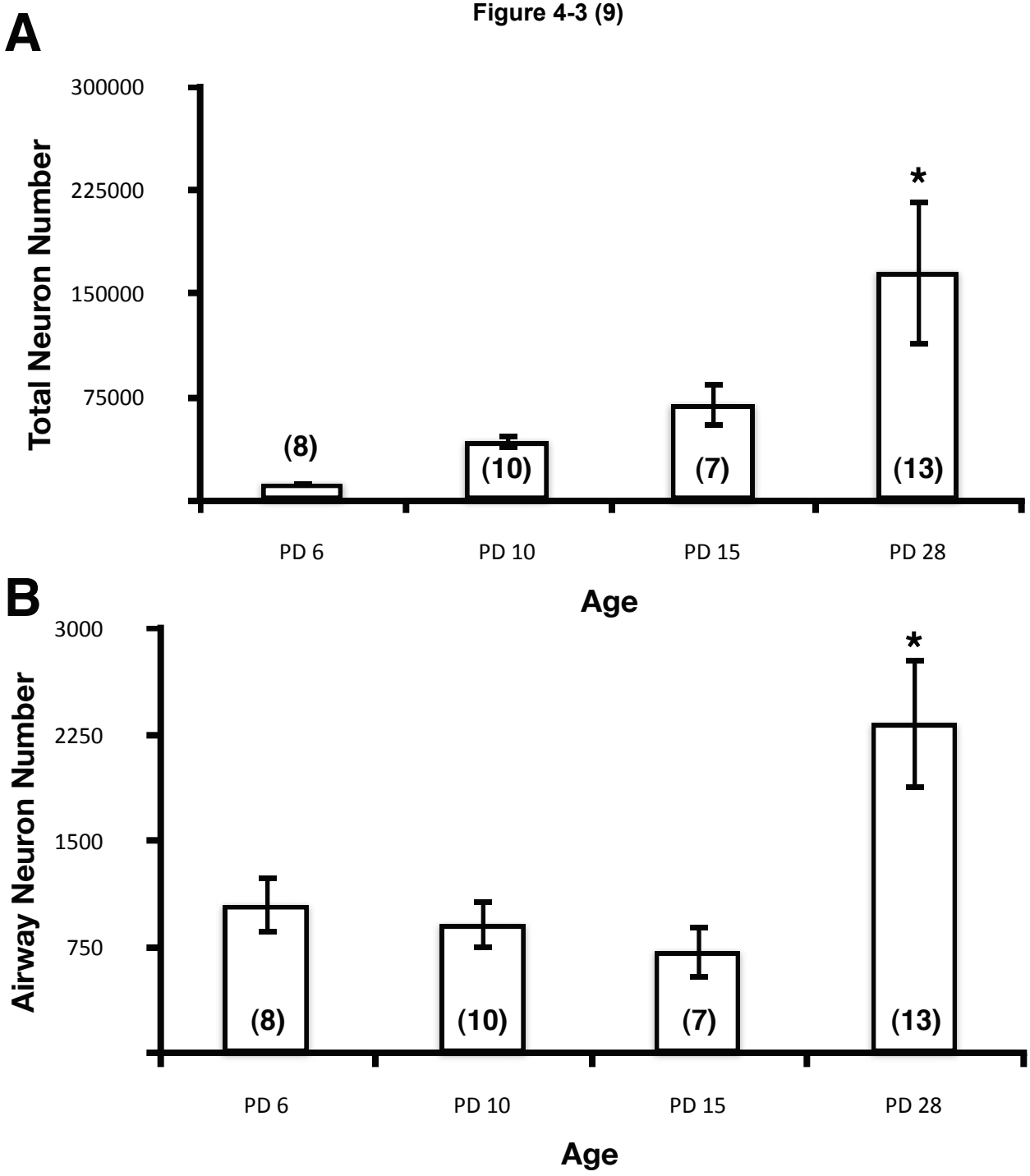

Figure 4-3. Number of total and airway neurons contained in nodose and jugular ganglia of postnatal day (PD) 6,10,15 and 28 rats as determined by flow cytometry. **(A)** Total neuron numbers in PD28 rat pups were significantly different from neuron numbers in PD6 animals. No other significant differences were found. **(B)** Airway neuron numbers in PD28 animals were significantly different from neuron numbers in PD10 and PD15 rats. Airway neuron numbers in PD6 rats were not significantly different from neuron numbers in any other age groups. Numbers in parenthesis represent the n value for each age group. *p <0.05

Figure 4-4 (10)

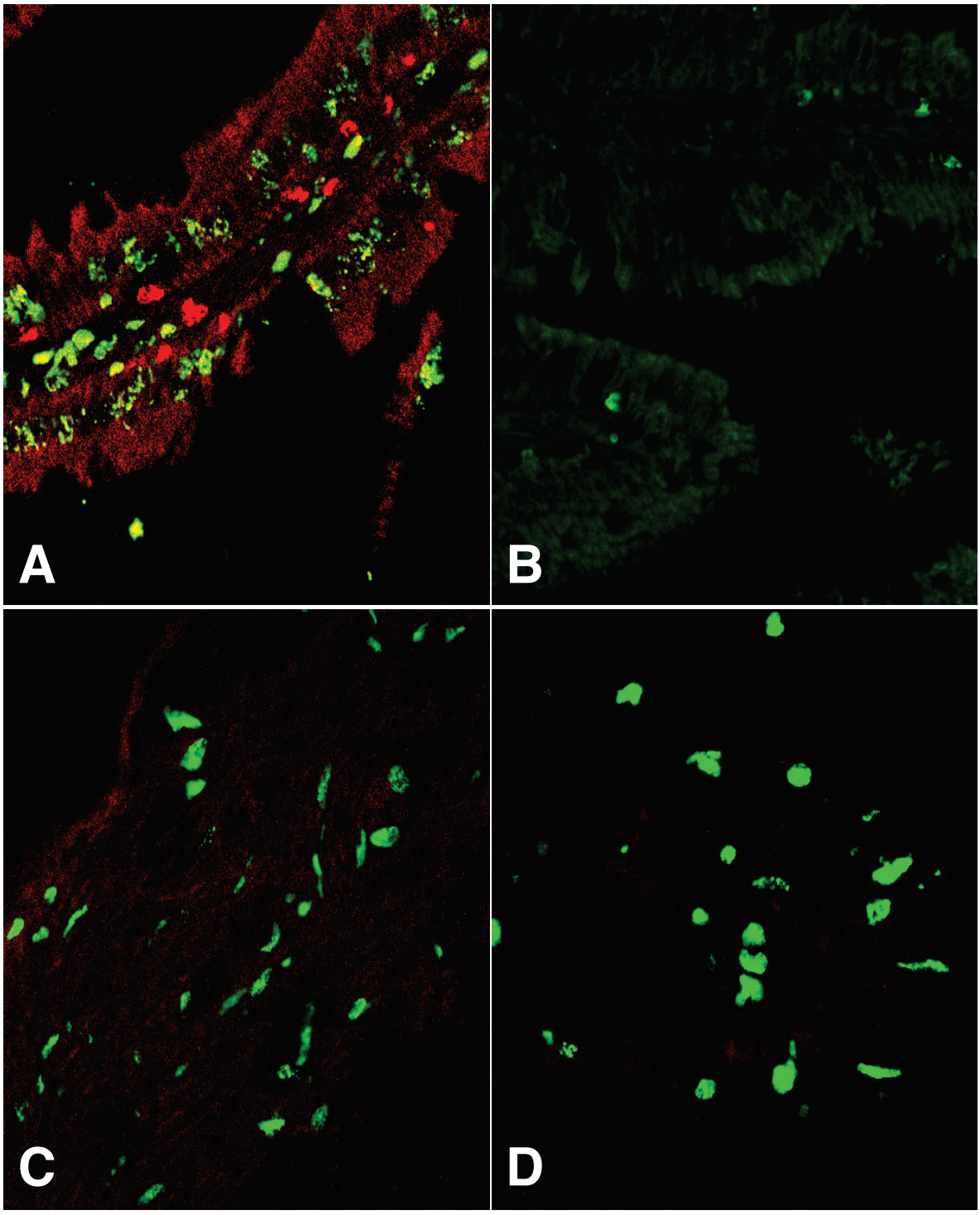

Figure 4-4. BrdU cell proliferation studies. **(A)** Representative image of gut section from a rat administered BrdU (red) in vivo and immunohistochemically stained for PGP-9.5 (green). **(B)** Representative image of gut section from animal receiving PBS in vivo and immunohistochemically stained for PGP-9.5 (green). **(C-D)** Representative Images of PGP-9.5 (green) and BrdU (red) staining in nodose and jugular ganglia.

Figure 4-5 (11)

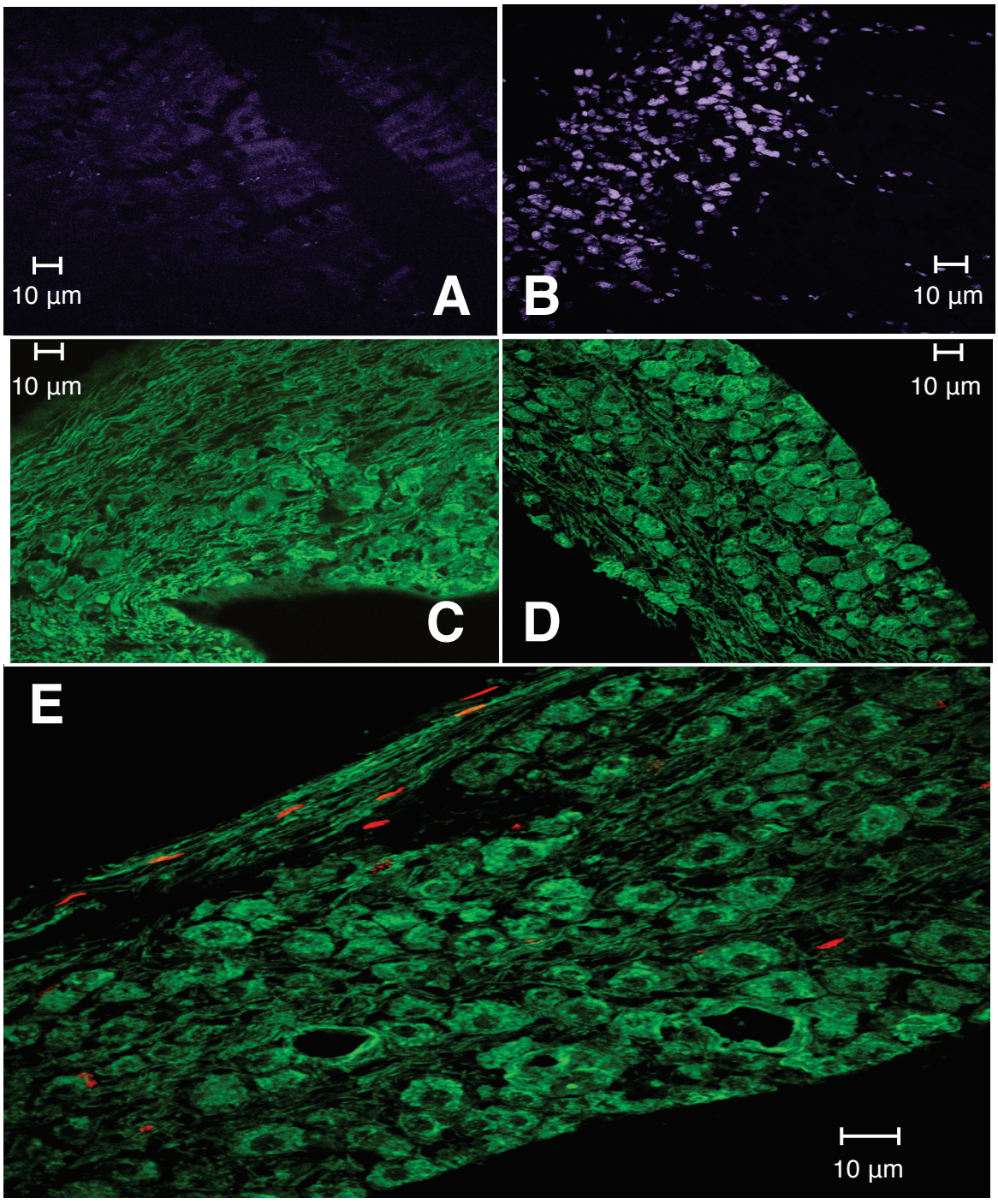

Figure 4-5. EdU cell proliferation studies. **(A)** Representative image of gut from an animal administered PBS in vivo. **(B)** Representative image of gut from an animal receiving EdU in vivo. **(C)** Representative image of nodose and jugular ganglia from rat receiving PBS in vivo. **(D)** Image of nodose and jugular ganglia from a rat administered EdU in vivo (Alexa Flour 647 not included in Click-iT® reaction cocktail). **(E)** Representative image of nodose and jugular ganglia section from a rat administered EdU (red) in vivo and immunohistochemically stained for PGP-9.5 (green).

4.4 Discussion

The results of this series of preliminary assessments indicated that analysis with flow cytometry was a more efficient assay to use than stereology for determining neuron number in the nodose and jugular ganglia. It was also determined that neuron proliferation does not account for increases in neuron number observed during late postnatal development (between PD15 and PD28), and that DAPI counterstaining is an effective technique to decrease variability in neuron counts performed using flow cytometry.

4.4.1 Neuron Counts

4.4.1a Airway Neuron Counts: Stereology

Neuron counts for these studies were initially conducted using fixed, frozen tissue sections because previously conducted studies that aimed to determine neuron number in the nodose ganglia did so using tissue sections. Stereological analysis was chosen in order to decrease bias in counts, and the Stereo Investigator software package “Meander Scanning” tool was used for counting airway neurons in nodose and jugular ganglia (Figure 4-1). Meander scanning allowed for the counting of labeled airway neurons across multiple sections without recounting the same neuron that might appear in several sections. The optimal section thickness for sections used for airway neuron counts was determined to be 25 μm because it allowed the user to count neurons in multiple focal planes in the shortest amount of time. Though beads are clearly visible at high magnifications and are easily captured in images, photobleaching was a concern. Meander scanning must be done in real time and, therefore, sections were exposed for long periods of time, which could result in counting few labeled neurons than are actually present. In addition, the sections used for airway neuron counts were also to be used for total neuron counts, and photobleaching of the DAPI counterstaining was a possible issue (Figure 4-2).

Another possible problem with using stereology as the counting method for nodose and jugular neurons was that the optimal section thickness needed for counting total neuron numbers was 35 μm or greater. As previously discussed above, the optimal section thickness for airway neurons was < 30 μm. Due to this difference in section thickness, additional sets of animals would have been required to complete total neuron counts.

4.4.1b Neuron Counts: Flow Cytometry

Investigation of the literature revealed that flow cytometry had previously been employed to count embryonic dorsal root ganglion neurons, though the application was different than what was used for the studies described in this work. Neuron dissociation techniques used in single cell electrophysiology recording experiments (8) demonstrated that nodose and jugular ganglia neurons could be isolated and individually identified. By moderately adapting this approach, nodose and jugular neurons were isolated and processed for analysis by flow cytometry.

Initial experiments using flow cytometry for neuron counts found that this method of examination reduced the possibility of human bias to nearly zero, as well as having a higher throughput of sample analysis than stereology trials. While flow cytometry proved to be the more rapid counting method, two concerns arose during the optimization process. The first issue was the very sizeable, unexpected increase in neuron number between PD15 and PD28 (Figure 4-3B). The second was that the small proportion of airway neurons to total neurons made detection of labeled airway neurons challenging. Since previous studies examining neuron number in the nodose ganglion were not in agreement as to the pattern of normal postnatal neuron development in the ganglion, studies to determine if neuron proliferation was the cause of the increase were conducted.

4.4.2 Cell Proliferation Studies

Several theories arose to explain why there was such a large increase in neuron number. Older animals have larger nodose and jugular ganglia than younger animals, and it was reasoned that the size increased was not due to and increase in connective tissue alone. Also since the airways are growing during this same time period, more sensory neural input is required, and as a result more neurons are need to meet the increased demand. Further evidence for the possibility of neuronal proliferation came from a study by Czaja et al. (4) in which it was found that following capsaicin-induced neuronal death, new nodose ganglion neurons developed. A similar mechanism might be involved during normal airway sensory neural development, in order to meet the innervation demands of growing airways.

4.4.2a BrdU

BrdU incorporation was initially used to address the first concern that neuron proliferation was a possible cause of the large increase in total neuron number between PD15 and PD28. BrdU was administered at the same time every other day starting on PD22, in an attempt to ensure that the thymidine analog would be present in a high enough concentration to

be incorporated into proliferating cells. This technique, however, proved inconclusive due to the extensive tissue damage that occurred during the detection process (Figure 4-4).

4.4.2b EdU

An alternative thymidine analog that employed a more mild detection process was evaluated in an effort to determine if nodose and jugular ganglion neurons were undergoing mitosis. EdU administration was conducted in the same manner that was used for BrdU administration. The different detection technique used for EdU detection was much less destructive to tissue sections, allowing for the collection of sufficient data to conclude that neuron proliferation was not occurring in nodose and jugular ganglia neurons between PD21 and PD28 (Figure 4-5). Having addressed concerns that neuron proliferation was occurring, the next task was to determine if the flow cytometry technique could be further enhanced to optimize detection of airway neurons as well as elucidate a potential cause for the increase in neuronal number.

4.4.3 Neuron Counts: Flow Cytometry (new staining protocol)

It was decided that a simple yet effective solution to both concerns raised from initial flow cytometry experiments would be to label the nuclei of all cells by counterstaining with DAPI. DAPI staining provided an additional parameter for the identification of neurons in that now only the population of cells having an intact nucleus would be further examined for the presence of the neuronal marker PGP-9.5. From the population of DAPI+PGP+ neurons, the neurons containing beads were much more easily detected because the total population of neurons was now clearly defined, and substantially smaller than the population of total neurons determined during initial flow cytometry experiments (Table 4-1).

4.4.4 Conclusions

These preliminary analyses were successful in indentifying the most effective method for determining neuron number in the nodose and jugular ganglia. Though stereology is a powerful and effective tool that would allow for morphological information to be collected during the process of counting neurons, it was shown to be less efficient than flow cytometry. Employing the flow cytometry assay virtually eliminated all human bias from neuron counts, increased sample throughput, decreased variability in results and allowed for counting total and airway neurons within the same animal. It was for those reasons that flow cytometry was chosen for all future analysis of nodose and jugular neuron number.

References

1. Bakal RS, Wright LL. Postnatal neuron death in the nodose ganglia of the rat. *Developmental Neuroscience* 1993;15:22-26

2. Colin W, Donoff RB, Foote WE. Fluorescent latex microspheres as a retrograde tracer in the peripheral nervous system. *Brain Res* 1989;486:334-339.

3. Cooper E. Synapse formation among developing sensory neurones from rat nodose ganglia grown in tissue culture. *J Physiol* 1984;351:263-274

4. Czaja K, Burns GA, Ritter RC. Capsaicin-induced neuronal death and proliferation of the primary sensory neurons located in the nodose ganglia of adult rats. *Neuroscience* 2008;154:621-630.

5. Hunter DD, Carrell-Jacks LA, Batchelor TP, Dey RD. Role of nerve growth factor in ozone-induced neural responses in early postnatal airway development. *Am J Respir Cell Mol Biol* 2010.

6. Hunter DD, Dey RD. Identification and neuropeptide content of trigeminal neurons innervating the rat nasal epithelium. *Neuroscience* 1998;83:591-599.

7. Katz LC, Burkhalter A, Dreyer WJ. Fluorescent latex microspheres as a retrograde neuronal marker for in vivo and in vitro studies of visual cortex. *Nature* 1984;310:498-500.

8. Kwong K, Lee L-Y. PGE(2) sensitizes cultured pulmonary vagal sensory neurons to chemical and electrical stimuli. *J Appl Physiol* 2002;93:1419-1428.

9. Stefanini M, De Martino C, Zamboni L. Fixation of ejaculated spermatozoa for electron microscopy. *Nature* 1967;216:173-174.

CHAPTER 5*:*

Early Postnatal Ozone Exposure Alters Rat Nodose and Jugular Sensory Neuron Development

Accepted for Publication in Toxicological and Environmental Chemistry

Authors: Zellner LC, Brundage KM, Hunter DD and Dey RD

5.1 Abstract

Sensory neurons originating in nodose and jugular ganglia that innervate airway epithelium (airway neurons) play a role in inflammation observed following exposure to inhaled environmental irritants such as ozone (O_3). Airway neurons can mediate airway inflammation through release of the neuropeptide substance P (SP). While susceptibility to airway irritants is increased in early life, the developmental dynamics of afferent airway neurons are not well characterized. The hypothesis of this study was that airway neuron number might increase with increasing age, and that an acute, early postnatal O_3 exposure might increase both the number of sensory airway neurons as well as the number SP–containing airway neurons. Studies using Fischer 344 rat pups were conducted to determine if age or acute O_3 exposure might alter airway neuron number. Airway neurons in nodose and jugular ganglia were retrogradely labeled, removed, dissociated, and counted by means of a novel technique employing flow cytometry. In Study 1, neuron counts were conducted on postnatal days (PD) 6, 10, 15, 21, and 28. Numbers of total and airway neurons increased significantly between PD6 and PD10, then generally stabilized. In Study 2, animals were exposed to O_3 (2 ppm) or filtered air (FA) on PD5 and neurons were counted on PD10, 15, 21, and 28. O_3 exposed animals displayed significantly less total neurons on PD21 than FA controls. This study shows that age-related changes in neuron number occur, and that an acute, early postnatal O_3 exposure significantly alters sensory neuron development.

5.2 Introduction

Sensory innervation in the airways is important in the pathogenesis of inflammation associated with asthma and other obstructive respiratory disorders (2, 19, 23). However, a few studies have been undertaken to describe the dynamics and development of airway innervation during early postnatal lung development. Furthermore, the lung continues to grow and develop throughout childhood (7) and early childhood is recognized as highly sensitive to the effects of airway irritants, including allergens, cigarette smoke and air pollutants (26).

There are several components of postnatal airway development that contribute to normal sensory innervation. One component originates from the sensory neurons in the nodose and jugular ganglia. These ganglia are largely responsible for the sensory innervation in the thoracic and abdominal viscera, including the heart, lung, and GI tract. Nerve tracing studies demonstrated that airway afferent fibers contain cell bodies located in the nodose and jugular ganglia (5, 11, 14) whose projections include nociceptive C-fibers that mediate airway inflammation through the release of the neuropeptide, SP (8, 15, 22).

Many airway environmental irritants including cigarette smoke, allergens and ozone (O_3) may affect the extent of neuropeptide expression in the airways (6, 13, 17, 18) and early life may be a particularly susceptible period. Hunter et al. (12) found that rats exposed to O_3 during early postnatal life (between postnatal days 2-6), and then re-exposed to O_3 later in life (postnatal day 28), have increased SP innervation compared to rats exposed only on PD28. However, the underlying mechanism generating this altered neural response to early-life O_3 exposure has not been established.

This investigation examined the possibility that neuron number changes in an age-specific manner and that O_3 exposures in early life increase the number of airway neurons as well as raising the number of SP-containing neurons in the nodose and jugular ganglia that innervate the airway. The approach involves a novel technique combining neural tracing of airway neurons, enzymatic dissociation of the nodose and jugular ganglia, and high-throughput cell quantification.

Experimental Design

In order to test the hypothesis, experiments were designed to quantify the number of neurons in the nodose and jugular ganglia innervating the airway epithelium that contain SP.

Study 1: Age Specific Dynamics of Sensory Neurons

The first experiment was designed to determine the normal pattern of development for airway innervating sensory neurons in the nodose and jugular ganglia. Rat pups were instilled with fluorescent microspheres on postnatal days (PD) 2 or 5 to retrogradely label neurons in sensory ganglia innervating airway epithelium. On PD6, 10, 15, 21, or 28 ganglia were removed and dissociated; neurons were isolated, purified, and counted using flow cytometry (Figure 5-1).

Study 2: Ozone or Filtered Air Exposure

The second experiment evaluated if a single acute O_3 exposure in early postnatal life might change the number of neurons containing the inflammatory neuropeptide SP that innervate the airway, or the number of neurons innervating the airway. Animals were instilled with fluorescent microspheres on PD5 to retrogradely label neurons in sensory ganglia innervating airway epithelium. On the same day (PD5), rat pups were exposed to O_3, 2 ppm or filtered air (FA) for 3 hr. Five, 10, 16 and 23 days post treatment (corresponding to postnatal ages 10, 15, 21, and 28 respectively) ganglia were removed, dissociated and neurons were isolated, purified, and counted using flow cytometry (Figure 5-2).

Figure 5-1 (12)

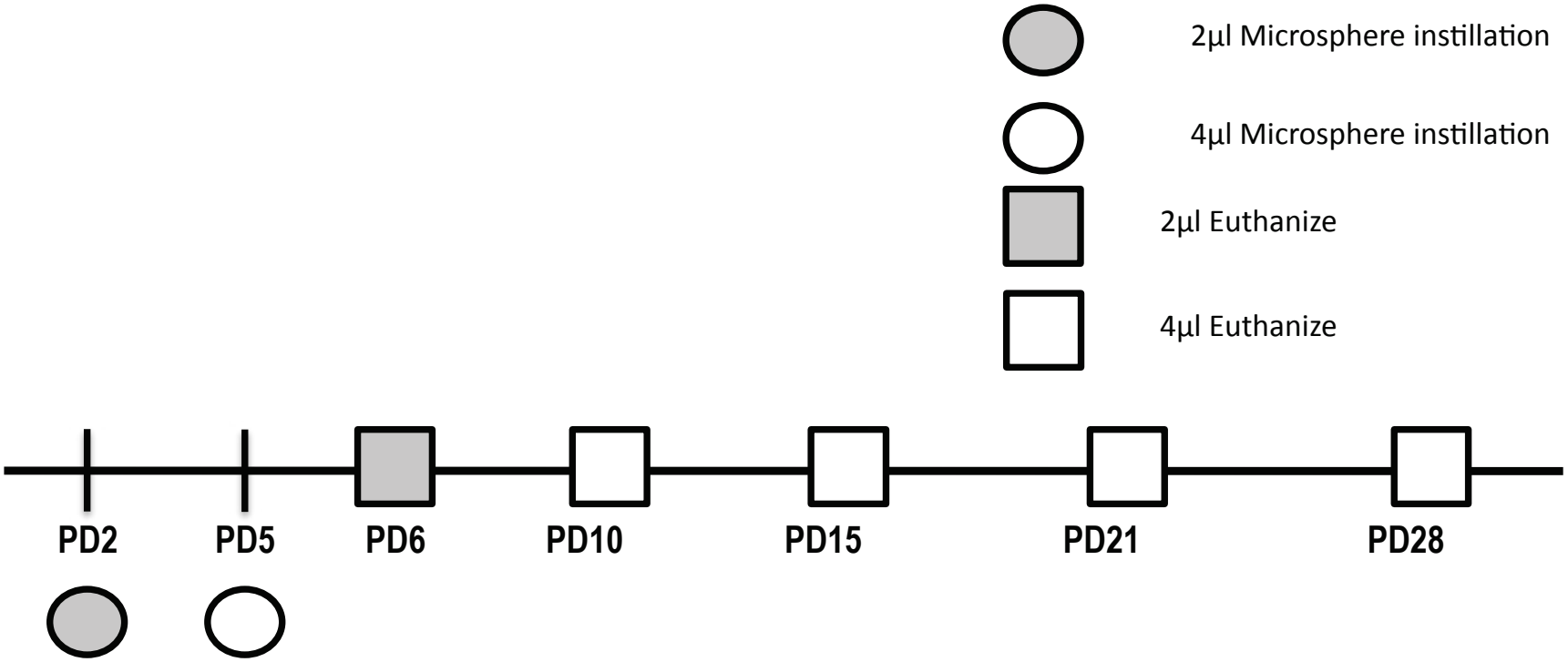

Figure 5-1. Experimental design for study 1: age specific dynamics of sensory neurons. To examine the normal pattern of development of nodose and jugular sensory neurons innervating the airways, tracheas of Fischer 344 rat pups were instilled with fluorescent microspheres on postnatal day (PD) 2 (gray circle) or 5 (white circle). On PD6, animals beaded on PD2 were sacrificed (gray square), while animals beaded on PD5 were euthanized on PD10, 15, or 28 (white square).

Figure 5-2 (13)

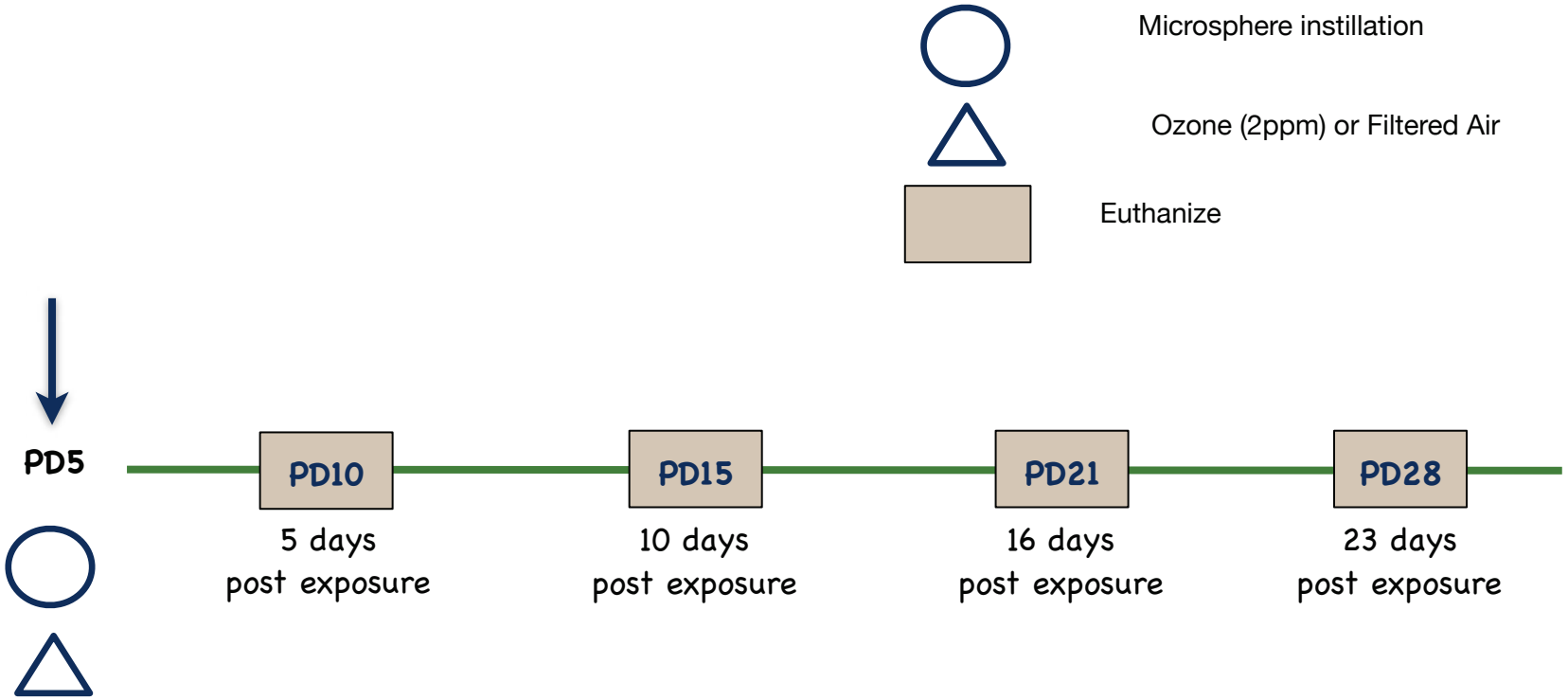

Figure 5-2. Experimental design for study 2: ozone or filtered air exposure. Study 2: To determine if neuron numbers were changing in response to an acute, early postnatal ozone (O_3) exposure, 5-day-old Fischer 344 rat pups were instilled with fluorescent microspheres to retrogradely label sensory neurons innervating airway epithelium (circle). On the same day, pups were exposed to either O_3 (2ppm) or filtered air for 3hr (triangle). Rat pups were returned to their mother's cages, where they remained until sacrifice 5, 10, 16, or 23 days after the exposure, which corresponded to PD10, 15, 21, and 28 respectively (square).

5.3 Materials and Methods

5.3.1 Animals

Late gestation pregnant female Fischer 344 rats were purchased from Harlan Laboratories and kept in filtered ventilated cages in an USDA approved, specific pathogen-free and environmentally controlled animal facility. While in the vivarium, animals were provided with HEPA-filtered air, autoclaved diet and tap water ad libitum and housed under controlled 12hr light-dark cycle and temperature (22-24°C) conditions. After rat pups were born they were kept in the same cage as the mother. Rat pups were analyzed on postnatal days (PD) 10, 15, 21 and 28. All procedures were done in accordance with IACUC regulations and approved IACUC protocols.

5.3.2 Fluorescent Microsphere Instillation

Retrograde tracers were instilled into the tracheal lumen in order to identify sensory neurons in the nodose and jugular ganglia that specifically innervate the airway epithelium. Briefly, on PD2 or 5 depending on the study, rat pups were anesthetized via ice immersion-induced hypothermia (3-5 min; 4). The pups were placed inside a latex sleeve, to protect their skin. When sufficiently anesthetized (unresponsive to foot pinch), trachea was exposed with a midline incision in the skin on the ventral surface of the neck. Next, 2 µl (PD2) or 4 µl (PD5) of Green Fluorescent RetroBeads™ (beads, LumaFluor Inc., Durham, NC) were instilled into the tracheal lumen using a 10 µl Hamilton syringe. Incisions were closed using surgical glue. Rat pups were revived using gentle warming and artificially ventilated if needed. When animals regained consciousness and were breathing normally, pups were returned to their mother. As the beads need a minimum of 4 days to travel from the epithelium to the cell body and It was shown that the beads reach maximal uptake within 7 days of instillation (10), animals being examined on PD6 received bead instillation on PD2, whereas all other age groups rat pups received beads on PD5. Through preliminary studies it was determined that intratracheal bead instillations did not result in airway inflammation as evidenced by a lack of neutrophil infiltration in lung lavage fluid. Optimization of bead instillation volumes were also completed and the selected volumes were found to result in the best survival rates at the specific ages.

5.3.3 Ozone Exposure

Technical details of our ozone exposure apparatus have been published (27). On PD5, following bead instillation, the rat pups were exposed for 3 hr to either O_3 (2ppm) or filtered air (FA) in a stainless steel-and-glass exposure chamber. Passing hospital-grade air through a drying and high-efficiency particle filter and then through an ultraviolet light source produced O_3. The O_3 concentration in the chamber was measured by chemiluminescence with a calibrated O_3 analyzer (model OA 350-2R, Forney, Carrollton, TX). In the FA exposed animals, procedures were identical to those described above except O_3 was not delivered to the exposure chamber.

5.3.4 Nodose and Jugular Ganglia Neuron Isolation

At PD 10, 15, 21, or 28 pups were euthanized with an i.p. injection of sodium pentobarbital (50 mg/ml), both vagus nerves were exposed and the left and right nodose and jugular ganglia were removed. Neurons were isolated using a method previously described by Kwong and Lee (16). Briefly, following removal, ganglia were desheathed, cut into smaller pieces and placed in a 0.125% collagenase type IV in Dulbecco's Modified Eagle Medium: Nutrient Mixture F12 (DMEM/F12) media solution overnight at 37°C. To terminate collagenase activity, the suspension was pelleted (150g, 5 min) and resuspended in a solution of 0.15% trypsin EDTA in Hank's Balanced Salt Solution (HBSS) (<1 min) repelleted (150g, 5 min) and resuspended in modified DMEM/F12 solution. This final suspension, containing a mixture of cells and cellular connective tissue fragments was layered on top of a solution of 15% bovine serum albumin (BSA) in DMEM/F12. Subsequent centrifugation (500g, 8 min) through the BSA solution resulted in the trapping of myelinated debris such that the remaining pellet contained mostly neurons free of cellular and connective tissue fragments. The pelleted neurons were collected and then prepared for flow cytometry.

5.3.5 Flow Cytometry Cell Preparation

Cell pellets containing isolated neurons were resuspended in 500 µl of DMEM/F12 media with 250 µl of BD Cytofix/Cytoperm Kit (BD Biosciences, San Jose, CA) for 20 min to fix and permeablize them. Cells were incubated with a guinea pig primary antibody (Chemicon/Millipore, Temecula, CA) against the pan-neuronal marker, protein gene product 9.5 (PGP-9.5) for 30 min at 4°C. After incubation, cells were washed twice to remove any unbound primary antibody, followed by the addition of a R-Phycoerythrin (RPE) conjugated donkey anti-guinea pig antibody (Jackson ImmunoResearch, West Grove, PA). Cells incubated with the

secondary antibody for 30 min at 4°C, and were then washed twice to remove any unbound antibody. All cells were then incubated for 10 min at 4°C with 4'6-diamindino-2-phenylindole (DAPI) (Sigma Aldrich, St. Louis, MO) in order to label nuclei of cells, washed to remove any unbound DAPI, and resuspended in a final volume of 300 µl. Prior to analysis, samples were passed through a 70µm cell strainer to remove any cellular debris that might remain. Cells were analyzed on a BD FACSAria (BD Biosciences, San Jose, CA) located in the WVU Flow Cytometry Core Facility using DIVA 6.1 software. For each sample, data were collected using a constant flow rate for 60 sec. An event was considered an intact cell if it was DAPI $^{+}$. Whole cells were deemed neurons if they were both DAPI^{+}PGP-9.5^{+}. Neurons that innervate the airways were identified as being FITC^{+} as an indicator of the retrograde transport of green RetroBeads™.

In the second set of experiments, cells from animals in the O_3/FA exposed groups were also labeled for tachykinin, SP. During the primary antibody incubation a mouse monoclonal primary antibody (R&D Systems, Minneapolis, MN) against SP was added at the same time as the anti-PGP-9.5 antibody. In order to detect the SP, a Cy-5 conjugated goat anti-mouse antibody (Jackson ImmunoResearch, West Grove, PA) was added along with the RPE-conjugated secondary antibody. Other than these additions the same procedural steps were taken as described above. This allowed for neurons to be further identified as SP^{+} neurons (non-airway SP-containing neurons, DAPI^{+}PGP-9.5^{+}SP^{+}) or SP^{+} airway neurons (SP-containing airway neurons, DAPI^{+}PGP-9.5^{+}FITC^{+}SP^{+}).

To calculate the number of neurons in each sample the following equation was used:

$$\frac{\text{Number of Events}}{\text{Volume Sampled}} = \frac{\text{Neuron Number}}{\text{Total Sample Volume}}$$

For each sample set analyzed, a tube containing a known volume of buffer was run through the FASCAria for the same time and at the same flow rate used for sample analysis. The volume sampled was determined by measuring the amount remaining in the tube.

5.3.6 Data Analysis

Results of experiments are expressed as mean (± SE). For an individual result to be included in the study, it had to be within 2 standard deviations of the mean. Statistical analysis was evaluated by using a one- or two-way (age and O_3/Air) ANOVA. When an effect was considered significant, a pair-wise comparison was made with a *post hoc* analysis. A value of p less than 0.05 was considered significant for each endpoint and n represents the number of animals studied per experimental group. An n=6 was used for each age group unless otherwise noted.

5.4 Results

5.4.1 Identification and Confirmation of Neurons

The number of neurons contained in the nodose and jugular ganglia was determined using flow cytometry. This method allows for unbiased, absolute counting, as well as the ability to identify multiple populations of neurons in a single run. Cells were first identified as being $DAPI^+$, which indicated the presence of an intact nucleus (Figure 5-3A: blue box). From the $DAPI^+$ population, the neuron specific marker, PGP-9.5, was used to determine which cells were neurons as shown in Figure 5-3B: lower right quadrant (total neurons; $DAPI^+PGP^+$). Neurons projecting to the airway epithelium were neurons that contained Retrobeads™ (airway neurons; $DAPI^+PGP^+FITC^+$) as seen in Figure 5-3B: upper right quadrant. Samples prepared for flow cytometry were also observed by confocal microscopy to confirm the structural and labeling attributes of neurons. Figure 5-4 shows an example of a non-airway neuron. It is labeled for PGP-9.5, indicating a neuron, DAPI showing that it is a whole cell with a nucleus, and had no microspheres indicating it was not a neuron projecting to the airway epithelium. The neuron in Figure 5-5 was labeled for both PGP-9.5 and DAPI, and was also labeled with green microspheres transported from the airway, indicating that this neuron projected to the airway epithelium.

In order to determine the numbers of SP containing neurons in O_3/FA exposed animals, total and airway neurons were first identified. From the $DAPI^+$ population, cells were classified as neurons ($PGP\text{-}9.5^+$) and were then categorized as either being non-airway SP-containing neurons (SP^+ neurons, $DAPI^+PGP^+SP^+$), or SP-containing airway neurons (SP^+ airway neurons,

$DAPI^+PGP^+FITC^+SP^+$) as seen in Figure 5-3C (lower right quadrant and upper right quadrant, respectively). Figure 5-6 is a representative image of a SP-containing airway neuron, demonstrating labeling with DAPI, PGP-9.5, green beads (FITC) and SP.

5.4.2 Age Specific Dynamics of Sensory Neurons

Nodose and jugular ganglia sensory neurons were isolated from rat pups during early postnatal life (PD6, 10, 15, 21, and 28) in order to determine the pattern of normal sensory neuron development of all neurons in the nodose and jugular ganglia and of a subpopulation of neurons innervating the airway epithelium (refer to Figure 5-1).

5.4.2a Total Nodose and Jugular Ganglia Neurons ($DAPI^+PGP\text{-}9.5^+$)

Using FACS, it was determined that the number of neurons at PD6 was 924(±470; Figure 5-7A). There was a significant increase in total neurons between PD6 and PD10 (8197±1170), which remained elevated at all subsequent ages examined (PD15=9677±2596; PD21=6185 ±547; PD28=6765 ±1745). Neuron numbers on PD10 through PD28 were not significantly different from each other. To confirm the quantitative and significant increase in neuron number between PD6 and PD10, ganglia from both ages were removed, weighed, processed for immunohistochemistry and visualized using confocal microscopy. Ganglia removed from PD10 animals (n=3) weighed significantly more than ganglia from PD6 (n=3) rats (Figure 5-8).

5.4.2b Airway Neurons ($DAPI^+PGP\text{-}9.5^+FITC^+$)

The number of airway neurons at PD6 was 83 (±35). Neuron numbers rose significantly to 439 (±51) on PD 10. Airway neuron numbers remained significantly elevated relative to PD6 on PD15 (253 ±73) and PD28 (453 ±105). PD21 (169 ±26) was not significantly different from any other age (Figure 5-7B). Altogether, these results indicate that a substantial increase in total nodose and jugular neurons and in airway neurons occurs during the early periods between PD6 and 10, and that neuron numbers stabilize from PD10 through PD28.

5.4.3 Ozone or Filtered Air Exposure

On PD5, rat pups were instilled with RetroBeads™, exposed to O_3 or FA, then nodose and jugular ganglia sensory neurons were isolated and counted 5, 10, 16, and 23 days after exposure to elucidate if a single acute O_3 exposure might affect sensory neuron development (see Figure 5-2).

5.4.3a Total Neurons ($DAPI^+PGP\text{-}9.5^+$)

Total nodose and jugular ganglia neuron numbers in PD21 rat pups exposed to O_3 (2845 $\pm$1132; n=9) were significantly less than the number of neurons seen in PD21 FA exposed rat pups (10542 $\pm$3150; n=7). Although no other significant differences were seen between groups, total nodose and jugular neuron numbers in O_3 exposed animals were less than the numbers noted in FA exposed animals at PD15, 21, and 28 (Figure 5-9A). Ganglia removed from PD 21 animals exposed to both FA (n=3) and O_3 (n=3) revealed that ganglia from O_3 exposed animals weighed less than ganglia from FA controls (Figure 5-10). Thus, O_3 exposure resulted in a marked reduction in total neuron number in the entire nodose and jugular ganglia compared to FA controls.

5.4.3.b SP^+ neurons ($DAPI^+PGP^+SP^+$)

The numbers of SP^+ neurons in the total nodose and jugular ganglia of the O_3 group were less than the numbers of SP^+ neurons in the FA group at every time point except PD28 (Figure 5-9B). Although no significant differences were observed at any postnatal age, the difference at PD21 rose numerically, (FA- exposed, 1938 $\pm$ 793, n=7 and O_3- exposed, 525 $\pm$ 129, n=8) suggesting a possible reduction in total SP neuron numbers after O_3 exposure.

5.4.3c Airway Neurons ($DAPI^+PGP\text{-}9.5^+FITC^+$)

Although no significant differences were found in airway neuron numbers between the O_3 and FA groups at any time point, the numbers of airway neurons in O_3 exposed animals were quantitatively lower than airway neuron numbers seen in FA controls at PD10, 15, and 21, (Figure 5-11A). While airway neuron numbers in both exposure groups were maximally increased at PD21, as was the case with the numbers of total nodose and jugular neurons, a single early postnatal O_3 exposure did not produce a similarly large decrease in airway neuron number.

5.4.3d SP^+ airway neurons ($DAPI^+PGP^+FITC^+SP^+$)

The numbers of SP^+ airway neurons in O_3 exposed groups were not markedly different from the numbers found in FA groups (Figure 5-11B). However, at PD28, 23 days post exposure, the numbers of SP^+ airway neurons in the O_3 group (41 $\pm$9; n=14) were quantitatively greater than in the FA exposed group (18 $\pm$6). Data indicate that an acute, early postnatal O_3 exposure might play a role in sustaining a specific subpopulation of airway neurons known to play an important role in inflammatory responses in the airways.

Figure 5-3 (14)

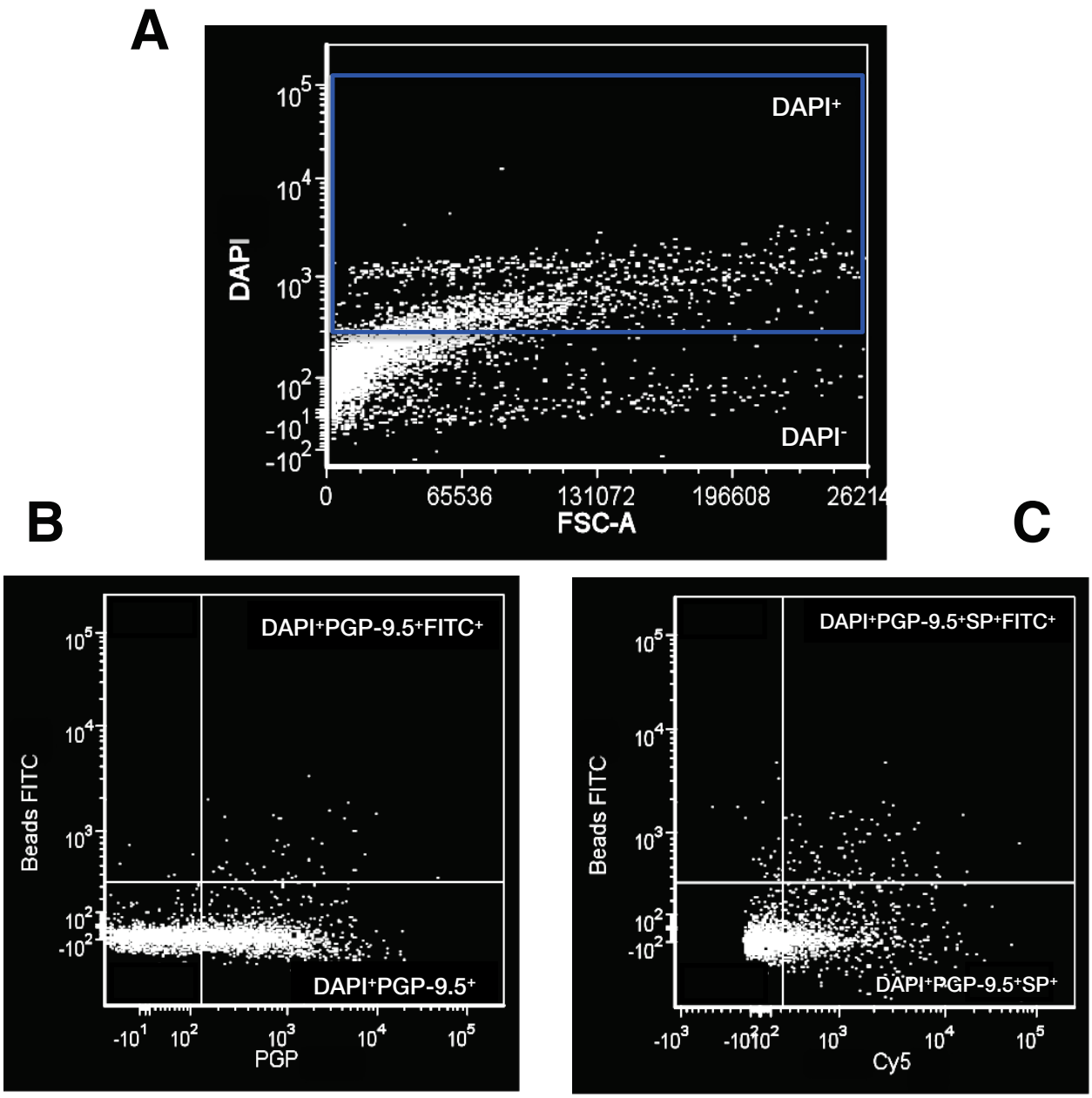

Figure 5-3. Identification of Nodose and Jugular Ganglia Neuron Populations using flow cytometry. Representative scatter plots from flow cytometry experiments. Neurons contained in the nodose and jugular ganglia were identified using flow cytometry as being (A) *whole cells*; DAPI$^+$, (B) *neurons*; DAPI$^+$ PGP-9.5$^+$, *airway neurons*; DAPI$^+$ PGP-9.5$^+$ FITC$^+$, (C) *Substance P neurons*; DAPI$^+$ PGP-9.5$^+$ SP$^+$, or *Substance P airway neurons*; DAPI$^+$ PGP-9.5$^+$ FITC$^+$ SP$^+$.

Figure 5-4 (15)

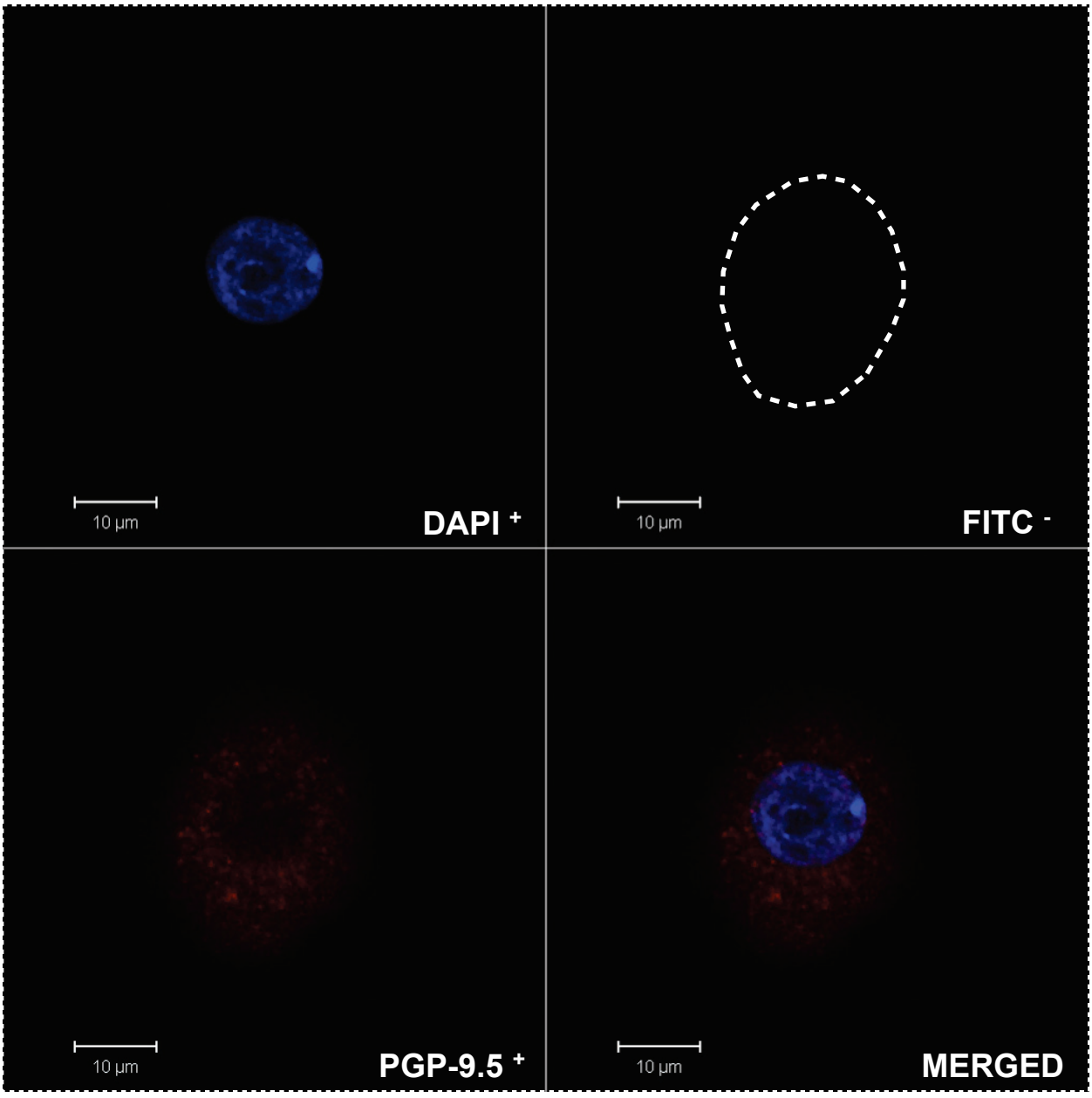

Figure 5-4. Representative confocal microscopy image of a nodose and jugular neuron following flow cytometry quantification. Image was taken on a Zeiss LSM 510 confocal microscope using a 63x/1.4 oil immersion objective. A z-stack (5 sections at 1µm intervals) was taken of each neuron, flattened and a median filter applied using Zeiss AIM software. Contrast was adjusted to enhance detail.

Figure 5-5 (16)

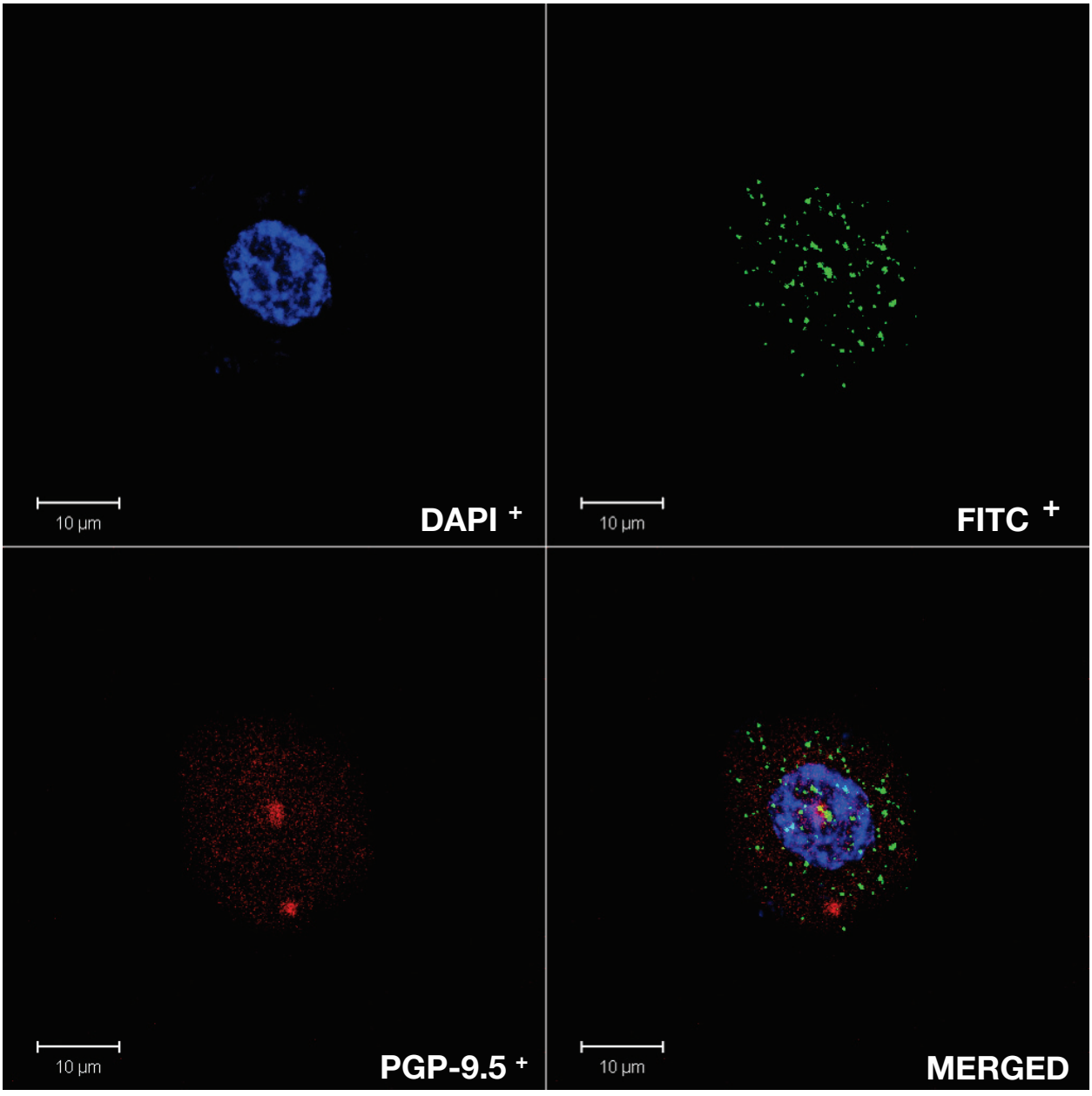

Figure 5-5. Representative confocal microscopy image of a nodose and jugular airway neuron following flow cytometry quantification. Image was taken on a Zeiss LSM 510 confocal microscope using a 63x/1.4 oil immersion objective. A z-stack (5 sections at 1µm intervals) was taken of each neuron, flattened and a median filter applied using Zeiss AIM software. Contrast was adjusted to enhance detail.

Figure 5-6 (17)

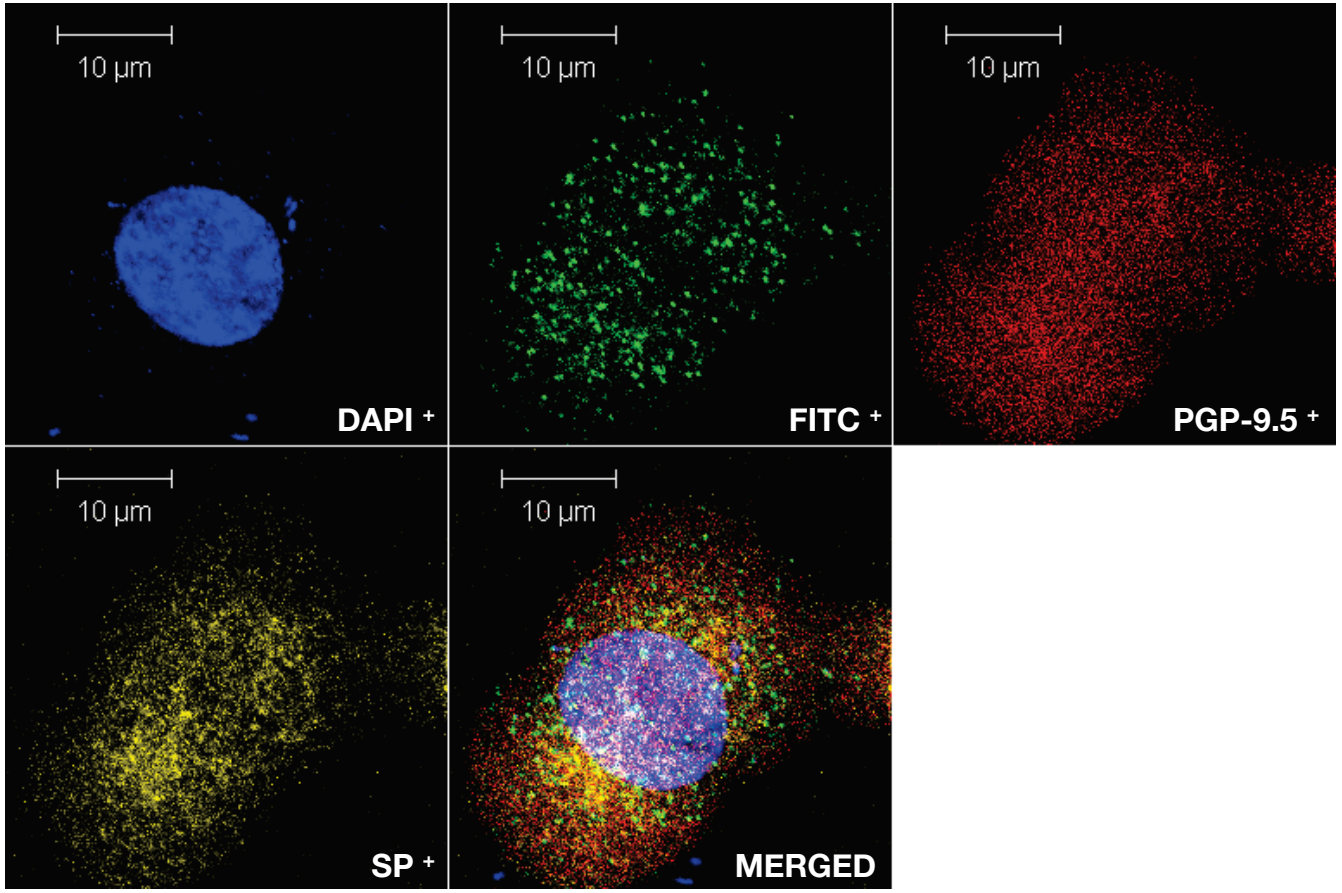

Figure 5-6. Representative confocal microscopy image of a substance P (SP) airway neuron following flow cytometry quantification. Image was taken on a Zeiss LSM 510 confocal microscope using a 63x/1.4 oil immersion objective. A z-stack (5 sections at 1µm intervals) was taken of each neuron, flattened and a median filter applied using Zeiss AIM software. Contrast was adjusted to enhance detail.

Figure 5-7 (18)

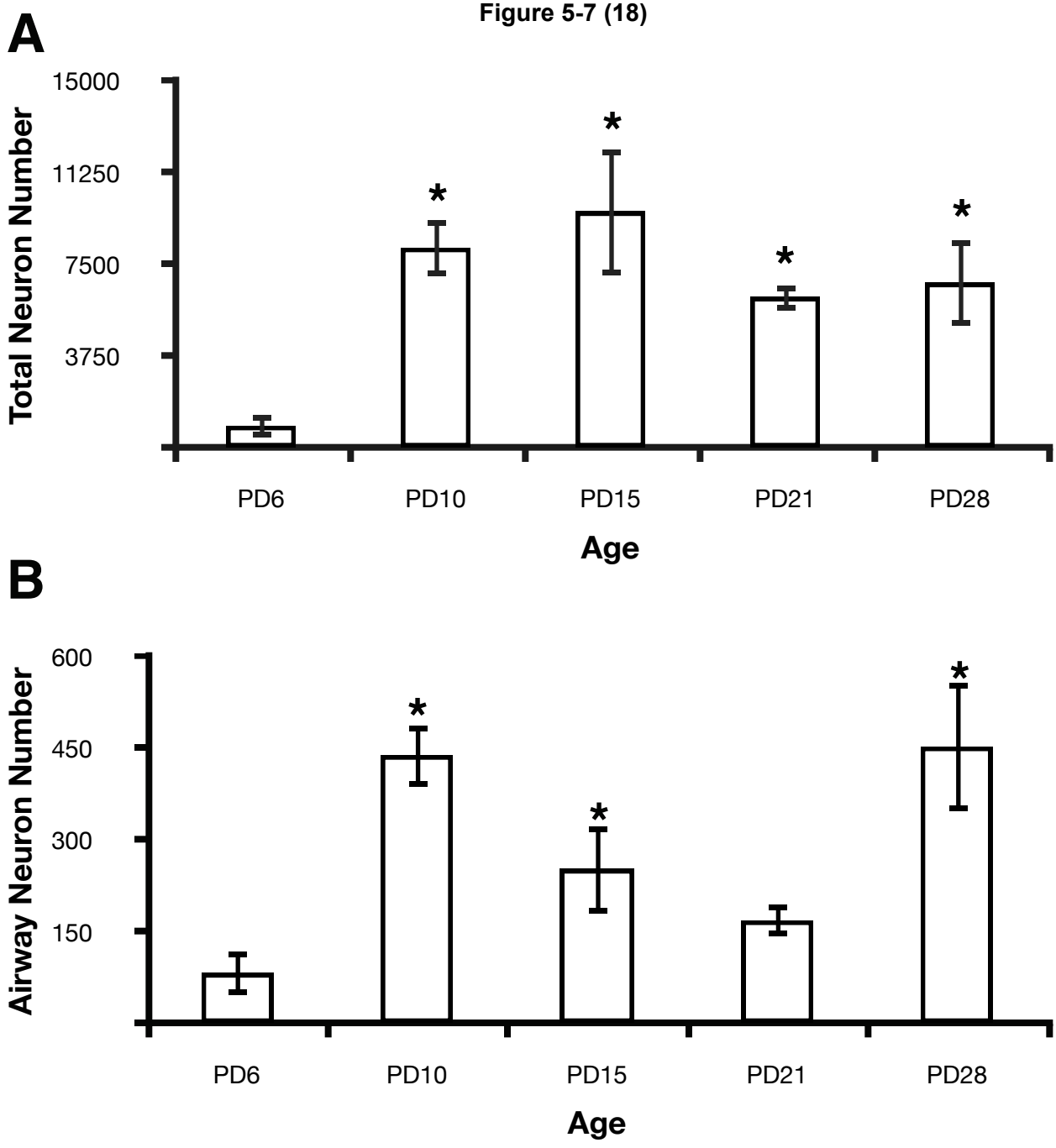

Figure 5-7. Age specific dynamics of sensory nodose and jugular ganglia neurons in postnatal day (PD) 6,10,15, 21, and 28 rats. Total and airway neurons were quantified in this study. All quantifications were done on the FASCSAria Flow Cytometer. Neuron numbers represent the average of all animals sampled for a particular age group. (A) Quantification of total nodose and jugular ganglia neurons ($DAPI^+$ $PGP\text{-}9.5^+$) found that PD6 rat pups significantly less total neurons than PD 10, PD15, PD21, and PD28 animals (* $p<0.05$). (B) Neurons that innervated the airway were labeled using a green fluorescent retrograde tracer, identified as $DAPI^+PGP\text{-}9.5^+FITC^+$ and then quantified. PD10, PD15 and PD28 animals significantly more neurons than PD6 (* $p<0.05$) rats. The number of airway neurons in PD21 animals was not significantly different from any other day examined. n=6 for each age group.

Figure 5-8 (19)

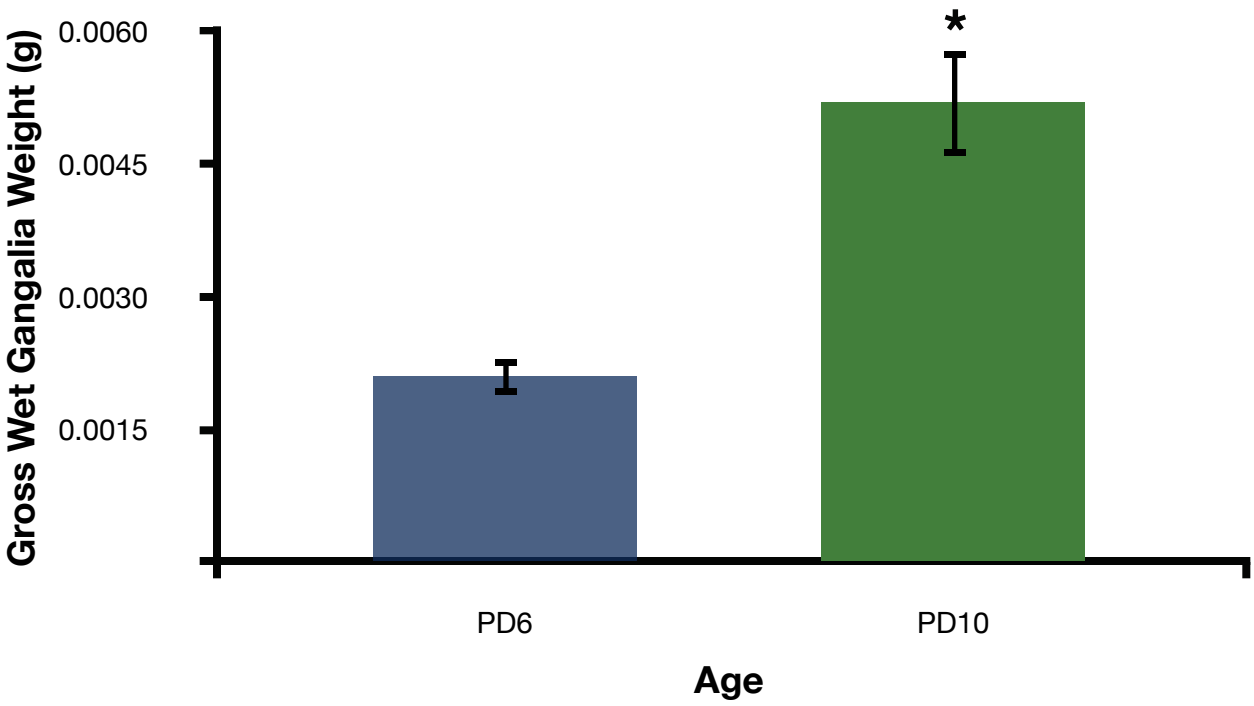

Figure 5-8. Differences in nodose and jugular ganglia gross wet weight postnatal day (PD) 6 and PD10 rats. Ganglia were removed from PD6 (n=3) and PD10 (n=3) animals, weighed and immunohistochemically processed for PGP-9.5 and counterstained with DAPI. Ganglia from PD10 rats weighed significantly more than ganglia from PD6 pups (* = $p<0.05$).

Figure 5-9 (20)

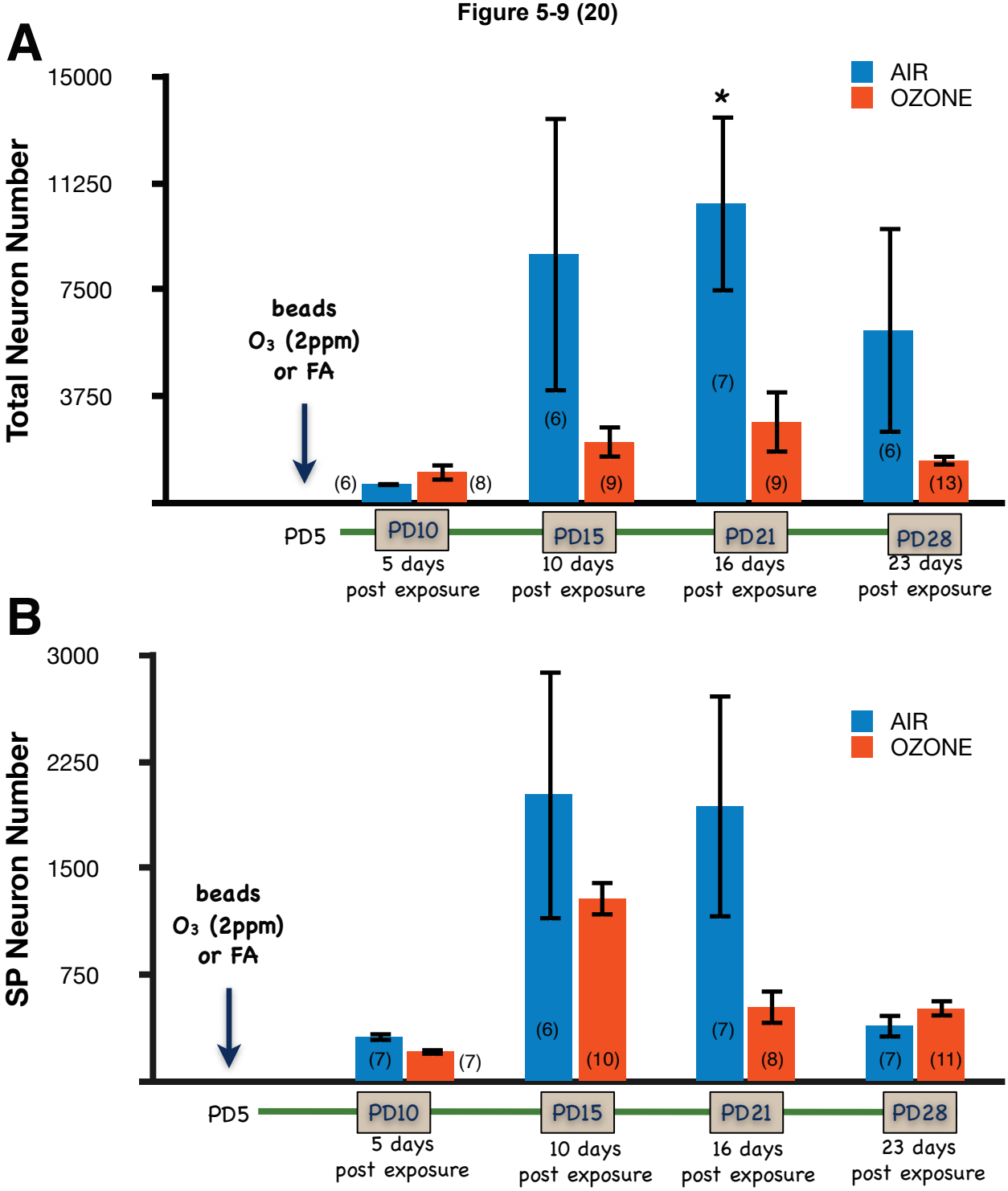

Figure 5-9. Effect of acute postnatal ozone exposure on total nodose and jugular neuron number and total substance P containing neuron number in rats. Rat pups were exposed to ozone (O_3; 2ppm) or filtered air (FA) for 3hr on postnatal day (PD) 5, and then euthanized on PD10, 15, 21, or 28. Total neurons and total substance P (SP) neurons were quantified. All quantifications were done on the FASCSAria Flow Cytometer. Neuron numbers represent the mean of all animals sampled for a particular age group. (A) On PD21, the number of total neurons in O_3 exposed animals was significantly less than the neuron number in the FA group (* $p<0.05$). (B) There were no significant differences between exposure groups in the number of SP neurons. The n value for each age group is listed in parentheses.

Figure 5-10 (21)

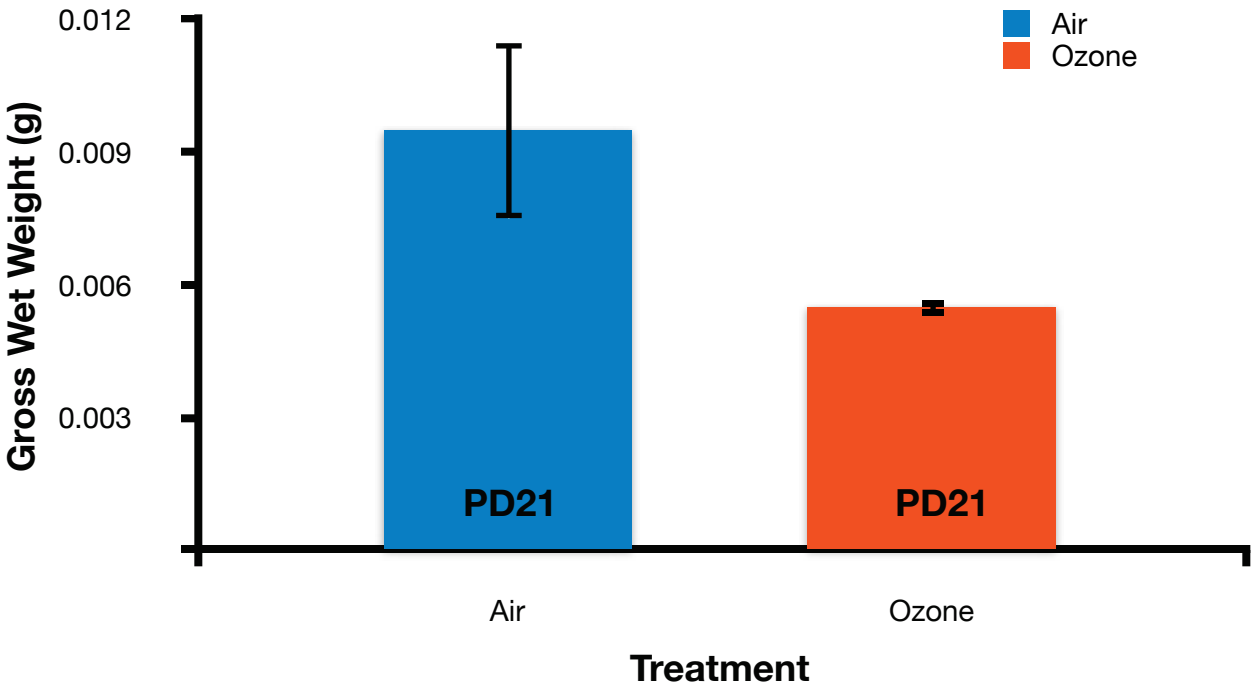

Figure 5-10. Differences in nodose and jugular ganglia gross wet weight in postnatal day (PD) 21 rats following ozone or filtered air exposure on PD5. Rat pups were exposed to ozone (O_3; 2ppm; n=3) or filtered air (FA; n=3) for 3hr on postnatal day (PD) 5, and then euthanized on PD21. Nodose and jugular ganglia were removed, weighed, and immunohistochemically processed for PGP-9.5 and counterstained with DAPI. Ganglia from PD21 animals exposed to FA weighed more than ganglia removed from animals exposed to O_3.

Figure 5-11 (22)

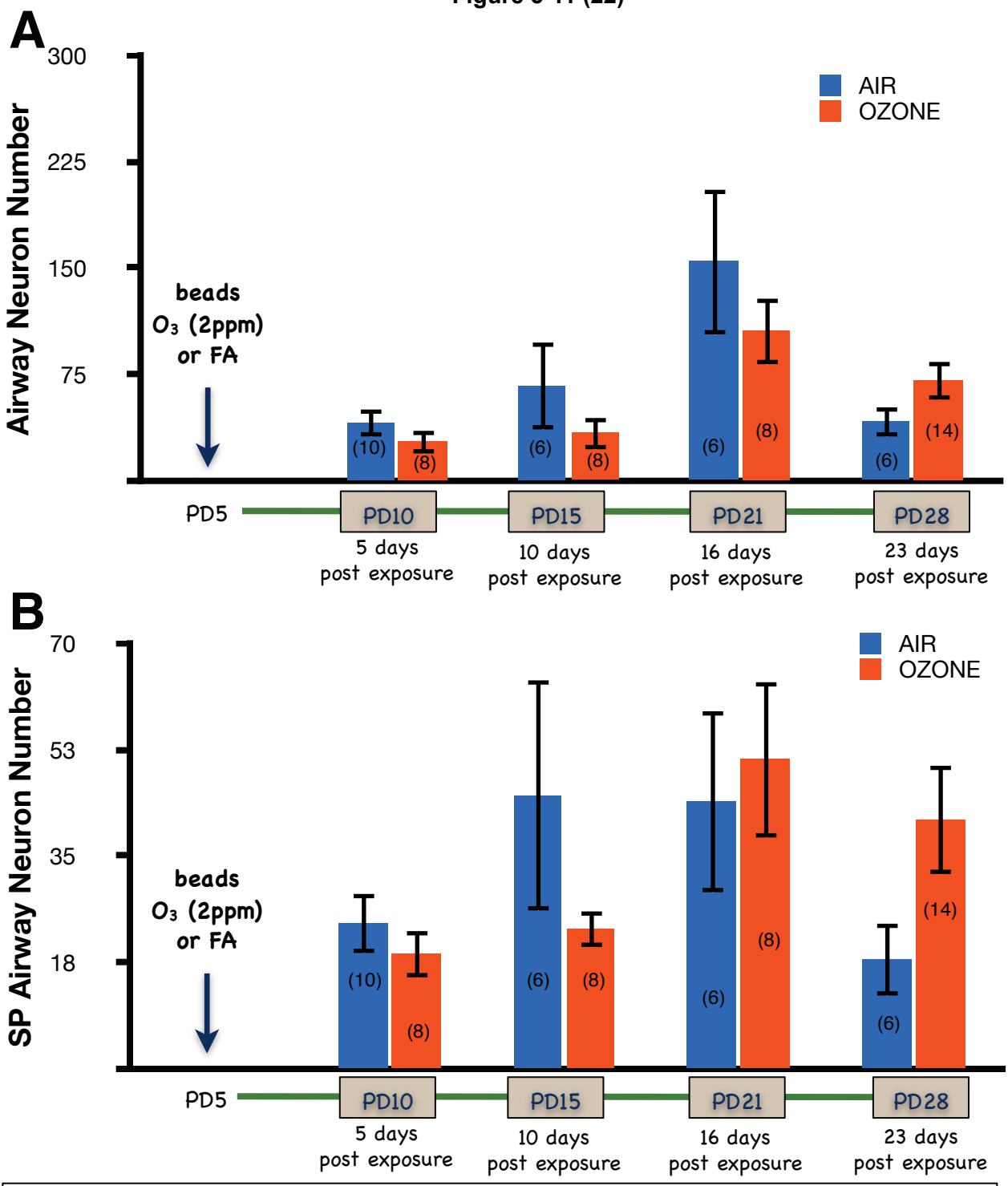

Figure 5-11. Effect of acute postnatal ozone exposure on airway neuron number and substance P containing-airway neuron number in rats. On postnatal day (PD) 5 rat pups were intra-tracheally instilled with fluorescent microspheres, to identify nodose and jugular airway neurons, exposed to ozone (O_3; 2ppm) or filtered air (FA) for 3hr, and then euthanized on PD10, 15, 21, or 28. The number of airway neurons and the number of substance P (SP) airway neurons quantified. All quantifications were done on the FASCSAria Flow Cytometer. Neuron numbers represent the mean of all animals sampled per age group. (A) No significant difference in airway neuron number was found between O_3 and FA exposed groups. (B) Quantification of SP airway neurons found no significant differences between exposure groups. The n value for each age group is listed in parentheses.

5.5 Discussion

The results of this study show that the numbers of labeled airway sensory neurons and the total number of neurons of the nodose and jugular ganglia during early postnatal development, increase between PD6 and 10 and then generally stabilize. Animals exposed to O_3 early in postnatal life show a quantitative reduction in total nodose and jugular ganglia neurons on PD 15, 21, and 28, compared to FA controls. Airway neuron numbers in O_3-exposed animals were also quantitatively decreased compared to FA control animals. The numbers of total SP-containing neurons were no different from numbers found in FA controls. The number of SP-containing airway neurons in O_3 exposed rats were increased on PD28 (23 days post exposure), while in FA controls the numbers of SP^+ airway neurons at the same time point were decreased.

5.5.1 Use of Flow Cytometry for Neuron Counts

Traditionally neuron counts are conducted using immunohistochemistry in conjunction with confocal microscopy, followed by analysis using stereology software. For this study however, flow cytometry was chosen as the preferred counting method for several reasons. Firstly, flow cytometry allowed us to count whole, three-dimensional (3-D) neurons, as opposed to the two-dimensional (2-D) counting that is accomplished with confocal microscopy. The advantage of counting neurons in 3-D, is that the chances of counting the same neuron twice are virtually eliminated. Secondly, by counting neurons using flow cytometry, the sample throughput is increased exponentially. The process of preparing neurons for counting essentially requires the same amount of time as it would to prepare sections for counting, however 40 samples or more can be analyzed in a single day using flow cytometry as opposed to weeks it might take to count neurons from the same number of animals using tissue sections. A third advantage of flow cytometry is that human bias is virtually removed from counting. Instead of a person deciding if a neuron is positive, as is the case in counting by eye, neurons pass a highly sensitive detector that determines if fluorescence is higher than unstained and positive control samples. One final reason flow cytometry was employed in this study, is because it allowed for multiple neuronal markers to be analyzed simultaneously in a single sample. However, possible limitations of this technique that could lead to potential variation in results are that 100% of airway neurons will not be labeled with Retrobeads ™ nor will 100% of neurons be recovered following ganglia dissociation. Additional limitations include variation in dissecting techniques and in antibody labeling due to disparities in manufacturing. Nevertheless

the advantages far outweighed the positives of using traditional sectioning to determine neuron number in the nodose and jugular ganglia.

5.5.2 Age Specific Changes in Neuron Number

5.5.2a Total Nodose and Jugular Ganglia Neurons

The numbers of total neurons determined in this study differ from numbers found in studies by Bakal and Wright (1) and Cooper (3). Bakal and Wright (1) found that total neuron number in the nodose ganglion decreased between postnatal days 1 and 14, while Cooper (3) noted that nodose neuron numbers remained constant from birth. The current study showed that neuron numbers rise between PD6 and PD10, and then stabilize (Figure 5-7A). Both of the previous studies used microscopy techniques to estimate total neuron number. In the current study, neurons from the nodose and jugular ganglia were isolated and counted individually, using flow cytometry, allowing for more exact counting and decreased stereological bias. Because neuron isolation was used in this study, no distinction was made between nodose and jugular ganglia, which is the most likely explanation for the overall larger neuronal number in our study.

5.5.2b Airway Neuron Number

The utilization of retrograde tracing to identify neurons innervating the airway epithelium in this study allowed for the examination of a specific neuronal population that is known to mediate defensive and inflammatory responses in the lung, including the release of SP and neuronal reflexes (20, 21). This is the first time the numbers of this subpopulation of neurons was examined *in vivo* in the context of postnatal development.

The significant increase in airway neuron number between PD6 and PD10 (Figure 5-7B) might be interpreted in several different ways. The first is that neuron proliferation is occurring and that new neurons send new axons to the airway epithelium where they are subsequently labeled with Green Retrobeads. However, this seems to be an unlikely explanation because the growth and development of a new, airway-innervating neuron that would be retrogradely labeled with beads would take longer than the maximum 4 days. Yet, given the quantitative increase in airway neuron numbers, this possibility should not be discounted and requires further study. A second, and more likely possibility is that the rise in neuron number may be attributed to neurons, present in the nodose and jugular ganglia at PD6, whose axons were destined to innervate the airway epithelium but had not yet reached that target until PD10. If the axons were not yet in the epithelium to take up the beads the cell body would not be labeled when

analyzed at PD6 but would be labeled when neuron counts were performed at PD10.

5.5.3 Changes in Neuron Number Following Early Postnatal Acute O_3 Exposure

5.5.3a Total Neuron Number

This study determined that the number of total neurons in the nodose and jugular ganglia of animals exposed to O_3 on PD5, was markedly lower than the neuron number found in FA controls at all ages and significantly lower at PD21 (Figure 5-9A). Despite this sizeable reduction in neuron number, no marked differences were noted between FA and O_3 exposed rats in either body weight or behavior (feeding, grooming, activity, etc). One possible explanation for this significant decrease might be that neurons in the nodose and jugular ganglia also innervate other organs including the heart and stomach. The large fall in neuron number might be attributed to a reduction in neurons innervating those organs. While the studies conducted here focused on the effects of an inhaled O_3 exposure, as animals are placed in an exposure chamber, systemic O_3 exposure is unavoidable. O_3 entering the GI tract may directly interact with nodose and jugular afferent fibers, which might adversely affect neuronal survival. In addition O_3 penetrating the body through skin enters the bloodstream where the gas immediately reacts with biologically active molecules resulting in the formation of free radicals. Circulating free radicals can damage cells, as well as alter protein synthesis and DNA replication (24, 25). Any of these adverse conditions might result in cell death, which may be a possible explanation for the significant fall in total neuron number found in this study.

5.5.3b SP^+ Neuron Number

The number of SP^+ nodose and jugular neurons in O_3 exposed animals was quantitatively lower than the number seen in FA exposed controls at PD 10, 15, and 21 (Figure 5-9B). The lack of change in total number of SP^+ neurons between FA controls and O_3 exposed animals was expected, as the SP+ neurons are a small subpopulation of the total neurons.

5.5.3c Airway Neuron Number

The numbers of nodose and jugular airway neurons in O_3 exposed rat pups were numerically lower (Figure 5-11A). Although this result was unexpected it is particularly interesting when taking into account the quantitative decrease in total nodose and jugular neuron number that was seen following O_3 exposure. Our finding that early postnatal O_3 exposure lowered total neuron number, which had no marked effect on airway neuron number, may indicate that airway neurons possess protective mechanisms allowing them to survive following O_3, while non-airway neurons are more adversely affected.

5.5.3d SP^+ Airway Neuron Number

No significant difference in SP^+ airway neuron number was found between FA controls and O_3 exposed rat pups (Figure 5-11B), however the quantitative increase on PD28 in SP^+ airway neurons 23 days post O3 exposure, is noteworthy. It may lend insight into why Hunter et al. (9) found a rise in the % of SP+ airway neurons in rat pups administered Nerve Growth Factor (NGF) on PD6 and later exposed to O_3 on PD28. O_3 exposure increased both NGF measured in bronchoalveolar lavage fluid and relative levels of NGF mRNA in tracheal epithelial cells (9). In sensory neurons, neuropeptide gene and peptide expression is upregulated by NGF (21). The quantitative changes in SP^+ airway neurons following acute early postnatal O_3 might be mediated by alterations in the amount of NGF present in the airway at developmentally critical periods. While experiments determining how instillation of NGF into the airways affects the numbers of both airway neurons and SP^+ airway neurons, the results of this study may play a role in helping to elucidate the intermediary steps in the mechanism of O_3-induced changes in sensory airway innervation that are occurring during postnatal airway development.

5.5.4 Conclusions

Overall this study shows that the development of sensory neurons in nodose and jugular ganglia is a dynamic process that is not only occurring in an age-related manner, but might also be altered by acute O_3 exposure in early postnatal life.

5.6 Acknowledgements

Flow cytometry experiments were performed in the West Virginia University Flow Cytometry Core Facility, which is supported in part by NIH grants RR016440 and RR020866.

Imaging experiments and image analysis were performed in the West Virginia University Imaging Facility, which is supported by the Mary Babb Randolph Cancer Center and NIH grant P20 RR016440.

Research Support Funding: NIH HL35812, NIH F31085916, NIH HL080566-04

References

1. Bakal RS, Wright LL. Postnatal neuron death in the nodose ganglia of the rat. *Dev Neurosci* 1993;15:22-26.

2. Carr MJ, Hunter DD, Jacoby DB, Undem BJ. Expression of tachykinins in nonnociceptive vagal afferent neurons during respiratory viral infection in guinea pigs. *Am J Respir Crit Care Med* 2002;165:1071-1075.

3. Cooper E. Synapse formation among developing sensory neurones from rat nodose ganglia grown in tissue culture. *J Physiol* 1984;351:263-274

4. Danneman PJ, Mandrell TD. Evaluation of five agents/methods for anesthesia of neonatal rats. *Lab Anim Sci* 1997;47:386-395.

5. Dey RD, Altemus JB, Zervos I, Hoffpauir J. Origin and colocalization of CGRP- and SP-reactive nerves in cat airway epithelium. *J Appl Physiol* 1990;68:770-778.

6. Fischer A, McGregor GP, Saria A, Philippin B, Kummer W. Induction of tachykinin gene and peptide expression in guinea pig nodose primary afferent neurons by allergic airway inflammation. *J Clin Invest* 1996;98:2284-2291.

7. Harding R, Pinkerton KE, Plopper CG, editors. The Lung: Development, Aging and the Environment London: Elsevier Academic Press; 2004.

8. Helke CJ, Hill KM. Immunohistochemical study of neuropeptides in vagal and glossopharyngeal afferent neurons in the rat. *Neuroscience* 1988;26:539-551.

9. Hunter DD, Carrell-Jacks LA, Batchelor TP, Dey RD. Role of nerve growth factor in ozone-induced neural responses in early postnatal airway development. *Am J Respir Cell Mol Biol* 2010.

10. Hunter DD, Dey RD. Identification and neuropeptide content of trigeminal neurons innervating the rat nasal epithelium. *Neuroscience* 1998;83:591-599.

11. Hunter DD, Undem BJ. Identification and substance p content of vagal afferent neurons innervating the epithelium of the guinea pig trachea. *Am J Respir Crit Care Med* 1999;159:1943-1948.

12. Hunter DD, Wu Z, Dey RD. Sensory neural responses to ozone exposure during early postnatal development in rat airways. *Am J Respir Cell Mol Biol* 2010;43:750-757.

13. Kajekar R, Pieczarka EM, Smiley-Jewell SM, Schelegle ES, Fanucchi MV, Plopper CG. Early postnatal exposure to allergen and ozone leads to hyperinnervation of the pulmonary epithelium. *Respir Physiol Neurobiol* 2007;155:55-63.

14. Kalia M, Mesulam MM. Brain stem projections of sensory and motor components of the vagus complex in the cat: I. The cervical vagus and nodose ganglion. *J Comp Neurol* 1980;193:435-465.

15. Kalia M, Mesulam MM. Brain stem projections of sensory and motor components of the vagus complex in the cat: Ii. Laryngeal, tracheobronchial, pulmonary, cardiac, and gastrointestinal branches. *J Comp Neurol* 1980;193:467-508.

16. Kwong K, Lee L-Y. PGE(2) sensitizes cultured pulmonary vagal sensory neurons to chemical and electrical stimuli. *J Appl Physiol* 2002;93:1419-1428.

17. Kwong K, Wu ZX, Kashon ML, Krajnak KM, Wise PM, Lee LY. Chronic smoking enhances tachykinin synthesis and airway responsiveness in guinea pigs. *Am J Respir Cell Mol Biol* 2001;25:299-305.

18. Larson SD, Schelegle ES, Walby WF, Gershwin LJ, Fanuccihi MV, Evans MJ, Joad JP, Tarkington BK, Hyde DM, Plopper CG. Postnatal remodeling of the neural components of the epithelial-mesenchymal trophic unit in the proximal airways of infant rhesus monkeys exposed to ozone and allergen. *Toxicol Appl Pharmacol* 2004;194:211-220.

19. Lee LY, Kwong K, Lin YS, Gu Q. Hypersensitivity of bronchopulmonary C-fibers induced by airway mucosal inflammation: Cellular mechanisms. *Pulm Pharmacol Ther* 2002;15:199-204.

20. Lee LY, Pisarri TE. Afferent properties and reflex functions of bronchopulmonary c-fibers. *Respir Physiol* 2001;125:47-65.

21. Lindsay RM, Harmar AJ. Nerve growth factor regulates expression of neuropeptide genes in adult sensory neurons. *Nature* 1989;337:362-364.

22. Lundberg JM, Saria A, Brodin E, Rosell S, Folkers K. A substance p antagonist inhibits vagally induced increase in vascular permeability and bronchial smooth muscle contraction in the guinea pig. *Proc Natl Acad Sci U S A* 1983;80:1120-1124.

23. Maggi CA, Giachetti A, Dey RD, Said SI. Neuropeptides as regulators of airway function: Vasoactive intestinal peptide and the tachykinins. *Physiol Rev* 1995;75:277-322.

24. Pham-Huy LA, H. Hua, C. Pham-Huy. Free radicals, antioxidants in disease and health. *Int J Biomed Sci* 2008;4:89-96.

25. Ueno I, Hoshino M, Miura T, Shinriki N. Ozone exposure generates free radicals in the blood samples in vitro. Detection by the esr spin-trapping technique. *Free Radic Res* 1998;29:127-135.

26. Wang L, Pinkerton KE. Air pollutant effects on fetal and early postnatal development. *Birth Defects Res C Embryo Today* 2007;81:144-154.

27. Wu ZX, Satterfield BE, Dey RD. Substance P released from intrinsic airway neurons contributes to ozone-enhanced airway hyperresponsiveness in ferret trachea. *J Appl Physiol* 2003;95:742-750.

CHAPTER 6:

General Discussion and Conclusions

The normal postnatal development of airway sensory innervation is discussed, including age specific dynamics of nodose and jugular neuron number, changes in the amount of afferent nerve innervation, differing levels of NGF in the airway throughout postnatal development and the interactions between these different components. The effects of an early life irritant exposure on neurons in the nodose and jugular ganglia are subsequently discussed. Finally, general conclusions together with the implications of these results complete this chapter.

6.1 Discussion of Normal Postnatal Airway Sensory Neural Development

6.1.1 Summary of Results Respective of Age

The major findings of the studies contained within this dissertation reveal that early postnatal life is a time during which airway sensory neural development is undergoing dynamic changes. The amount of NGF measured in BALF at different postnatal ages was not static (Chapter 3; Figure 3-2). Innervation levels of the airway epithelium (nerve fiber density) also fluctuated during development (Chapter 3; Figure 3-1B). The number of total neurons in the nodose and jugular ganglia and the numbers of neurons specifically innervating the airways (airway neurons) also varied with age (Chapter 5; Figure 5-7). The following table (Table 6-1) summarizes differences in each parameter at the postnatal ages examined.

Table 6-1

Postnatal Age	Parameter	Difference with respect to ages
PD6	NGF in BALF*	Lowest concentration
	Epithelium NFD*	Significantly greater than PD28
	Airway Neurons^	Fewest number
	Total Neurons^	Fewest number
PD10	NGF in BALF*	Significantly increased over any other age
	Epithelium NFD*	Significantly increased over PD21 & PD28
	Airway Neurons^	Significantly increased over PD6 & PD21
	Total Neurons^	Significantly more than PD6
PD15	NGF in BALF*	Quantitatively more than PD6, PD21 & PD28
	Epithelium NFD*	Quantitatively more than PD21 & PD28
	Airway Neurons^	Quantitatively more than PD6 & PD21
	Total Neurons^	Greatest number, Significantly more than PD6
PD21	NGF in BALF*	Low concentration
	Epithelium NFD*	Low concentration
	Airway Neurons^	Quantitatively fewer than all days but PD6
	Total Neurons^	Significantly more than PD6; Quantitatively fewer than PD10, PD15, & PD21
PD28	NGF in BALF*	Low concentration
	Epithelium NFD*	Low concentration
	Airway Neurons^	Significantly more than PD6 & PD21
	Total Neurons^	Significantly more than PD6; Quantitatively fewer than PD10 & PD15, Quantitatively more than PD21

* Results found in Chapter 3; ^ Results found in Chapter 5

6.1.2 Airway Neuron Number

As previously described the significant increase in airway neuron number between PD6 and PD10 (Chapter 5, Figure 5-7B) could be interpreted in several different ways. The first is that neuron proliferation is occurring and that new neurons send new axons to the airway epithelium where they are subsequently labeled with Green Retrobeads. A second possibility is that the increase in neuron number could be attributed to neurons, present in the nodose and jugular ganglia at PD6, whose axons were destined to innervate the airway but had not yet reached that target until PD10. If the axons were not yet in the airway to take up the beads the soma would not be labeled when analyzed at PD6 but would be labeled when neuron counts were preformed at PD10. A third possibility is that this increase is a combination of the two aforementioned theories. As the beads need a minimum of four days to travel from the airway to the cell body (9), animals being examined on PD6 received bead instillation on PD2, whereas all other age groups rat pups received beads on PD5. Neurons from rats being analyzed for the

PD10 group would have had only one additional day for bead uptake, which we do not believe would be sufficient time to account for the large increase in neuron number that was observed. It has been shown that the RetroBeads reach maximal uptake within seven days of instillation (9), therefore increasing the number of days that beads were available for uptake should not play a role in the differences in neuron number seen at later time points.

The increase in airway neurons between PD21 and PD28 is harder to explain. It is possible that changes in the availability of trophic factors between PD21 and PD28 cause this increase in airway neuron number. A study conducted by Lommatzsch et al. in 2005 found that in the first few weeks after birth, specifically between PD1 and PD21, the levels of both NGF and BDNF decreased in the lungs, although the concentration of BDNF was always higher than the concentration of NGF. The same study found that BDNF concentrations increased from PD21 onward, while NGF levels remained low (19). In addition, adult neurons from the nodose placode are responsive to BDNF for growth and support (15), and isolated airway smooth muscles cells produce BDNF (14). Thus, it may be that trophic support by NGF in epithelium is receding while BDNF support from airway smooth muscle is increasing. This could explain the recovery of airway neuron numbers in the face of decreasing NGF at PD21 and 28.

Another possibility for the rebound of airway neuron numbers between PD21 and 28 is that Trk receptor expression changes. If airway neurons express more TrkB or less TrkA, in theory there would have an increased probability that these neurons would preferentially respond to BDNF rather than NGF. A decrease in the amount of NGF could be the signal that instigates receptor switching, or perhaps increasing levels of BDNF is a catalyst for initiating changes in receptor expression.

An additional factor that may have affected the developmental dynamics of airway neurons is that the animals were weaned during the time period between PD21 and 28, which could have affected neuronal development. There are several possible stressors that can occur as a result of weaning and stress has been shown to directly affect airway sensory neurons in adult mice (13).

6.1.3 Total Neuron Number

Older animals had significantly more total nodose and jugular ganglion neurons than PD6 rat pups (Chapter 5; Figure 5-7A). Though the highest number of neurons was recorded in PD15 animals, the results of this study revealed that total neuron number in these ganglia

begins to stabilize in the vicinity of PD10. The increase in neuron number was expected since ganglia size and weight (Chapter 5; Figure 5-8) increased as animals aged, and the increase in size is not thought to be strictly related to an increase in connective tissue within the ganglia. Though studies conducted using EdU (Chapter 4; Figure 4-5) did not uncover proliferation occurring in the ganglia, these studies were conducted to determine if mitosis was responsible for large increases in neuron numbers between PD21 – 28 observed in preliminary studies. Experiments to determine if proliferation was occurring at early postnatal ages were not repeated, and, therefore, the possibility of neuronal proliferation still exists. Also because neurons contained in the nodose and jugular ganglia innervate several different target organs, it is difficult to draw conclusions on the significance of the finding that total neuron numbers increase significantly between PD6 and 10.

When comparing findings from different parameters on the basis of postnatal age, a pattern appears to emerge (Table 6-1). Epithelial NFD, NGF in BALF, and airway neuron number, are highest on PD10, indicating that this age may be very important in terms of airway sensory neural development. Because all of these airway specific parameters were significantly increased at PD10, we attempted to discern if there was any correlation between the measured factors.

6.1.4 NGF Levels in BALF vs. Epithelium NFD

As discussed in Chapter 3, no correlation was found between NGF levels in BALF and epithelium NFD (r^2= 0.5531). However, the lack of correlation is not indicative that NGF levels in the airways are entirely unimportant in determining the amount of epithelial innervation (Chapter 3, Figure 3-3). Transgenic mice that over-express NGF specifically in Clara cells have hyperinnervated airways (7). Pioneering studies examining the effects of NGF on neurons demonstrated that neurite outgrowth was significantly increased in the presence of NGF(3). NGF is produced and released from epithelial cells as well as resident immune cells present in the airways (1, 4, 16, 21, 22). A study that determined relative NGF mRNA levels in isolated rat tracheal epithelial cells (RTEs) found that NGF mRNA expression was also greatest at PD10. Although an increase in mRNA expression does not necessarily equate to increased protein production and release this result may indicate that RTEs are a significant source of NGF in the airways (8). However, if the epithelium and immune cells are not stimulated to release NGF into the lumen, it would not be measured in the lavage fluid, and as such, NGF levels measured in lavage fluid do not represent the total amount of NGF in the airway.

6.1.5 NGF Levels in BALF vs. Nodose and Jugular Ganglia Airway Neuron Number

Correlation statistics showed that NGF levels in BALF correlated with the number of airway neurons in nodose and jugular ganglia up until PD21 (r^2= 0.9528, p=0.0472). When the PD28 age group was included no correlation was found (r^2=0.3444). A possibility for the lack of correlation in later postnatal life is that receptor expression on the afferent neurons projecting to the airways may also vary. Though not measured as part of this dissertation, changes in Trk receptor expression would affect the responsiveness of sensory afferents to trophic support in the epithelium. If TrkA receptor expression decreased, neurons would have an attenuated response to NGF and, in turn, neuronal number would be unaffected by changes in NGF.

Another possible reason that airway neuron numbers in PD28 animals do not correlate with NGF levels at the same age is that NGF concentrations in the airway may not be uniform. The studies conducted here used bronchoalveolar lavage to determine the levels of NGF in the airways at different postnatal ages. Bronchoalveolar lavage allows for the measurement of NGF contained in the airway lumen; however, the location of relative NGF concentrations in the airway cannot be determined. Studies conducted in guinea pigs examining the somatic origin of sensory airway innervation patterns have revealed that the sensory afferents in the trachea primarily originate from the jugular ganglia, while the majority of nodose ganglion neurons innervating the airways terminate within the intrapulmonary compartment (17). The differing airway locations of the nerve terminals of sensory afferents originating in the nodose and jugular ganglia present the possibility that a variance in the availability of neurotrophins exists. So while airway neurons may still be responsive to NGF later in life, afferent nerve location could be a large determinant of their access to NGF. Likewise, NGF measured in BALF is not a measurement of total NGF in the airways, as the amount of NGF contained within cells (i.e. not in the lumen) is not accounted for.

6.1.6 Epithelium NFD vs. Nodose and Jugular Ganglia Airway Neuron Number

Though both airway neuron number and epithelium NFD are increased at PD10 and decrease similarly through PD21, no correlation between the two parameters was found (r^2=0.0003). The lack of correlation is most likely due to axonal arborization within airway epithelium. A single airway neuron might have an epithelium innervating axon with multiple arborizations and therefore changes in epithelium NFD would not represent changes in neuron number. Likewise, if a single airway neuron died epithelium NFD might not decrease in a

similar fashion as axonal arborization from a surviving neuron might occur in an effort to maintain proper target innervation.

6.1.7 Airway Neuron Number vs. Epithelium NFD vs. NGF levels

A more compelling indicator of a possible relationship between the airway specific parameters measured during normal development is revealed when examining all three on the same graph. In Figure 6-1, the pattern that emerged in Figure 3-3 between epithelium NFD and NGF levels becomes more evident with the addition of airway neuron numbers. All parameters show rapid increases between PD6 and PD10; NFD, NGF levels and airway neuron numbers were all significantly increased at PD10; all measurements decreased after PD15; and with the exception of airway neuron numbers, remained low through PD28.

Figure 6-1

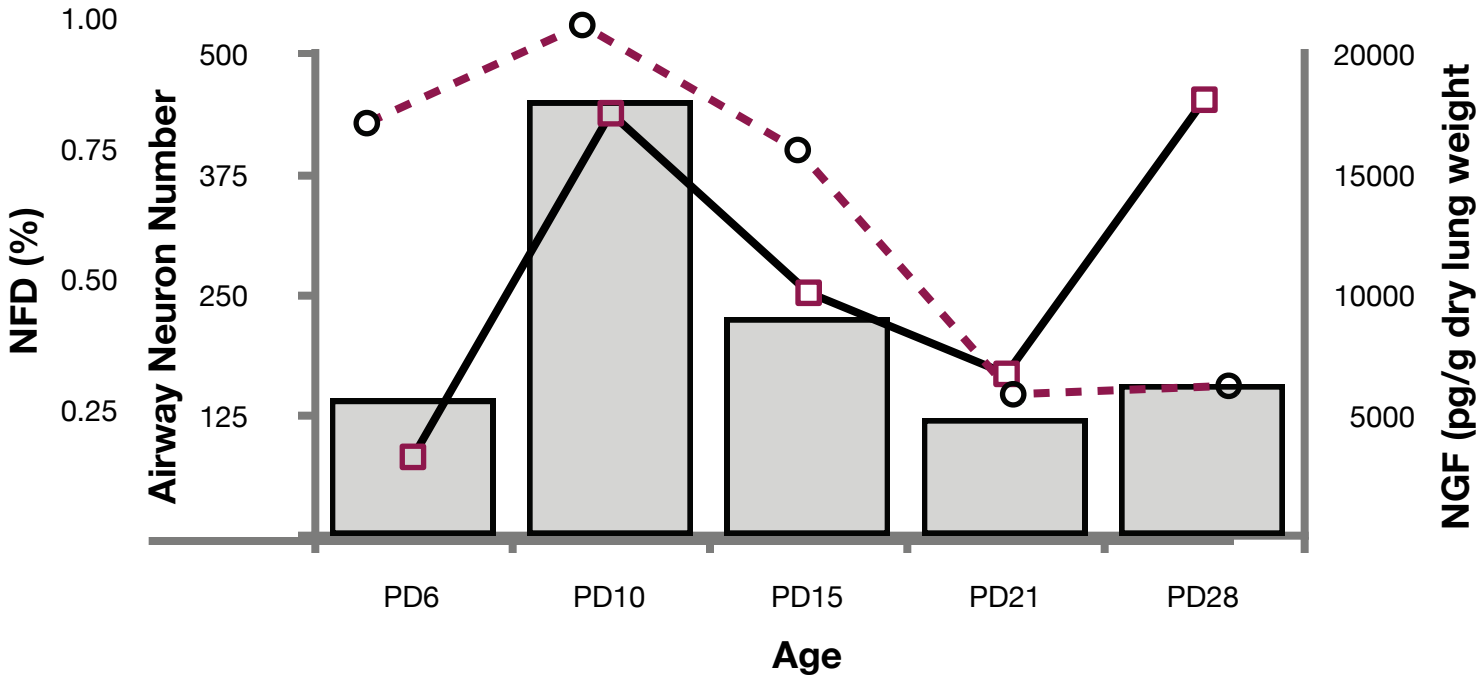

Figure 6-1. Comparison of airway neuron number, nerve growth factor levels and epithelium nerve fiber density during normal development. When graphed together a pattern emerges that appears to indicate a relationship between these three airway specific parameters.

6.2 Discussion of Postnatal Airway Sensory Neural Development Following Acute Early Ozone Exposure

6.2.1 Summary of Results Respective of Age

The major findings of the studies designed to examine the effects of an acute O_3 exposure on nodose and jugular neuron number show that a single O_3 exposure on PD5 can affect sensory neuron development in the nodose and jugular ganglia. In the four neuronal populations examined, animals exposed to O_3 in early postnatal life had fewer neurons than FA exposed counterparts. The number of total nodose and jugular ganglia neurons in O_3 exposed rats was substantially lower at all ages examined and significantly lower on PD21 (Chapter 5; Figure 5-9A). The number of SP+ neurons in rats exposed to O_3 was lower than neuron numbers found in FA exposed animals at all postnatal days (Chapter 5; Figure 5-9B). Airway neuron numbers were slightly lower at all ages except PD28 in O_3-exposed animals (Chapter 5; Figure 5-11A). O_3-exposed rat pups had slightly lower numbers of SP+ airway neurons on PD10 and 15, slightly greater on PD21, and nearly significantly greater on PD28 (Chapter 5; Figure 5-11B). The following table (Table 6-2) summarizes how each of the four neuronal populations examined change after a single O_3-exposure on PD5 when compared with neuronal numbers quantified from rats exposed to FA on PD5.

Table 6-2

Postnatal Age	Neuronal Population	Difference in neuron number in relation to FA exposed rats
PD10	Total Neurons	Quantitatively fewer, no significant difference
	SP^+ Neurons	Quantitatively fewer, no significant difference
	Airway Neurons	No significant difference
	SP^+ Airway Neurons	No significant difference
PD15	Total Neurons	Quantitatively fewer, no significant difference
	SP^+ Neurons	Quantitatively fewer, no significant difference
	Airway Neurons	Slightly fewer, no significant difference
	SP^+ Airway Neurons	No significant difference
PD21	Total Neurons	Significantly fewer
	SP^+ Neurons	Substantially fewer, no significant difference
	Airway Neurons	Quantitatively fewer, no significant difference
	SP^+ Airway Neurons	Quantitatively more, no significant difference
PD28	Total Neurons	Quantitatively lower, no significant difference
	SP^+ Neurons	Quantitatively lower, no significant difference
	Airway Neurons	Quantitatively more, no significant difference
	SP^+ Airway Neurons	Quantitatively more, near significant difference

6.2.2 Total Neuron Number

The large decrease in total neuron number following an acute early life O_3 exposure was not anticipated (Chapter 5; Figure 5-9A). As previously discussed, the substantially lower numbers of nodose and jugular neurons could be due to mixed target tissue innervation. By administering O_3 via inhalation, other organs, such as the heart and GI tract, which also receive sensory innervation from nodose and jugular ganglion neurons, were possibly exposed to an undetermined concentration of O_3, through the blood stream or through swallowing. Based on the experiments performed here, it is unclear whether the O_3 exposure resulted in systemic effects. Though the considerable decrease in the number of nodose and jugular neurons appears to be indicative of an effect of O_3 on neuronal survival.

6.2.3 Substance P Neuron Number

Previous work examining changes in SP neuron number in nodose and jugular ganglia following an exogenous stimulus (NGF, ozone, allergen) differ from work presented here in that previous studies investigated differences in SP immunoreactivity (SP-IR) only 24 hrs post agonist treatment (2, 8, 11). The results presented in those studies revealed that the number of

SP-IR neurons were increased 24 hrs after agonist administration. It might then be expected that the acute O_3 exposure on PD5 in this study would elicit a similar result; however that was not the case. No significant differences in SP neuron number following O_3 were seen at any age, though neuron numbers in O_3 exposed animals were lower than neuron numbers in FA exposed animals on PDs10, 15 and 21 (Chapter 5; Figure 5-9B). As the SP neurons are a subpopulation of the total neurons, the large changes observed in total neuron numbers between FA and O_3 groups result in no difference in the number of SP neurons, despite the seemingly large differences between FA and O_3 exposed groups.

6.2.4 Airway Neuron Number

Though O_3 exposed rats had slightly fewer airways neurons than FA-exposed animals, no significant difference in airway neuron number was noted (Chapter 5; Figure 5-11A). This result was unanticipated given the sizeable differences in total neuron numbers, as it would be expected that a large reduction in total neuron number would affect at least a small proportion of airway neurons. It might then be reasoned that in O_3-exposed rats observing no difference in airway neuron number, while at the same time noting large decreases in total neurons, could be indicative of a protective effect an acute O_3-exposure in early postnatal life has on the survival of airway neurons. The phenomenon of early postnatal O_3-exposure positively affecting neuronal number has, to my knowledge, not been previously described. The exposure paradigm and outcome measurements employed in these studies made it possible to observe the effects of an acute O_3 exposure on postnatal airway neuron development.

6.2.5 SP^+ Airway Neuron Number

The number of SP positive airway neurons in O_3 exposed animals was expected to be greater than the SP^+ airway neuron number determined in FA exposed animals; however, no differences were found (Chapter 5; Figure 5-11B). Studies conducted in rat show an effect of early O_3 exposure on airway reactivity, SP content in sensory afferent nerve fibers, and levels of NGF in the airway lumen. Hunter et al. (12) found a significant increase in SP NFD in the airways of rats initially exposed to O_3 on PD4 and then re-exposed to O_3 on PD28. This increase was not seen in groups that received initial O_3 exposures later in life (PD21), or in groups receiving FA rather than O_3 on PD28 (12). This work revealed that airway sensory neural development is potentially more susceptible to the adverse effects of O_3 exposures occurring during early postnatal life. The same group found that O_3 exposure increased NGF levels measured in the airways, 24 hrs post exposure (8). NGF is known to increase tachykinin gene

expression in sensory neurons (18), as well as increase the number of SP-IR nodose and jugular neurons (10).

Further examination of the effects of exogenous stimuli on early postnatal airway sensory neural development demonstrated that rats receiving intratracheal NGF administration on PD6, and O_3 exposure on PD28 had an increased percentage of SP-IR airway neurons (8). Airway neuron SP-IR was unchanged in groups that received NGF instillations later in postnatal life, vehicle rather than NGF, or FA instead of O_3 exposure. Therefore, with two potentially linked mechanisms for increasing SP-IR in nodose and jugular neurons, an increase in SP positive airway neurons following acute ozone in early postnatal life was probable. Though experiments conducted for this dissertation did not show a difference in SP positive airway neuron number, alterations in when data was collected following O_3 exposure, and differences in the exposure paradigm between the studies, most likely account for this.

Early postnatal increases of inflammatory mediators in the airway may result in altering the regulation of tachykinin gene expression, inasmuch that the amount of gene expression in older animals may be lower when no airway insult occurs in early life. Studies conducted in humans found that adults have lower levels of SP innervation than infants and children (6). This appears to indicate a decrease in preprotachykinin-1 (PPT-1) gene expression, although a decrease in translation of SP protein would also account for decreased levels of SP in adults. So perhaps a more accurate conclusion to draw would be that increases in early postnatal inflammatory mediators in the airways could result in altered SP protein synthesis, whether the difference lies at the level of transcription or translation or both needs to be elucidated.

6.3 Conclusions and Implications

Overall the studies conducted as part of this dissertation reveal that early postnatal life between birth and PD10 is a period of rapid growth and development in the airway. The airway specific parameters (epithelium NFD, NGF in BALF, and airway neuron numbers) measured during normal postnatal development changed in an age-related manner, and fluctuated in the same direction and on the same postnatal days. Based on data presented in Chapter 5 it can also be concluded that the postnatal development of sensory neurons in the nodose and jugular ganglia can be disrupted by a single early life O_3 exposure.

The large deficit in total neuron number following O_3 exposure may represent suppressed neuronal development rather than O_3-induced cell death. Ganglia removed from PD21 rats weighed markedly less in the O_3-exposed groups compared with FA-exposed rat pups, which might also indicate developmental deficiencies. Despite the large differences in total neuron numbers between O_3-exposed and FA-exposed animals no differences were noted in the numbers of airway neurons. This result might signify a protective effect of O_3 exposure on airway neurons, a mechanism that may be mediated through the release of neurotrophins in the airways. Early postnatal O_3 exposure increases NGF protein and mRNA in the airways 24 hrs after exposure (8) and populations of neurons in both vagal ganglia are reliant on NGF for trophic support during development (5, 20); indicating that increased availability of trophic factors in the airways might allow airway neurons to overcome the developmental deficiencies that affected non-airway neurons. When also taking into account the increases in the numbers SP positive airway neurons, the results of these studies may provide insight for how early life O_3 exposure results in enhanced airway sensitivity to secondary exposures in later life.

References

1. Braun A, Appel E, Baruch R, Herz U, Botchkarev V, Paus R, Brodie C, Renz H. Role of nerve growth factor in a mouse model of allergic airway inflammation and asthma. *Eur J Immunol* 1998;28:3240-3251.

2. Chuaychoo B, Hunter DD, Myers AC, Kollarik M, Undem BJ. Allergen-induced substance P synthesis in large-diameter sensory neurons innervating the lungs. *The Journal of Allergy and Clinical Immunology* 2005;116:325-331.

3. Cohen S, Levi-Montalcini R, Hamburger V. A nerve growth-stimulating factor isolated from sarcom as 37 and 180. *Proc Natl Acad Sci U S A* 1954;40:1014-1018.

4. Ehrhard PB, Erb P, Graumann U, Otten U. Expression of nerve growth factor and nerve growth factor receptor tyrosine kinase trk in activated CD4-positive T-cell clones. *Proc Natl Acad Sci U S A* 1993;90:10984-10988.

5. Forgie A, Kuehnel F, Wyatt S, Davies AM. In vivo survival requirement of a subset of nodose ganglion neurons for nerve growth factor. *The European Journal of Neuroscience* 2000;12:670-676

6. Hislop AA, Wharton J, Allen KM, Polak JM, Haworth SG. Immunohistochemical localization of peptide-containing nerves in human airways: Age-related changes. *Am J Respir Cell Mol Biol* 1990;3:191-198.

7. Hoyle GW, Graham RM, Finkelstein JB, Nguyen KP, Gozal D, Friedman M. Hyperinnervation of the airways in transgenic mice overexpressing nerve growth factor. *Am J Respir Cell Mol Biol* 1998;18:149-157.

8. Hunter DD, Carrell-Jacks LA, Batchelor TP, Dey RD. Role of nerve growth factor in ozone-induced neural responses in early postnatal airway development. *Am J Respir Cell Mol Biol* 2010.

9. Hunter DD, Dey RD. Identification and neuropeptide content of trigeminal neurons innervating the rat nasal epithelium. *Neuroscience* 1998;83:591-599.

10. Hunter DD, Myers AC, Undem BJ. Nerve growth factor-induced phenotypic switch in guinea pig airway sensory neurons. *Am J Respir Crit Care Med* 2000;161:1985-1990.

11. Hunter DD, Undem BJ. Identification and substance P content of vagal afferent neurons innervating the epithelium of the guinea pig trachea. *Am J Respir Crit Care Med* 1999;159:1943-1948.

12. Hunter DD, Wu Z, Dey RD. Sensory neural responses to ozone exposure during early postnatal development in rat airways. *Am J Respir Cell Mol Biol* 2010;43:750-757.

13. Joachim RA, Cifuentes LB, Sagach V, Quarcoo D, Hagen E, Arck PC, Fischer A, Klapp BF, Dinh QT. Stress induces substance P in vagal sensory neurons innervating the mouse airways. *Clinical and Experimental Allergy: Journal of the British Society for Allergy and Clinical Immunology* 2006;36:1001-1010

14. Kemi C, Grunewald J, Eklund A, Hoglund CO. Differential regulation of neurotrophin expression in human bronchial smooth muscle cells. *Respir Res* 2006;7:18.

15. LeMaster AM, Krimm RF, Davis BM, Noel T, Forbes ME, Johnson JE, Albers KM. Overexpression of brain-derived neurotrophic factor enhances sensory innervation and selectively increases neuron number. *The Journal of Neuroscience: The Official Journal of the Society for Neuroscience* 1999;19:5919-5931

16. Leon A, Buriani A, Dal Toso R, Fabris M, Romanello S, Aloe L, Levi-Montalcini R. Mast cells synthesize, store, and release nerve growth factor. *Proceedings of the National Academy of Sciences of the United States of America* 1994;91:3739-3743.

17. Lieu T, Kollarik M, Myers AC, Undem BJ. Neurotrophin and GDNF family ligand receptor expression in vagal sensory nerve subtypes innervating the adult guinea pig respiratory tract. *Am J Physiol Lung Cell Mol Physiol* 2011;300:L790-798.

18. Lindsay RM, Harmar AJ. Nerve growth factor regulates expression of neuropeptide genes in adult sensory neurons. *Nature* 1989;337:362-364.

19. Lommatzsch M, Quarcoo D, Schulte-Herbruggen O, Weber H, Virchow JC, Renz H, Braun A. Neurotrophins in murine viscera: A dynamic pattern from birth to adulthood. *Int J Dev Neurosci* 2005;23:495-500.

20. Snider WD. Functions of the neurotrophins during nervous system development: What the knockouts are teaching us. *Cell* 1994;77:627-638.

21. Tam SY, Tsai M, Yamaguchi M, Yano K, Butterfield JH, Galli SJ. Expression of functional TrkA receptor tyrosine kinase in the HMC-1 human mast cell line and in human mast cells. *Blood* 1997;90:1807-1820.

22. Torcia M, Bracci-Laudiero, L., Lucibello, M., Nencioni, L., Labardi, D., Rubartelli, A., Cozzonlino, F., Aloe, L., Garaci, E.,. Nerve growth factor is an autocrine survival factor for memory B lymphocytes. *Cell* 1996;85:345-356.

Curriculum Vitae

Education:

Current **Doctor of Philosophy**, Cellular and Integrative Physiology
West Virginia University, Morgantown, WV
Dissertation: Effects of Age and Early Life Ozone Exposure on the Developmental Dynamics of Afferent Airway Neurons in Postnatal Rats

Research interests: sensory neural development, airway innervation, inflammation and neuronal responses to inhaled irritants, neurotrophins

1998-2002 **Bachelor of Science,** Marine Science Chemistry,
The University of Tampa, Tampa FL

Research:

- Development of novel technique employing flow cytometry for neuron quantification
- Retrograde tracing and immunohistochemical identification of neurons
- Morphometric analysis of airway innervation
- Quantification of neurotrophin levels in airway lavage fluid using ELISA
- Experience with mRNA isolation, RT-PCR, protein extraction

Publications:

2011 **Zellner LC**, Brundage KM, Hunter DD, Dey RD. Early postnatal ozone exposure alters rat nodose and jugular sensory neuron development.
Accepted for publication in Toxicological and Environmental Chemistry

Conference Abstracts and Presentations:

2010 **Zellner L**, Brundage K, Hunter D, Dey R. Altered airway sensory neuron development in rats following acute early postnatal ozone exposure. *Van Liere Research Convocation:* Morgantown, WV.

2009 **Zellner L**, Brundage K, Dey R. Quantitative analysis of rat nodose, jugular and petrosal ganglia neurons using flow cytometry. *Van Liere Research Convocation:* Morgantown, WV.

Zellner L, Hunter D, Brundage K, Dey R. Tracheal epithelium innervation and sensory neuron number in the nodose and jugular ganglia of rats. *FASEB Annual Scientific Meeting*: New Orleans, LA

2008 Puce A, McNeely M, Carrick O, Berrebi M, Epling J, Thompson JC, Hardee JE, **Zellner L**, Brefczynski-Lewis J. N170 amplitude reflects the seen number of faces irrespective of low-level stimulus variables. *OHBM Annual Scientific Meeting.* #714

Zellner L, Batchelor T, Hunter D, Dey R. Sensory innervation of the tracheal epithelium: a role for NGF". **1st place poster competition** *Van Liere Research Convocation*: Morgantown, WV.

2007 **Zellner L**, Hunter D, Batchelor T, Dey R. Postnatal development of airway sensory neurons. *American Thoracic Society International Meeting*: San Francisco, CA.

Zellner L, Hunter D, Batchelor T, Dey R. Airway sensory neuron development in postnatal fisher 344 rats. **Platform presentation and poster** *Minority Trainee Research Forum*: Miami, FL.

Zellner L, Batchelor T, Dey R. Postnatal development of airway sensory neurons. *Van Liere Research Convocation*: Morgantown, WV.

Honors and Awards:

2007- 2010 *Fellow*; F31 Predoctoral Ruth L Kirschstein National Research Service Award

2008 *1st Place Poster Competition*: WVU Van Liere Research Convocation

2007 *Travel Award*; American Thoracic Society International Annual Scientific Meeting

Abstract Award: Minority Trainee Research Forum

Teaching:

2009 *Coursework*: Teaching practicum (PSIO 790), Dr. Mark Paternostro, West Virginia University

2008 *Tutor;* Elementary physiology (PSIO 241), coordinator Dr. Stan Yokota, West Virginia University

2007 *Lecturer*; Mechanisms of Body Function (PSIO 441), coordinator Dr. Laurie Sherwood West Virginia University

2006 *Lecturer*; Mechanisms of Body Function (PSIO 441), coordinator Dr. Laurie Sherwood West Virginia University

2005 *Moderator;* Physiology Small Group in Human Function (CCMD 730), coordinator Dr. Robert Goodman West Virginia University

2004 *Moderator;* Physiology Small Group in Human Function (CCMD 730), coordinator Dr. Robert Goodman West Virginia University